Neuroplastic Changes in a Mouse Model of Pancreatic Ductal Adenocarcinoma

by

Rachelle Eve Stopczynski

B.S. Biological Sciences: Neuroscience, University of Rochester, 2006

Submitted to the Graduate Faculty of

School of Medicine in partial fulfillment

of the requirements for the degree of

Doctor of Philosophy

University of Pittsburgh

2013

UNIVERSITY OF PITTSBURGH

School of Medicine

This dissertation was presented

by

Rachelle Eve Stopczynski

It was defended on

June 10, 2013

and approved by

Brian M. Davis, PhD, Professor of Medicine and Neurobiology

Derek C. Molliver, PhD, Assistant Professor of Medicine

Linda M. Rinaman, PhD, Professor of Neuroscience

David C. Whitcomb, MD, PhD, Professor of Medicine, Cell Biology and Physiology, and Human Genetics

Andrew D. Rhim, MD, Instructor A of Medicine, University of Pennsylvania Perelman School of Medicine

Dissertation Advisor: Kathryn M. Albers, PhD, Professor of Medicine and Neurobiology

Neuroplastic Changes in a Mouse Model of Pancreatic Ductal Adenocarcinoma

Rachelle Eve Stopczynski, PhD

University of Pittsburgh, 2013

Tumor-nerve interactions including tumor invasion of intra- and extra-pancreatic nerves and pain have been extensively documented in pancreatic malignancies. However, little is known about the relationship between tumor development and neuroplastic changes in the pancreas. Studies of human tissue demonstrate increased neurotrophic factor expression in pancreatic ductal adenocarcinoma (PDAC), and neurotrophic factors are known to enhance nerve sprouting and sensitization in peripheral afferents. Furthermore, animal studies show that chronic pancreatic inflammation produces hypertrophy and hypersensitivity of pancreatic afferents and that sensory fibers may themselves drive inflammation via neurogenic mechanisms. These observations led us to hypothesize that PDAC-related pain is due to changes in sensory afferent gene expression, driven by tumor-derived neurotrophic factors, and that sensitized afferents accelerate the transition from precancerous lesions to cancer via neurogenic inflammation. Using a genetically engineered mouse model of PDAC we found that although disease time course varied, pancreatic cancer typically developed by 16 weeks of age, however pancreatic neurotrophic factor mRNA expression was up-regulated and pancreatic innervation increased dramatically prior to this time point. These changes correlated with pain-related decreases in exploratory activity and increased expression of nociception-related genes in sensory ganglia. Cells of pancreatic origin could also be found invading the celiac or sensory ganglia. These results demonstrate that the nervous system participates in all stages of PDAC, including those that precede appearance of cancer.

TABLE OF CONTENTS

LIST OF TABLES

LIST OF FIGURES

LIST OF ABBREVIATIONS

5-FU- 5- fluorouracil

Actb- beta actin

ANOVA- analysis of variance

ARTN- artemin

ATF3- activating transcription factor 3

ATM- ataxia-telangiectasia mutated gene

B2m- beta2- microglobulin

B6.Cg- congenic C57BL/6 mouse strain

BB- blocking buffer

BDNF- brain-derived neurotrophic factor

BRCA1- breast cancer 1, early onset

BRCA2- breast cancer 2, early onset

BSA- bovine serum albumin

C57BL/6- C57 black 6 mouse strain

CA19-9- carbohydrate antigen 19-9

Ca^{2+}- calcium

$CaCl_2$- calcium chloride

CDK- cyclin-dependent kinase

CDKN2A- cyclin-dependent kinase inhibitor 2A

CGRP- calcitonin-related polypeptide α

CPB- celiac plexus blockade

Ct- threshold cycle

CX3CL1- chemokine (C-X3-C motif) ligand 1

CX3CR1- chemokine (C-X3-C motif) receptor 1

Cy2- Cyanine 2

ΔΔCt- normalized threshold cycle relative to control

ΔF340/380- ratio of absorbance at 340nm to absorbance at 380nm

DBTC- dibutyltin dichloride

DMEM/F12- Dulbecco's modified eagle medium: nutrient mixture F-12

DNA- deoxyribonucleic acid

DRG- dorsal root ganglion/ganglia

DiI- 1.1'-diotadecyl-3,3,3'3'-tetramethylindocarbocyanine perchlorate

ECM- extracellular matrix

EDTA- ethylenediaminetetraacetic acide

EGF- epidermal growth factor

EMT- epithelial- mesenchymal transition

EtOH- ethanol

FAMMM- familial atypical multiple mole-melanoma

FBS- fetal bovine serum

FGF- fibroblast growth factor

FOLFIRINOX- 5-fluorouracil, leucovorin, irinotecan, oxaliplatin

FVB- friend virus B mouse strain

GAP-43- growth associated protein 43

GAPDH- glyceraldehyde 3-phosphate dehydrogenase

GDNF- glial cell line-derived neurotrophic factor

GFRα1- glycoslyphosphatidylinositol-linked receptor alpha 1

GFRα2- glycoslyphosphatidylinositol-linked receptor alpha 2

GFRα3- glycoslyphosphatidylinositol-linked receptor alpha 3

Gt(ROSA)26Sor- gene trap ROSA 26, Philippe Soriano

GTP- guanosine-5'-triphosphate

Gusb- beta-glucuronidase

HBSS- Hank's balanced salt solution

HGF- hepatocyte growth factor

High K^+- 50mM potassium chloride

HNPCC- hereditary non-polyposis colorectal cancer

Hprt- hypoxanthine phosphoribosyl-transferase 1

HSC-3- human tongue squamous cell carcinoma

IGF- insulin-like growth factor

IL-1β- interleukin 1, beta

IL-6- interleukin 6

IPMN- intraductal papillary mucinous neoplasm

K_v4.3- potassium voltage-gated channel 4.3

KCl- potassium chloride

KRAS- v-Ki-ras2 Kirsten rat sarcoma viral oncogene homolog

$Kras^{G12D}$- conditional Kras allele with a glycine to aspartate point mutation in codon 12

L1-CAM- L1 cell adhesion molecule

LAS- Leica application suite

LSL- lox-stop-lox

MAG- myelin-associated glycoprotein

MAPK/ERK- mitogen-activated kinase/extracellular signal-regulated kinase

MCN- mucinous cystic neoplasm

MEM- minimal essential media

$MgSO_4$- magnesium sulfate

MLH1-mutL homolog 1, colon cancer, nonpolyposis type 2 (E. coli)

MMP-2 metalloproteinase-2

MSH2- mutS homolog 2, colon cancer, nonpolyposis type1 (E. coli)

MUC1- type 1 transmembrane mucin

$Na_v1.8$- sodium voltage-gated channel 1.8

NaCl- sodium chloride

$NaHCO_3$- sodium bicarbonate

NBS- normal bath serum

NFκB- nuclear factor kappa B

NGF- nerve growth factor

NK1R- tachykinin receptor 1

NRTN- neurturin

$p14^{ARF}$- 14 kilodalton protein, alternate reading frame

$p16^{INK4A}$- 16 kilodalton protein, inhibitor cdk4 and cdk6

$p19^{ARF}$- 19 kilodalton protein, alternate reading frame

p48-Cre- Ptf1a-p48-Cre recombinase

$p53^{Lox}$- conditional p53 allele with LoxP sites in intron 1 and intron 10

PanIN- pancreatic intraepithelial neoplasia

PAR2- protease-activated receptor 2

PB- 0.1M phosphate buffer, pH 7.4

PCR- polymerase chain reaction

PDAC- pancreatic ductal adenocarcinoma

Pdx1- pancreas duodenum homeobox 1

Pen/Strep- penicillin/streptomycin

PFA- paraformaldehyde

Pgk- phosphoglycerokinase

PGP 9.5- protein gene product 9.5

PI3K- phosphoinositide-3-kinase

PNI- perineural invasion

Ppia- cyclophilinA

PRSS1- protease, serine, 1 (trypsin 1)

PSC- pancreatic stellate cell

Ptf1a-p48- pancreas specific transcription factor 1a

RNA- ribonucleic acid

ROBO1- roundabout, axon guidance receptor, homolog 1 (Drosophila)

ROBO2- roundabout, axon guidance receptor, homolog 2 (Drosophila)

ROBO3- roundabout, axon guidance receptor, homolog 3 (Drosophila)

Rpl13a- 60S ribosomal protein L13A

Rpm- revolutions per minute

RPMI- Roswell Park Memorial Institute medium

RT- room temperature

RT-PCR- reverse transcription polymerase chain reaction

SCC- squamous cell carcinoma

SDS- sodium dodecyl sulfate

SEMA3A- sema domain, immunoglobulin domain (Ig), short basic domain, secreted, (semaphoring) 3A

SEMA3E- sema domain, immunoglobulin domain (Ig), short basic domain, secreted, (semaphoring) 3A

SLIT2- slit homolog 2 (Drosophila)

SMAD4- Smad family member 4

SP- substance P

STK11- serine/threonine kinase 11

TAE- 40mM Tris acetate, 1mM EDTA buffer

tdTomato- tandem dimer Tomato

TE- 10mM Tris, 1mM EDTA buffer

TGFβ- transforming growth factor beta

TH- tyrosine hydroxlase

TNBS- trinitrobenzene sulfonic acid

TNFα- tumor necrosis factor alpha

TP53- tumor protein p53 (human)

Tris- tris(hydroxymethyl)aminomethane

TRK- tropomyosin-related kinase

TRKA- tropomyosin-related kinase receptor type 1

TRKB- tropomyosin-related kinase receptor type 2

Trp53- tumor protein p53 (mouse)

TRPA1- transient receptor potential cation channel ankyrin 1

TRPV1- transient receptor potential cation channel vanilloid 1

VEGF- vascular endothelial growth factor

PREFACE

This dissertation could not have been completed without the generous support of my co-mentors, Dr. Kathryn Albers and Dr. Brian Davis. Dr. Albers has been a constant source of encouragement and scientific wisdom and expertise, especially with regard to the molecular experiments in this study. Dr. Davis has also been a tremendously valuable resource during my training and his endless energy makes it impossible to stay discouraged when experiments do not go as expected. Dr. Albers and Dr. Davis have not only guided my development as a successful scientist, but have supported my success and happiness in life outside of the laboratory as well. I sincerely thank them for everything they have done for me over the past five years.

The Albers/Davis laboratory has been a fun, productive, and collaborative environment in which to train. I am grateful to all of the past and current members who have contributed to my scientific knowledge and training especially Dr. Jennifer DeBerry, Dr. Xiaotang Jing, Dr. Ting Wang, Dr. Kathleen Salerno, Christopher Sullivan, and Charlotte Diges.

I would like to thank the members of my dissertation committee who have provided significant insight and valuable feedback about my project as it has progressed. Heartfelt thanks to Dr. Linda Rinaman for serving as my committee chairperson, Dr. Derek Molliver for serving on all of my graduate training milestone committees, Dr. David Whitcomb for his renowned expertise in pancreatic disease and for facilitating interactions with the Pancreas Working Group

as well as other prominent pancreas experts, and Dr. Andrew Rhim for serving as my outside examiner and for his collaborative contributions to the project over the past year.

I would also like to acknowledge our collaborators: Dr. Ronald DePinho and Dr. Haoqiang Ying for their help establishing the PDAC mouse colony and collecting preliminary data, Dr. Douglas Hartman for reviewing and scoring the pancreas histology slides, Dr. Daniel Normolle for his statistical expertise and for analyzing the behavior data in this study, Dr. Herbert Zeh III for his laboratory's help in creating murine PDAC cell lines, and Dr. Klaus Bielefeldt for helping originate this project.

My graduate training has been enriched through interactions with the Pittsburgh Center for Pain Research, the Center for Neuroscience at the University of Pittsburgh, and the University of Pittsburgh/Carnegie Mellon University Medical Scientist Training Program. I am grateful to the faculty and to all of my friends in these centers that have provided support over the years and made graduate training enjoyable.

Finally, I would like to thank my parents, family, friends, and The Boz for their love and support throughout my graduate training and in life. Mom, Megan, and Jaclyn, thank you for always being there with encouragement and much needed laughter. Most of all, I could not have made it through without the constant love and never-ending support from my fiancé. Anoopum, thank you for inspiring me every day and just generally making life great.

1.0 INTRODUCTION

1.1 PANCREATIC CANCER

1.1.1 Incidence, mortality, and epidemiology

In the United States, pancreatic cancer is the tenth most common cancer diagnosis in men and the ninth most common cancer diagnosis in women[1]. It is estimated that 45,220 new cases of pancreatic cancer will be diagnosed in 2013 and approximately 38,460 patients are expected to die of the disease[1]. This makes pancreatic cancer the fourth leading cause of cancer death in both men and women, accounting for 7% of all cancer deaths in the United States[1]. Approximately 95% of pancreatic neoplasms are exocrine tumors, which includes all tumors related to ductal cells, acinar cells, and their stem cells, while 5% of malignancies arise from the endocrine pancreas[1]. Pancreatic ductal adenocarcinoma (PDAC) is the most common type of pancreatic cancer, representing greater than 90% of exocrine tumors and 85% of all pancreatic neoplasms. In contrast, other exocrine tumors such as acinar carcinoma and pancreatic endocrine neoplasms make up just 1-2% of pancreatic malignancies[2]. Most pancreatic cancers, up to 85%, are localized to the periampullary region of the pancreas including the head, neck and uncinate process, with the remainder in the body and tail[3,4].

The lifetime risk of developing pancreatic cancer is 1.5% in both men and women[1]. Pancreatic cancer is approximately 30% more common in men than women overall and at every age over 35 years[1]. Increased age is a significant risk factor, with the likelihood of developing pancreatic cancer in the next ten years four times higher at age 70 than at age 50, and a median age of 71 at diagnosis[1]. Other risk factors include race and ethnicity (highest incidents rates are in African Americans, lowest in Asian Americans)[1,5], low socioeconomic status[5], tobacco use[6], obesity[7,8], heavy alcohol use[9], diabetes[10–12], and chronic pancreatitis[13–17].

Family history, particularly in a first-degree relative, and certain genetic factors are also associated with increased risk of developing pancreatic cancer (reviewed in[18–23]). Approximately 10% of PDAC cases are thought to be familial[22]. Germline mutations in the breast cancer 2, early onset *(BRCA2)* gene, which are associated with hereditary breast and ovarian cancer syndrome, account for the highest proportion of known causes of inherited pancreatic cancer[24–26], and both breast cancer 1, early onset *(BRCA1)* and *BRCA2* mutations are associated with increased risk of pancreatic cancer[24,25,27–29]. Germline mutations in the gene linked to familial atypical multiple mole-melanoma (FAMMM) syndrome, cyclin-dependent kinase inhibitor 2A *(CDKN2A)*, also confer increased risk of developing pancreatic cancer[29–31]. Other hereditary cancer syndromes such as Peutz-Jeghers syndrome (linked to mutations in serine/threonine kinase 11; *STK11*) and Hereditary Non-polyposis Colorectal Cancer syndrome (HNPCC; linked to mutations in MutL homolog 1, colon cancer, nonpolyposis type 2*; MLH1* and mutS homolog 2, colon cancer, nonpolyposis type 1*;MSH2*) are associated with increased risk of pancreatic cancer[32–34]. Germline mutations in the ataxia-telangiectasia mutated gene (*ATM*) have also been described in families with familial pancreatic cancer.[35] Patients with hereditary pancreatitis, which is associated with mutations in protease, serine, 1 *(PRSS1)*[36], also have a significantly

increased risk of developing PDAC[13–15,36,37]. In these patients, the lifetime risk of developing pancreatic cancer is 40-55%, which is a 70 times greater risk than the general population[13].

1.1.2 Prognosis and treatment

Despite increased research focus, the estimated 5-year survival rate for PDAC remains just 6%, with median survival time after diagnosis ranging from 24.1 months for patients diagnosed with stage IA disease to 4.5 months for patients with stage IV disease[38]. Several factors are thought to be responsible for the high fatality rate associated with this disease including poor early detection, early metastatic spread and lymph node involvement, and local invasion of retroperitoneal structures such as the superior mesenteric artery and the celiac plexus[1,39–43].

For patients with PDAC, treatment is largely based on the resectability of the tumor at presentation. Complete surgical resection is currently the only potentially curative treatment for patients with pancreatic cancer. Unfortunately, 80-85% of patients have stage III or IV disease at the time of diagnosis and are not candidates for surgical resection[1,38]. Criteria for un-resectability of PDAC tumors include superior mesenteric artery or celiac artery encasement, unreconstructable superior mesenteric vein or portal vein occlusion, aortic invasion or encasement, metastases to lymph nodes beyond the field of resection, and distant metastases[44].

Although surgical resection has the potential to be curative, five-year survival is approximately 20-25% in patients with negative margins following surgical resection and approximately 10% in patients with positive margins[1,4,45]. Predictors of poor survival following surgery include positive resection margins, poor tumor differentiation, tumor size, lymph node involvement, the presence of perineural invasion, and high preoperative or persistently elevated carbohydrate antigen 19-9 (CA19-9)[4,38,40,45–57]. Adjuvant treatment with chemotherapy or

chemoradiotherapy has been shown to improve survival outcome after surgery[48,58,59]. Additionally, the value of neoadjuvent chemotherapy or chemoradiotherapy to identify patients most likely to benefit from surgical resection, to increase the likelihood of achieving negative margins following tumor resection, and to potentially treat early micrometastatic disease is currently being studied[59,60].

In patients with metastatic disease, response to mono-treatment with 5-fluorouracil (5-FU) or gemcitabine is generally poor, however combination therapy with 5-FU, leucovorin, irinotecan, and oxaliplatin (FOLFIRINOX) has been shown to prolong life in patients who are able to tolerate the increased toxicity. Symptom management and palliative care are important components of PDAC treatment and often focus on relieving PDAC-related pain, depression, gastric outlet obstruction, delayed gastric emptying, obstructive jaundice, and pancreatic insufficiency (reviewed in[1,61,62]). Both monotherapy with gemcitabine as well as FOLFIRINOX have been shown to significantly improve quality of life for patients with metastatic PDAC[63,64].

1.1.3 Symptoms

In patients with PDAC the most common presenting symptoms, regardless of disease stage, are pain, jaundice, and weight loss[1,3,42,62,65] (reviewed in[66–68]). In the case of tumors in the body or tail of the pancreas, symptoms may not be apparent until very late in disease progression, when metastatic disease is often present[67]. In one study of 185 patients diagnosed with exocrine pancreatic cancer, asthenia and anorexia were present in >80% of patients whereas nausea, diarrhea, and vomiting were present in 33-51% of patients[3]. This study also found that jaundice was the most frequent sign at the time of diagnosis in 55% of patients and hepatomegaly was the next most common in 39%[3]. PDAC pain is generally epigastric or abdominal, radiating to the

sides or back, although severe back pain in the absence of abdominal pain is reported by some PDAC patients[68]. For a more detailed discussion of pain related to PDAC, see **1.3 CANCER PAIN**. Jaundice associated with PDAC is significantly more common in patients with tumors in the head of the pancreas, particularly at early stages of the disease[68]. Additionally, painless jaundice is more frequent at early stages of disease whereas jaundice with abdominal or back pain, is more common at advanced stages[68].

Other symptoms are less common at the time of disease presentation but may develop as the disease progresses (reviewed in[39]). This includes duodenal obstruction leading to gastric outlet obstruction[62], delayed gastric emptying associated with nausea and vomiting[69], abdominal ascites[39], depression[70–72], and cachexia[73]. Metastatic disease in PDAC commonly affects the liver, peritoneum, and lungs (reviewed in[39,74]).

1.1.4 Precursor lesions and PDAC histopathology

Several types of noninvasive epithelial neoplasms have been shown to give rise to PDAC, including intraductal papillary mucinous neoplasms (IPMNs), mucinous cystic neoplasms (MCNs), and pancreatic intraepithelial neoplasia (PanIN). Of these, PanIN lesions are the most common and their progression to PDAC has been extensively documented[75,76] (reviewed in[74]). PanIN typically occur in smaller pancreatic ducts and can be found in the pancreas of healthy patients, particularly with advanced age[74,75,77,78]. PanIN are also found in the pancreas of patients who are at high risk for developing PDAC[77]. A classification system has been developed to grade PanIN lesions based on graded stages of dysplasia, increasing architectural disorganization, and appearance of nuclear abnormalities[76]. Squamous metaplasia typically proceeds PanIN lesions and describes a process in which cuboidal ductal epithelium is replaced

by mature stratified squamous or transitional epithelium[76]. PanIN-1A and -1B are epithelial lesions with tall columnar cells and basally located nuclei and supranuclear mucin[76]. PanIN-2 is a mucinous epithelial lesion that may be flat or papillary and contains nuclear abnormalities. PanIN-3 is classified as epithelial lesions that are typically papillary or micropapillary, cribriforming, clusters of epithelial cells in the duct lumen, luminal necrosis, loss of nuclear polarity, and nuclear abnormalities[76]. High grade PanIN transition to PDAC is evidenced by the presence of invasion beyond the basement membrane[76]. The progression from PanIN to PDAC is associated with an accumulation of genetic mutations (discussed in **1.1.5 Molecular pathogenesis of PDAC**).

Less commonly, larger precursor lesions give rise to PDAC. IPMNs are also mucinous epithelial lesions, however these involve the main pancreatic duct or major branches and are large enough to be grossly or radiologically visable[76]. MCNs are also larger than PanIN and are cystic lesions characterized by the presence of ovarian-type stroma around the cyst and lack of connection to the duct system[76]. Similar to PanIN, IPMNs and MCNs are accompanied by accumulation of genetic mutations[74,79,80].

One study of precancerous lesions in the pancreas of patients at high risk of developing a pancreatic malignancy, found multifocal IPMN and PanIN lesions ranging from grade 1A-3[77]. In the majority of cases examined, regions of lobular parenchymal atrophy, characterized by loss of acinar cells, aggregation of islets, fibrosis, and fatty replacement of the pancreas, were associated with PanINs or IPMNs[77]. A different study found a significant association between PanINs and fibrosis in the pancreas of individuals older than 60 years of age[78]. Fibrotic changes associated with PanINs and IPMNs are thought to be due to small duct obstruction caused by the neoplasia[77,78].

Grossly, exocrine tumors of the pancreas are solid, scirrhous masses with poorly defined borders. PDAC tumors range from well- to moderately- to poorly- differentiated based on the extent to which the tumor cells morphologically resemble normal cells of the tissue. Differentiation has been shown to influence prognosis with well- or moderately- differentiated tumors associated with better prognosis, regardless of tumor stage[81]. PDAC tumors are characterized by a dense desmoplastic stroma, perineural tumor invasion (discussed in detail in **1.1.6 Tumor microenvironment, inflammation, and metastatic spread** and **1.2.1 Perineural invasion**), and limited vascularization.

1.1.5 Molecular pathogenesis of PDAC

While controversy remains as to what the cellular origins of PDAC are, pancreatic tumorigenesis involves progression from normal ducts to cancer precursor lesions to carcinoma driven by a combination of genetic mutations that are both inherited and acquired over time. Over 90% percent of pancreatic cancers have mutations in the *v-Ki-ras2 Kirsten rat sarcoma viral oncogene homolog* (*KRAS*) gene, a human homolog of a gene isolated from the Kirsten rat sarcoma virus[82–85]. KRAS, a GTP-binding protein, is a member of the RAS protein family and mediates a variety of cellular functions including proliferation, differentiation, and survival (reviewed in[74]). Activating mutations in *KRAS* cause the protein product to have decreased enzymatic activity and to be insensitive to GTPase activating proteins[86]. However, though enzymatic activity is inactivated, KRAS is actively signaling as long as it binds GTP, which in the case of the activating mutations means that KRAS is constitutively active[86]. Most commonly, activating mutations are point mutations in codon 12, resulting in substitution of glycine with valine, arginine, or most often, aspartate (reviewed in[74]). Interestingly, *KRAS*

mutations are also found in precursor lesions known to progress to PDAC. Mutations in *KRAS* have been shown to be in IPMNs[87], MCNs[80], and PanIN[88]. Furthermore, the prevalence of *KRAS* mutations found in precursor lesions increases, as the degree of dysplasia increases[80,87]. The early appearance of *KRAS* mutations in the pancreas suggests that oncogenic *KRAS* is involved in the formation of cancer precursor lesions as well as the development and maintenance of PDAC. This hypothesis is further supported by studies of transgenic mouse models of PDAC in which mutations in *KRAS* drive the formation of PanIN and eventually PDAC[89,90] (see **1.4.2 Genetically engineered mouse models of PDAC**).

Other important genetic mutations in PDAC are inactivating mutations in the tumor suppressor genes *tumor protein p53 (TP53), CDKN2A*, and *Smad family member 4* (*SMAD4*), which occur in more than 50% of pancreatic cancers[83,85,91–95]. The *CDKN2A* gene encodes for the protein $p16^{INK4A}$, a G1 cyclin-dependent kinase (CDK), and is located on chromosome 9p[91,92]. Somatic inactivating mutations in *CDKN2A* occur in approximately 95% of pancreatic tumors[91,92] and germline mutations in the gene are one of the causes of FAMMM syndrome. Inactivation of *CDKN2A* is thought to occur early[88] and cooperates in the development of PDAC with activated *KRAS*. The *CDKN2A* locus also encodes an overlapping tumor suppressor protein, $p14^{ARF}$, that inhibits TP53 degradation (reviewed in[74]). Mutations in the other two tumor suppressor genes generally occur in more advanced stages of neoplasia, after the acquisition of *KRAS* and *CDKN2A* mutations (reviewed in[74]). The *TP53* gene, one of the most commonly mutated genes in human cancers, is involved in many cellular functions including regulation of proliferation and apoptosis[93]. Inactivation of *TP53* occurs in 75-80% of pancreatic tumors, often via intragenic mutation coupled with loss of the second allele[83,93]. Inactivation of the *SMAD4* gene occurs[83,94] in approximately 60% of pancreatic tumors, and loss of heterozygosity is found

in 90% of tumors (reviewed in[74]). The protein product of *SMAD4* functions in the intracellular signaling pathway of transforming growth factor beta (TGFβ) receptor activation[96] and mutations in genes coding for other components the TGFβ signaling pathway have also been reported in pancreatic tumors[97].

How each of these mutations contributes to the development of neoplasia and subsequent transition to PDAC is not entirely understood. However, downstream effects could include alterations in a wide variety of signaling pathways including TGFβ, mitogen-activated kinase/extracellular signal-regulated kinase (MAPK/ERK), phosphoinositide-3-kinase (PI3K), nuclear factor κB (NFκB), epidermal growth factor (EGF), insulin-like growth factor (IGF), hepatocyte growth factor (HGF), fibroblast growth factor (FGF), and vascular endothelial growth factor (VEGF) (reviewed in[74]) Developmental signaling pathways, such as Hedgehog, Notch, and Wnt, likely also play a role in PDAC pathogenesis (reviewed in[74]).

1.1.6 Tumor microenvironment, inflammation, and metastatic spread

The tumor microenvironment also plays a critical role in PDAC pathogenesis (reviewed in[98–101]). PanIN formation is typically accompanied by focal fibrosis and inflammation, suggesting that both may plan an important role early in disease pathogenesis (reviewed in[102]). Inflammatory changes in the pancreas cause tissue damage and the release of cytokines, growth factors, and reactive oxygen species, which induce cell proliferation and DNA damage associated with tissue repair that could drive the accumulation of genetic changes related to malignant transformation and tumor development (reviewed in[103,104]). The strong relationship between chronic pancreatitis and the development of PDAC[13–17,37], as well as the presence of *KRAS*[105] mutations and PanIN lesions[75,106] in chronic pancreatitis support this hypothesis. Furthermore, studies using

transgenic mouse models of PDAC have shown that acute pancreatitis accelerates the development of cancer in mice expressing activating *Kras* mutations[107–111] (discussed in **1.4.2 Genetically engineered mouse models of PDAC**).

Similar processes of pancreatic stellate cell (PSC) recruitment and extracellular matrix (ECM) remodeling associated with stroma formation have been described in both PDAC and chronic pancreatitis, suggesting that inflammation in the pancreas may be an initiating event in PDAC-related stroma formation as well. A variety of cytokines and growth factors associated with inflammation in the pancreas have been shown to activate PSCs, and activated PSCs are thought to be responsible for secreting ECM components that form the desmoplastic stroma[112,113] (reviewed in[98,99]). The dense, desmoplastic stroma contains a cellular component that includes invading tumor cells, PSCs, fibroblasts, and inflammatory cells, and an extracellular component that includes glycoproteins, collagen, and proteases (reviewed in[98,100]). Growth factors and signaling molecules such as Hedgehog, HGF, FGF, and TGFβ create a positive feedback loop between tumor cells and PSCs driving tumor proliferation and migration, ongoing inflammation, and the expansion of the stroma (reviewed in[98–100,114]). One study demonstrated that stroma activity correlates with poorer prognosis[115] and the dense stroma surrounding the tumor as well as its avascular nature are thought to contribute to chemoresistance in PDAC. Blocking these components has been shown to increase tumor response to treatment with gemcitabine in a mouse model of PDAC[116].

Inflammation has also been shown to promote epithelial-mesenchymal transition (EMT)[117], which is thought to be an early step in metastatic spread. EMT allows tumor cells to dissociate from the epithelial layer via the down-regulation of molecules involved in cell-cell adhesion and acquisition of migratory capabilities (reviewed in[99]). Interestingly, in a mouse

model of PDAC, EMT and dissemination of pancreatic cells into the bloodstream was shown to occur at precancerous stages of tumor development, before PDAC was histologically evident[117]. This suggests that not only might inflammation in the pancreas influence the progression from PanIN to PDAC, but it may also drive the early dissemination of pancreatic cells related to metastases.

1.2 TUMOR-NERVE INTERACTIONS

1.2.1 Perineural invasion

Tumor-nerve interactions have been documented in a variety of cancers including PDAC, prostate cancer, skin cancer of the head and neck cancer, and oral cancers (reviewed in[118–127]). Metastases along nerves and perineural invasion (PNI) are commonly associated with these malignancies and previous studies have shown that intrapancreatic perineural invasion is present in up to 100% of PDAC cases (reviewed in[118,128,129]). Perinerual invasion is typically defined as the presence of malignant cells in the perineural space, but can involve tumor cell invasion of the epineurium, perineurium, or endoneurium.

1.2.1.1 Perineural invasion and disease prognosis

Intra- and extra-pancreatic perineural invasion correlate with worse disease prognosis. Extra-pancreatic PNI tumor invasion represents an important component of locally invasive disease and is a significant predictor of positive tumor margins following tumor resection. PNI has also been shown to correlate with post-operative recurrence and decreased survival time[52–57,130–133].

Tumor spread along pancreatic nerves could also serve as a mode of dissemination of distant metastases. One study found continuity between cancer cells invading peripheral nerves and cancer cells invading lymph nodes[134], and perineural invasion has been shown to be significantly correlated with lymph node invasion[52,135]. This suggests that PNI may contribute to lymph node involvement in the disease, another significant predictor of poor outcome in PDAC[52–54,133,135].

Lymph node involvement and retroperitoneal tumor invasion, potentially via nerves, directly affect resectability criteria in patients and perineural invasion of extra-pancreatic nerve plexuses has also been proposed as a potential reservoir of tumor cells left behind following tumor resection that could contribute to local recurrence of the disease[129]. Given that surgical tumor resection represents the only potentially curative intervention for patients with PDAC, PNI may be a significant barrier to disease treatment and improved survival.

Perineural tumor invasion not only provides a mode for local and distant spread of disease, it is also thought to play a role in the development of PDAC-related pain[122,136] (discussed in **1.3.2 Mechanisms of pancreatic pain**). PNI damages peripheral afferents and exposes the nerves to an intense inflammatory milieu containing a variety of cytokines and growth factors that can induce changes in sensory afferent phenotype, resulting in pain.

1.2.1.2 Proposed mechanisms of PNI in PDAC

The mechanisms underlying perineural tumor invasion in PDAC are not currently known, but likely involve reciprocal signaling between tumor cells and pancreatic afferents. The list of potential signaling molecules includes neurotrophic factors (discussed in **1.2.2.1 Neurotrophic factors in PDAC**), axon guidance proteins, cytokines, neurotransmitters, and adhesion molecules (reviewed in[119]).

A recent study using genomic sequencing and pathway-based mutation analysis identified mutations and copy-number variants in genes related to axon guidance in resected tumors from a cohort of patients with stage I and stage II PDAC[85]. Specifically, alterations in the proteins involved in axon guidance during development, such as slit homolog 2 (Drosophila) (*SLIT2)* and/or roundabout, axon guidance receptor, homolog 1/2 (Drosophila) (*ROBO1/2)* were identified, and decreased *ROBO2* expression was associated with poorer survival, as was increased expression of *ROBO3*, an inhibitor of ROBO2 signaling[85]. Significant amplification of class 3 semaphorins (*SEMA3A* and *SEMA3E*), another group of proteins involved in growth cone axon guidance, was also observed and increased *SEMA3A* expression was associated with poor survival[85] These data suggest that signaling between tumor cells and pancreatic nerves may invoke mechanisms similar to those involved in axon guidance during development. Furthermore, it points to a similarity between neural progenitor cells present during normal development and PDAC tumor cells.

Activated sensory afferents are known to release a variety of molecules including glutamate, calcitonin-related polypeptide α (CGRP), and substance P (SP). Release of these molecules in the pancreas has been implicated in neurogenic inflammation associated with pancreatitis (reviewed in[137]), and they may also play a significant role in perineural invasion. Both SP and its receptor, tachykinin receptor 1 (NK1R), are expressed in pancreatic cancer cell lines and SP induces cancer cell proliferation, invasion, and expression of metalloproteinase-2 (MMP-2) *in vitro*[138]. SP/NK1R signaling provides a link between perineural invasion and neurogenic inflammation in the pancreas, which suggests that a common mechanism, such as peripheral afferent sensitization, could underlie both phenomena.

Cytokines and chemokines from a variety of sources such as tumor cells, infiltrating immune cells, and PSCs have also been linked to perineural neural invasion in PDAC. Chemokine (C-X3-C motif) receptor 1 (CX3CR1) is expressed by PDAC cell lines and in PDAC tissue, whereas its ligand chemokine (C-X3-C motif) ligand 1 (CX3CL1), or fractalkine, is expressed by neurons and peripheral nerve fibers. CX3CR1 signaling induces tumor cell migration *in vitro*, and promotes peripheral nerve infiltration by transplanted tumors *in vivo*[139].

Increased expression of *L1 cell adhesion molecule* (*L1-CAM*) in PDAC tissue is significantly correlated with perineural invasion and poorer prognosis, implicating adhesion molecule signaling in the mutual tropism between tumor cells and pancreatic nerves[140] as well. Other studies have shown that a type 1 transmembrane mucin, MUC1, is overexpressed in pancreatic cancer and enhances adhesion between pancreatic cancer cells and Schwann cells *in vitro* via binding of myelin-associated glycoprotein (MAG), which is expressed on oligodendrocytes and Schwann cells and binds myelin to neurons[141]. Given the variety of molecules associated with tumor cell migration and invasion *in vitro* and perineural invasion in PDAC tissue, it is likely that a pattern of gene expression, rather than a single factor, is necessary for the initiation and progression of perineural tumor invasion in PDAC.

1.2.2 Neurotrophic factors

The neurotrophins and glial cell line-derived neurotrophic factor (GDNF) family ligands regulate survival, development, and plasticity of the peripheral nervous system (reviewed in[142,143]). Members of the neurotrophins include nerve growth factor (NGF) and brain-derived neurotrophic factor (BDNF) and members of the GDNF family ligands include GDNF, artemin (ARTN), and neurturin (NRTN). NGF and BDNF signal through tropomyosin-related kinase

receptor type 1 (TRKA) and type 2 (TRKB), respectively, which then dimerize and activate intracellular signaling cascades (reviewed in[144]). GDNF family ligands each bind a preferred, high affinity glycoslyphosphatidylinositol-linked receptor- α (GFRα), and the ligand-receptor complex then binds the extracellular domain of the receptor tyrosine kinase (RET), triggering downstream intracellular signaling cascades (reviewed in[142]). GDNF preferentially binds GFRα1, NRTN preferentially binds GFRα2, and ARTN preferentially binds GFRα3. Our lab and others have shown that these neurotrophic factors also drive postnatal sprouting and sensitization of primary sensory afferents[145–154] The tumor microenvironment contains a variety of inflammatory mediators and neurotrophic factors in the pancreas which can act on exposed pancreatic sensory afferents, stimulating nerve hypertrophy, promoting perineural invasion, and enhancing sensory neuron excitability and pain (discussed in **1.3.2 Mechanisms of pancreatic pain**).

1.2.2.1 Neurotrophic factors in PDAC

Studies of resected tumor tissue have shown that a variety of neurotrophic factors and neurotrophic factor receptors are expressed in PDAC. GDNF, GFRα1, NGF, TRKA, ARTN, and GFRα3 are increased in human PDAC tissue compared to normal control pancreas[140,155–162] and NGF and ARTN are significantly correlated with the degree of nerve hypertrophy[155,156]. Similar observations of nerve hypertrophy and remodeling associated with increased neurotrophic factor expression have been described in studies of chronic pancreatitis[163–167], suggesting that these changes are also associated with pancreatic inflammation and fibrosis and thus, likely begin at pre-malignant time points in PDAC development. Increased nerve hypertrophy and neural density in resected tissue from patients with PDAC and chronic pancreatitis are correlated with increased expression of growth associated protein 43 (GAP-43),

increased perineural invasion, and severity of patient-reported abdominal pain[136]. The effects of tumor-derived neurotrophic factors on afferents have also been demonstrated *in vitro*. Significant increases in neurite density were observed in isolated myenteric plexuses exposed to extracts from human PDAC[156,168] compared to normal medium, and this effect was blocked when NGF or ARTN was depleted from the tumor extract[156]. One group suggests that PDAC-related hyperglycemia could induce the release of neurotrophic factors such as NGF from pancreatic tumor cells as well as directly damage pancreatic afferents via glucose toxicity[169–171].

PDAC cell lines have been shown to express a variety of growth factor receptors including TRKA, TRKB, GFRα1, GFRα2, and GFRα3, suggesting that neurotrophic factors in the tumor microenvironment can also influence tumor cells[119]. Increased NGF, TRKA, TRKB, and GDNF expression in human PDAC tissue correlates with the degree of PNI[157,158,160,162,172] and *in vitro* studies show that ARTN, GDNF, and NGF promote invasive behavior of human PDAC cell lines[155,161,173–178]. One proposed mechanism for neurotrophic factor-induced tumor cell migration and invasion is increased expression of MMPs such as MMP-2[177]. Another *in vitro* study implicated GDNF-mediated activation of the ERK and PI3K pathways in pancreatic tumor cell migration and invasion[178]. Thus, neurotrophic factor signaling in the pancreas could contribute to disease progression directly by enhancing proliferation, migration, and invasion in tumor cells or indirectly via sensitization of pancreatic afferents. Increased NGF, TRKA, and GDNF expression in PDAC is also correlated with the severity of patient reported pain[119,157,159,162], suggesting that intrapancreatic neurotrophic factor expression in PDAC sensitizes pancreatic sensory afferents, resulting in pain.

1.3 CANCER PAIN

Many cancer patients will experience moderate to severe pain at some point during disease development and progression, with pain frequency and intensity increasing at later stages of disease (reviewed in[179–181]). Pain may be present at the time of cancer diagnosis or develop later as a direct result or side effect of cancer treatments and procedures or due advanced disease, metastases, or paraneoplastic syndromes (reviewed in[180,181]). Both tumor- and treatment-related pain syndromes can be chronic or acute in nature, complicating the balance between symptom management and disease treatment. Cancer-related pain has a profoundly negative effect on patient quality of life[71,72], and a significant number of patients report inadequate pain control. A number of different issues contribute to undermanaged cancer pain including incomplete knowledge of the underlying molecular mechanisms (reviewed in[181]). A better understanding of the pathophysiology of cancer pain will provide better, more efficacious treatment options with few side effects, thereby improving quality of life and survival in cancer patients.

1.3.1 Pancreatic pain

PDAC is associated with significant morbidity, particularly pain, which is associated with increased incidence of depression[71,72], decreased quality of life[71,72], and worse prognosis[68,136]. Similarly, pain is one of the most common and debilitating symptoms of patients with chronic pancreatitis (reviewed in[182]). Pancreatic pain can be caused by a variety of intra- and extra-pancreatic processes such as increased ductal pressure due to obstruction, ischemia, fibrosis, sensitized pancreatic afferents, duodenal stenosis, or common bile duct stenosis (reviewed in[183]).

Pancreatic pain has proven difficult to treat effectively. Use of nonsteriodal anti-inflammatory drugs and narcotic analgesics to relieve pain are generally the first line treatment, however they demonstrate limited efficacy and are associated with numerous adverse effects as well as the development of opioid dependence[184]. Celiac plexus blockade (CPB), either temporary or permanent, is one of the current options for treating patients with pancreatic pain (reviewed in[182,185–187]). Typically, an injection of a local anesthetic such as bupivacain and a corticosteroid is made into the celiac plexus for temporary CPB, and injection of alcohol or phenol into the celiac plexus produces permanent CPB. Unfortunately, the response rate following either temporary or permanent CPB is variable for patients with pancreatic pain and even for patients that experience a reduction in pain, the post-interventional pain-free interval is limited (reviewed in[185–188]). Thus far no randomized control trials have directly compared the efficacy of opioid analgesics and CPB in pancreatic cancer patients. Current evidence suggests the two treatments may be comparable, though CPB is associated with a lower risk of side effects and may be effective in patients in who are refractory to narcotic analgesics (reviewed in[182,185–188]). Similarly, denervation of the pancreas via bilateral transection of splanchnic nerves provides some patients with chronic pancreatitis short-term pain relief, though resection of the head of the pancreas remains the most efficacious treatment (reviewed in[186,187]). One potential reason for the poor sustained response to pancreatic denervation is that patients with pancreatic pain demonstrate evidence of central sensitization and impaired descending inhibitory pain modulation[189], suggesting that either interventions targeting peripheral afferent denervation should occur earlier in disease progression to prevent central sensitization, or that treatments occurring later require centrally-mediated interventions.

1.3.2 Mechanisms of pancreatic pain

Numerous molecules and processes likely contribute to the development of pancreatic neuropathy and pain including nerve damage and neurogenesis, immune cell infiltration, chemokines and cytokines, neurotrophic factors, and glial activation (reviewed in[179,180,190–192]). Inflammatory cytokines, such as interleukin 1, β (IL-1β), interleukin 6 (IL-6), and tumor necrosis factor α (TNFα), released by a variety of immune cells and pancreatic stromal cells have been shown to act directly on peripheral sensory afferents and induce hypersensitivity in a variety of neuropathic, inflammatory pain models (reviewed in[193,194]). Increased cytokine expression and astrocyte activation in the spinal cord have also been associated with chronic pancreatitis pain in a trinitrobenzene sulfonic acid (TNBS) induced rodent chronic pancreatitis model[195,196] and several studies using rodent models of bone and facial cancer pain have also implicated altered central glial activation and up-regulated cytokine signaling in the pathophysiology of cancer pain[197–203] (reviewed in[179]).

Additionally, chemokines such as fractalkine have also been implicated in pancreatic pain, as strong neuro-immunoreactivity for fractalkine and its receptor, CX3CR1, correlates with more severe pain in patients with chronic pancreatitis[204,205]. Increased fractalkine in human chronic pancreatitis is also associated with enhanced pancreatic infiltration of lymphocytes and macrophages and pancreatic neuritis[205]. Pancreatic neuritis is frequently observed in pancreatitis as well as PDAC tissue and increased neuritis is associated with a higher patient-reported pain score [136,166,185,206], increased neural density[136], and nerve hypertrophy[136]. Cytotoxic T-lymphocytes, macrophages, and mast cells are most commonly found infiltrating intra-pancreatic nerves and increased perineural mast cells is associated with the presence of pain[206].

Along with nerve injury due to pancreatic neuritis and the effects of inflammatory mediators on pancreatic afferent hypersensitivity, activation of two non-specific cation channels, transient receptor potential cation channel vanilloid 1 (TPRV1) and transient receptor potential cation channel ankyrin 1 (TRPA1) is associated with pancreatic afferent activation and pain (reviewed in[207]). TRPV1 responds to a variety of stimuli including capsaicin, noxious heat temperatures (> 42°C), and acid, while TRPA1 responds to stimuli including noxious cold (<17°C) temperatures, mustard oil, cinnamon oil, and bradykinin (reviewed in[208,209]). In mouse models of acute and chronic caerulein-induced pancreatitis, significantly more cultured pancreatic afferents respond to capsaicin or mustard oil application[210,211] and agonist-evoked intracellular calcium transients are potentiated[211]. Other rodent studies have also demonstrated TRPV1 and TRPA1 activation and enhanced pancreatic afferent excitability associated with pancreatitis[212–214]. Furthermore, exposure of cultured dorsal root ganglion (DRG) neurons to neurotrophic factors potentiates TRPV1-induced calcium transients[215], and blockade of NGF attenuates pancreatic hyperalgesia and decreases TRPV1 activation and expression in pancreatic sensory neurons[214]. Thus, inflammation- or cancer-derived neurotrophic factors in the pancreas likely drive pancreatic afferent sensitization via TRPV1 and TRPA1 activation.

1.3.3 Pancreatic pain and neurogenic inflammation

Studies of pancreatitis pain suggest that stimulation of sensory afferents and subsequent TRPV1 and TRPA1 activation also drives neurogenic inflammation in the pancreas[210,211,216–219] (reviewed in[137,207]). Neurogenic inflammation is characterized by vasodilation, edema, and thermal and mechanical hyperalgesia and is thought to be due release of CGRP and SP in the pancreas (reviewed in[137,207]). Furthermore, caerulein-induced pancreatic inflammation and edema is

attenuated by treatment with TRPV1 and/or TRPA1 antagonists[210,211,220] or treatment with a NK1R antagonist[220]. Sensory denervation of the pancreas, via neonatal capsaicin injection, prior to dibutyltin dichloride (DBTC) or caerulein induced pancreatitis inhibited pancreatic inflammation and attenuated the rate of pancreatic fibrosis and glandular atrophy in rats[216,221]. Ablation of TRPV1-expressing sensory neurons by resiniferatoxin, a neurotoxin and TPRV1 agonist, similarly ameliorated caerulein induced pancreatitis[218]. However, genetic deletion of TRPV1 in mice does not protect against pancreatitis[218] suggesting that another signaling cascade leading to sensory afferent sensitization and neuropeptide release exists, such as TRPA1. Taken together, these studies of neurogenic inflammation in rodent models of pancreatitis provide evidence that peripheral afferents play an important role in pancreatic pain and inflammation. Furthermore, additional studies using genetically engineered mouse models of PDAC are necessary to determine whether sensitized pancreatic afferents drive pain, inflammation, and disease progression in PDAC as well.

1.4 ANIMAL MODELS

1.4.1 Animal models of cancer pain

Previous studies of pancreatic cancer pain in a mouse model of acinar cell carcinoma[222], a relatively rare pancreatic exocrine malignancy, demonstrated increased density of sensory and sympathetic fibers, increased microvascular density, and increased NGF-expressing macrophage infiltration in the pancreas at precancerous and early stage disease[223]. In this model, pain-related hunching and vocalizations were not significantly increased as compared to wild type controls

until late stages of disease, when large tumors were present. Pain-related hunching severity in cancer mice with advanced stage disease was attenuated by acute administration of morphine sulfate[223] and administration of the central nervous system-penetrant opioid receptor antagonists, naloxone and naltrexone, induced hunching and vocalizations in cancer mice with pre-malignant or early stage disease[224]. These data suggest that endogenous opioid signaling may suppress pain at pre-malignant and early stages of cancer development, potentially delaying the detection of an underlying pancreatic malignancy.

Other groups have studied the molecular mechanisms of cancer pain using rodent models of metastatic bone, oral, or head and neck cancer. Bone cancer pain is typically related to metastatic spread, therefore rodent models of bone cancer pain typically utilize injection of prostate or mammary gland cancer cells into the tibia or femur, producing spontaneous pain-related behavior and evoked mechanical and thermal hyperalgesia, to recapitulate human disease and identify neuroplastic changes associated with tumor-induced pain [201,203,225–230]. In one model of bone cancer pain in which osteolytic murine sarcoma cells are surgically implanted into the femur, blockade of TRK signaling attenuates tumor-induced sprouting of sensory and sympathetic nerve fibers, neuroma formation, and pain[231]. Early and sustained treatment with the selective small molecule TRK inhibitor was necessary to prevent sarcoma-induced neural remodeling and pain[231]. In a similar model of murine bone pain, early, preventative or late treatment with an NGF-sequestering antibody attenuates sensory nerve sprouting, neuroma formation and nociceptive behaviors induced by canine prostate carcinoma cells implantation in the femur[226,232–234].

Another model of murine cancer pain in which fibrosarcoma cells are implanted in and around the calcaneus bone produces hyperalgesia to mechanical stimuli in the ipsilateral paw that

is dose-dependently attenuated by morphine administration[235], partially blocked by intra-tumor injection of a CGRP receptor anatagonist[236], and significantly alleviated with systemic antagonism of TNFα[237,238]. In this model, a subset of C-fibers adjacent to the tumor developed spontaneous activity and exhibited decreased heat thresholds within two weeks of tumor growth, and these changes in sensory afferent phenotype were accompanied by increased branching of epidermal nerve fibers in the skin overlaying the tumor[239], supporting the hypothesis that similar processes underlie both tumor-induced hyperinnervation and afferent sensitization.

A chemically induced model of head and neck cancer and injection of oral squamous cell carcinoma cells (SCC) or SCC supernatant have been established as models of chronic head and neck cancer pain, persistent oral cancer pain, and acute oral cancer pain, respectively[240]. In these models, interaction between protease-activated receptor 2 (PAR2) and serine proteases is critical for the development of acute and chronic cancer pain[240]. Furthermore, serine protease inhibition attenuates persistent cancer pain whereas chronic cancer pain development is prevented in PAR2-deficient mice[240]. In a similar model of oral cancer pain in which human oral cancer cells (HSC-3) are implanted into the plantar surface of the hindpaw or into the floor of the mouth, treatment with an anti-NGF antibody decreased nociception and weight loss as well as inhibited tumor proliferation[241]. Anti-NGF treatment also decreased expression of TRPV1, TRPA1 and PAR2 in trigeminal ganglia neurons[241].

1.4.2 Genetically engineered mouse models of PDAC

The relatively limited improvement in early detection, treatment, and survival in pancreatic cancer over the past 50 years led to an increased focus on developing preclinical models of the disease, and a variety of xenograft, carcinogen-induced, and genetically engineered models of

the disease are currently available (reviewed in[74,242–247]). Activating *KRAS* mutations such as *KRAS*^{G12D} are found in nearly all human PDAC tumors as well as precancerous PanIN lesions (discussed in **1.1.5 Molecular pathogenesis of PDAC**). Expression of *Kras*^{G12D} targeted to murine pancreatic cells leads to acinar-to-ductal metaplasia and the formation of PanIN lesions in the pancreas of transgenic mice[89] (reviewed in[242,245]). Furthermore, the importance of *Kras*^{G12D} in PDAC development and progression was recently demonstrated in transgenic mice expressing an inducible *Kras*^{G12D} in which expression of oncogenic *Kras*^{G12D} leads to formation of precursor lesions, whereas inactivation of *Kras*^{G12D} during cancer progression leads to regression of precancerous lesions[90].

Insertion of a *LoxP* flanked gene silencing "Stop" cassette (*LSL*) upstream of the *Kras* promoter restricts expression of the endogenous mutated *Kras*^{G12D}, based on Cre recombinase[248] excision of the silencing cassette. Specific expression of a conditional *LSL-Kras*^{G12D} allele[249,250] in pancreatic progenitor cells is achieved by crossing the *LSL-Kras*^{G12D} knock-in strain with a transgenic strain expressing either *pancreas duodenum homeobox 1-Cre* (*Pdx1-Cre*) or *pancreas specific transcription factor 1a-Cre* (*Ptf1a-p48-Cre*)[89]. Both *Pdx1* and *Ptf1a-p48* are expressed in early pancreatic progenitors cells that give rise to endocrine and exocrine cell lineages[251] (reviewed in[246]).

Inactivating mutations in the tumor suppressor genes *TP53, p16*^{INK4}*/CDKN2A*, and *SMAD4*, occur in more than 50% of human PDAC tumors (discussed in **1.1.5 Molecular pathogenesis of PDAC**), and each has been targeted in the development of transgenic mouse models of PDAC as well. Progression from precancerous lesions to invasive and metastatic adenocarcinoma was infrequently observed in *Ptf1a-p48-Cre; LSL-Kras*^{G12D} and *Pdx1-Cre; LSL-Kras*^{G12D} mice[89,252–254]. However, when expression of the mutated *Kras*^{G12D} is combined with

p16^{Ink4a}/*p19*^{Arf}, *Smad4*, or *Trp53* inactivation, PanIN lesions rapidly progress to invasive adenocarcinoma in transgenic mice[252–254]. In these transgenic mouse models, histology, pathology, pathophysiology, molecular, and clinical aspects of PDAC closely parallel what is observed in human PDAC (reviewed in[243]). Interestingly, recent studies have demonstrated that pancreatitis also significantly accelerates the progression from PanIN to PDAC in transgenic mice expressing *LSL-Kras*^{G12D} [107–111], which is consistent with the significant association between chronic pancreatitis and PDAC development in human disease.

1.5 DISSERTATION GOALS

The goal of my dissertation is to test the hypothesis that PDAC-related pain is due to changes in sensory afferent gene expression, driven by tumor-derived neurotrophic factors. These changes in growth factor expression and sensory afferent gene expression are further hypothesized to sensitize pancreatic afferents and in so doing, drive neurogenic inflammation in the pancreas and promote the development and progression of PDAC. In order to test this hypothesis, and to elucidate the temporal dynamics of disease progression, pain development, intra-pancreatic innervation, neurotrophic factor expression changes, and changes in sensory afferent gene expression, I measured behavioral, gene expression, anatomical, and calcium ion handling parameters over time in an established transgenic mouse model of PDAC.

1.6 SUMMARY

In this study, we demonstrate that changes in pain-related behavior are evident in PDAC mice as the disease progresses, though there is considerable variability in time course among PDAC mice. We describe neuroplastic changes in the pancreas of PDAC mice that closely parallel the neuroplastic changes previously described in human PDAC specimens, and importantly, these changes begin prior to the appearance of cancer. Finally, neuroplastic changes in the pancreas are accompanied by up-regulation of genes related to nociception and neurogenic inflammation in sensory afferent neurons.

2.0 METHODS

2.1 MOUSE STRAINS

We established the line of PDAC transgenic mice from breeders generously supplied by the laboratory of Dr. Ronald DePinho (MD Anderson Cancer Center, Houston, TX). PDAC mice produced on C57BL/6 and FVB backgrounds were backcrossed 4 times with C57BL/6 mice, resulting in transgenic mice that are genetically 93.75% identical to the C57BL/6 strain. PDAC mice express a conditional activated (mutant) *Kras* allele targeted to the endogenous *Kras* locus under *Lox-Stop-Lox* control (*LSL-Kras*^{G12D})[249,250], a conditional *Trp53* allele with *LoxP* sites in intron 1 and intron 10 of the *Trp53* gene (*p53*^{Lox})[254,255], and *Ptf1a-p48-Cre* (*p48-Cre)*[89,251], as described previously [89,117,254]. Mice with the genotypes *LSL-Kras*^{G12D}*; p53*$^{+/+}$, *LSL-Kras*^{G12D}*; p53*$^{lox/+}$, *LSL-Kras*^{G12D}*; p53*^{LoxlLox} or any conditional allele alone were used as age- and sex-matched littermate controls. To better visualize cells of pancreatic origin, PDAC mice were crossed with a *ROSA-LSL-tdTomato* reporter strain (B6.Cg-*Gt(ROSA)26Sor*$^{tm9(CAG-tdTomato)Hze}$/J; The Jackson Laboratory, Bar Harbor, ME) to produce tPDAC mice in which all cells of pancreatic origin express tdTomato, a red fluorescent protein. Transgenic mice expressing *p48-Cre* and *ROSA-LSL-tdTomato* but neither *LSL-Kras*^{G12D} nor *p53*^{Lox} were used as age- and sex-matched control tdTomato mice.

Transgenic offspring were genotyped at 2 weeks of age using DNA isolated from tail skin. Mice were lightly anesthetized with inhaled isoflurane and a small (5mm) tail snip was removed. Tails were digested in 480µl of lysis buffer (200mM NaCl, 100mM Tris pH 8.0, 10mM EDTA, 0.5% SDS) and 20µl of proteinase K (10 mg/ml) overnight at 55°C. To extract the DNA,165µl of 5N NaCl was added and tubes were centrifuged for 5 minutes at 10,000 revolutions per minute (rpm). DNA was precipitated in 800µl of 100% ethanol (EtOH), centrifuged for 10 minutes at 10,000 rpm to form a pellet, rinsed twice in 75% EtOH, and centrifuged for 5 minutes at 10,000 rpm after each rinse. The DNA pellet was dried for 5 minutes and reconstituted in 200µl of TE buffer (10mM Tris pH 8.0, 1mM EDTA pH 8.0). Polymerase chain reaction (PCR) analysis of 100ng of DNA was done using HotStar Taq DNA polymerase (Qiagen, Valencia, CA) using primer set sequences provided by the DePinho laboratory (*LSL-Kras*^{G12D}, *p53*^{Lox}, and *p48-Cre*) and The Jackson Laboratory (*ROSA-LSL-tdTomato*), listed in **Table 1**. Amplified DNA was separated by gel electrophoresis on a 2% agarose (GeneMate, BioExpress, Kaysville, UT) gel with ethidium bromide (0.5µg/ml; Invitrogen, Life Technologies, Grand Island, NY) in TAE buffer (40mM Tris acetate, 1mM EDTA pH 8.0).

Table 1. Primer squences for genotyping PDAC and tPDAC transgenic strains

Transgene	Primers	5'→ 3'
LSL-Kras^{G12D}	3'-Flank-3' LoxP1	TCCGAATTCAGTGACTACAGATG
	5'-Kozak-3' LoxP1	CTAGCCACCATGGCTTGAGT
p53^{Lox}	Intron 1 Forward	CACAAAAACAGGTTAAACCCAG
	Intron 1 Reverse	AGCACATAGGAGGCAGAGAC
Ptf1a-p48-Cre	Cre 26	CCTGGAAAATGCTTCTGTCCG
	Cre 36	CAGGGTGTTATAAGCAATCCC
	Gabra 12	CAATGGTAGGCTCACTCTGGGAGATGATA
	Gabra 70	AACACACACTGGCAGGACTGGCTAGG
ROSA-LSL-tdTomato	IMR 9020	AAGGGAGCTGCAGTGGAGTA
	IMR9021	CCGAAAATCTGTGGGAAGTC
	IMR 9103	GGCATTAAAGCAGCGTATCC
	IMR 9105	CTGTTCCTGTACGGCATGG

PDAC and tPDAC mice were analyzed at time points between weaning (post-natal day 21) through terminal disease, typically 25-30 weeks of age. Tissue was harvested at 3-4 weeks, 6-8 weeks, 10-12 weeks, and greater than 16 (>16) weeks. Due to the relatively few PDAC and tPDAC mice produced in each litter, both male and female mice were used to reach appropriate experimental group sizes.

All animals were housed in the Association for Assessment and Accreditation of Laboratory Animal Care-accredited Division of Laboratory Animal Resources at the University of Pittsburgh in a 12 hour light/dark cycle with a temperature-controlled environment and ad libitum access to water and food. Animals were cared for and studies were performed in accordance with guidelines of the Institutional Animal Care and Use Committee at the University of Pittsburgh and the National Institutes of Health *Guide for the Care and Use of Laboratory Animals*.

2.2 SICKNESS AND HUNCHING ASSESSMENT

PDAC, tPDAC, and littermate control mice were weighed weekly beginning at postnatal day 28 to monitor sickness severity. Animals were additionally monitored for the appearance of tumor sequelae such as jaundice, abdominal swelling due to ascites, and decreased locomotion. Additionally, PDAC and tPDAC mice were scored weekly based on a hunching/sickness scale adapted from the one previously developed by Mantyh and colleagues in a mouse model of pancreatic acinar carcinoma [223,224]. Scores were assigned as follows: 0= no rounded-back posture and healthy-appearing coat; 1= mild rounded-back posture and healthy-appearing coat; 2= moderate rounded-back hunched posture and slight piloerection; 3= moderate to severe rounded-back hunched posture and moderate piloerection; 4= severe rounded-back hunched posture, whole body piloerection, altered gait, and limited locomotion. Hunching score served as a surrogate marker of sickness severity and animals receiving a hunching score 4 were euthanized.

2.3 PANCREAS AND METASTASIS HISTOLOGY AND IMMUNOHISTOCHEMISTRY

2.3.1 Tissue preparation

Histological analysis and pancreatic innervation was examined in PDAC, tPDAC, and control mice at age 3-4 weeks, 6-8 weeks, 10-12 weeks, and >16 weeks. Animals were euthanized by overdose of inhaled isoflurane and transcardially perfused with 4% paraformaldehyde (PFA) in

0.1M phosphate buffer (PB, pH 7.4). The pancreas, stomach, and duodenum were dissected out *en bloc* and separate parts of liver and lung were removed if metastases were grossly visible. The tissue was post-fixed in 4% PFA for 2 hours at room temperature (RT), cryoprotected in 25% sucrose in 0.1M PB overnight at 4°C, embedded in Tissue-Tek OCT compound (Sakura Finetek, Torrance, CA), sectioned on a cryostat at 30µm, and serially mounted on Superfrost Plus slides (Fisher Scientific Company, Pittsburgh, PA).

2.3.2 Hematoxylin and eosin staining

Pancreas and metastasis histology was visualized with hematoxylin and eosin staining. Tissue sections were dehydrated in serial alcohols as follows: 2x water for 5 minutes, 2x 50% EtOH for 30 seconds, 2x 75% EtOH for 30 seconds, 2x 95% EtOH for 1 minute, 2x 100% EtOH for 2 minutes, and 2x Fisherbrand Citrisolv clearing agent (Fisher Scientific Company, Pittsburgh, PA) for 5 minutes. Sections were then rehydrated through the sequence of EtOH in the reverse order, dipped in hematoxylin (Thermo Scientific, Pittsburgh, PA) for 10 seconds, rinsed in water, dipped quickly 5 times in eosin (Thermo Scientific, Pittsburgh, PA), and rinsed in water. Sections were again dehydrated through serial alcohols as described above, coverslipped with DPX mounting medium (Electron Microscopy Sciences, Hatfield, PA), and viewed and photographed on a LEICA DM 4000B microscope (Leica Microsystems, Wetzlar, Germany) using Leica Application Suite (LAS) software (Leica Microsystems, Wetzler, Germany. Sections of pancreas from at least four PDAC mice per age group were reviewed and scored by Dr. Douglas J. Hartman, Assistant Professor of Pathology, University of Pittsburgh.

2.3.3 Immunohistochemistry

Immunofluorescence was used to visualize nerves in the pancreata and metastatic spread in tPDAC and control tdTomato mice. Tissue sections were washed in 0.1M PB, incubated in blocking buffer [BB; 5% normal horse serum (Thermo Scientific, Pittsburgh, PA) and 0.25% Triton X-100 (Thermo Scientific, Pittsburgh, PA) in 0.1M PB] for 30 minutes at RT, incubated in primary antibody diluted in BB overnight at RT, and washed with 0.1M PB. Primary antibodies used were rabbit anti-protein gene product 9.5 (PGP 9.5; 1:1000, UltraClone Limited, Wellow, Isle of Wight, England), rabbit anti-tyrosine hydroxylase (TH; 1:200, Cell Signaling Technology, Danvers, MA), and rabbit anti-calcitonin-related peptide α (CGRP; 1:1000, Sigma-Aldrich, St. Louis, MO). Binding of primary antibodies was visualized with donkey anti-rabbit secondary antibody conjugated to Cy2 (1:500, Jackson ImmunoResearch Laboratories, West Grove, PA) diluted in in 0.1M PB. Tissue sections were incubated in secondary antibody for 2 hours at RT, washed in in 0.1M PB, dehydrated in Fisherbrand Citrisolv clearing agent, and coverslipped with DPX mounting medium. Sections were photographed using LAS software and a LEICA DM 4000B microscope.

2.4 OPEN-FIELD EXPLORATORY BEHAVIOR

To assess pain-related behavior throughout tumor development in PDAC mice, open-field exploratory behavior was analyzed at time points ranging from 7-31 weeks of age. As previously described [210,211], mice were placed in plexiglass boxes and open-field exploratory activity was measured photoelectrically at a 0.75 cm spatial resolution for a period of 15 minutes

using TruScan software (Coulbourn Instruments, Whitehall, PA). The software analyzed movements, time spent moving, velocity of movement, distance travelled, and time spent in different areas of the behavior arena. Both horizontal measurements in which the animals were moving along the floor of the arena and vertical measurements in which the animals were extending or rearing upward were analyzed. Some animals were tested repeatedly, at a frequency of approximately two weeks, however no habituation to the test was apparent in PDAC or control mice. The total monitoring period was divided into 3 blocks of 5 minutes and data for each behavior measurement were analyzed using a linear mixed effects models with age, genotype, and time block treated as fixed effects and each individual animal treated as a random effect to account for intra-animal correlation. Analyses were performed using the R package lme4 and p-values for the fixed effects were based on likelihood ratio tests. These statistical analyses were performed by Dr. Daniel P. Normolle, Associate Professor of Biostatistics, University of Pittsburgh. Data were also binned based on discreet age ranges corresponding to different stages in tumor development (6-8, 10-12, and >16 weeks) and differences between cancer and control mice were analyzed using a two-way analysis of variance (ANOVA). Within age comparisons between PDAC and control mice were performed using the Bonferroni correction (Matlab, MathWorks, Natick, MA). All statistical analyses performed in Matlab were done by Dr. Anoopum S. Gupta, Department of Medicine, UPMC.

2.4.1 Naloxone treatment

To determine the effect of endogenous opioid blockade on open-field exploratory behavior in PDAC mice, animals were injected with the μ-opioid receptor antagonist, naloxone hydrochloride (4 mg/kg in sterile saline, subcutaneously; Sigma, St. Louis, MO) 30 minutes prior

to activity monitoring as described above. PDAC mice and matched controls were 17- 31 weeks of age at the time of testing and each PDAC mouse was scored a 1 or 2 on the hunching scale. The number of cancer and control mice exhibiting decreased behavior was compared for each behavior measurement using Mann Whitney U tests (SPSS Statistics; IBM Corporation, Armonk, NY). A percent change score [(post-naloxone treatment – baseline)/baseline] for each behavior measurement was calculated for each mouse. Average percent change score for PDAC and control mice were compared for each beahavior measurement using Mann-Whitney U tests (Matlab, Mathworks).

2.5 CELIAC GANGLION AND DORSAL ROOT GANGLIA IMMUNOHISTOCHEMISTRY

2.5.1 Tissue preparation

Celiac ganglia from tPDAC and tdTomato control mice >16 weeks of age were analyzed for the presence of tdTomato$^+$ cells of pancreatic origin and expression of activating transcription factor 3 (ATF3), a marker of nerve injury. Animals were euthanized by overdose of inhaled isoflurane and transcardially perfused with 4% PFA. The celiac ganglion was dissected out, post-fixed for 1hour at RT, and cryoprotected in 25% sucrose in 0.1M PB overnight at 4°C. In one tPDAC mouse, a tdTomato$^+$ tumor metastasis was found encasing the spinal cord at the level of thoracic vertebra 9-12 (T9-12). This section of spinal cord with associated DRG was dissected, post-fixed, and cryoprotected. Cryoprotected tissue was embedded in 10% porcine gelatin (~300 bloom, Sigma-Aldrich, St. Louis, MO) in 0.1M PB, fixed for 30 minutes in 4% PFA, and gelatin

blocks were cryoprotected in 25% sucrose in 0.1M PB overnight at 4°C. Floating tissue sections were cut at 20µm using a sliding microtome.

2.5.2 Immunohistochemistry

Immunofluorescence was used to visualize tdTomato^{+} cells within the celiac ganglion and expression of ATF3 in celiac ganglion neurons. Sections of celiac ganglion were washed in 0.1M PB, incubated in BB for 30 minutes at RT, incubated in primary antibody diluted in BB overnight at RT, and washed with 0.1M PB. Primary antibodies used were rabbit anti-PGP 9.5 (1:1000, UltraClone Limited), rabbit anti-TH (1:200, Cell Signaling Technology), and rabbit anti-ATF3 (1:200, Santa Cruz Biotechnology). Binding of primary antibodies was visualized with donkey anti-rabbit secondary antibody conjugated to Cy2 (1:500, Jackson ImmunoResearch Laboratories) diluted in in 0.1M PB. Tissue sections were incubated in secondary antibody for 2 hours at RT, washed in in 0.1M PB, and mounted on Superfrost Plus slides in 0.1% porcine gelatin in 0.1M PB. Sections were coverslipped with Vectashield mounting media (Vector Laboratories, Burlingame, CA) and photographed using LAS software and a LEICA DM 4000B microscope. Sections of spinal cord with attached DRG were processed as described above for PGP9.5 and ATF3.

2.6 DRG RNA ISOLATION AND QUANTITATIVE REVERSE TRANSCRIPTION-PCR (qRT-PCR)

Changes in gene expression in the DRG of PDAC mice at 10-12 and >16 weeks of age were assessed using qRT-PCR. Animals were euthanized by overdose of inhaled isoflurane, transcardially perfused with 0.9% saline, and DRG from T9-T12 were removed bilaterally as these levels have previously been shown to receive the majority of innervation from the pancreas [256]. DRG were immediately frozen on dry ice and RNA isolated using RNeasy Mini kits (Qiagen, Valencia, CA). RNA was treated with DNAse (Invitrogen, Life Technologies, Grand Island, NY) to remove genomic DNA, and 300ng -1µg was reverse-transcribed using Superscript II (Invitrogen, Life Technologies, Grand Island, NY). SYBR Green-labeled PCR amplification using Absolute QPCR SYBR Green ROX mix (Thermo Scientific, Pittsburgh, PA) was performed on an Applied Biosystems 7000 real-time thermal cycler controlled by Prism 7000 SDS software (Applied Biosystems, South San Francisco, CA). Threshold cycle (C_t) value, the cycle number at which SYBR Green fluorescence rises above background, was recorded as a measure of initial template concentration. Relative fold changes in RNA levels were calculated using the $\Delta\Delta C_t$ method [257] with glyceraldehyde 3-phosphate dehydrogenase (*Gapdh*) used as a reference standard for normalization. Significance was determined using Mann-Whitney U-tests (SPSS Statistics). Primers sets for GAPDH, transient receptor potential cation channel vanilloid 1 (*Trpv1*), transient receptor potential cation channel ankyrin 1 (*Trpa1*), sodium voltage-gated channel 1.8 (*Na_v. 1.8*), potassium voltage-gated channel 4.3 (*K_v 4.3*), *Cgrp*, substance P (*SP*), and *Atf3* were designed using ABI software (Molecular Biology Insights, Cascade, CO) or found in PrimerBank (Massachusetts General Hospital, Boston, MA) [258] and are listed in **Table 2**.

Table 2. Murine primer sequences for qRT-PCR

Gene	Forward (5'→ 3')	Reverse (5'→ 3')
Artn	GGCCAACCCTAGCTGTTCT	TGGGTCCAGGGAAGCTT
Atf3	TGAGCCACTTTGTGCCAACA	TGTGCCCAGGGTTCTTCCT
Bdnf	CACTGGCTGACACTTTTGAGCAC	GCTGTGACCCACTCGCTAATACTG
Cgrp	TCAGCATCTTGCTCCTGTACCA	CTGGGCTGCTTTCCAAGATT
Gapdh	ATGTGTCCGTCGTGGATCTGA	ATGCCTGCTTCACCACCTTCTT
Gdnf	GCACCCCCGATTTTTGC	AGCTGCCAGCCCAGAGAATT
Gfrα1	GTGTGCAGATGCTGTGGACTAG	TTCAGTGCTTCACACGCACTTG
Gfrα2	TGACGGAGGGTGAGGAGTTCT	GAGAGGCGGGAGGTCACA
Gfrα3	CTTGGTGACTACGAGTTGGATGTC	AGATTCATTTTCCAGGGTTTGC
K_v4.3	TGAATCTTTCTGGTACACCATAGT	GCTAAAGTTGGAGACTATCACAGG
Na_v1.8	GCCACCCAGTTCATTGCCTTTTC	TCCCCAGATTCTCCCAAGACATTC
Ngf	ACACTCTGATCACTGCGTTTTTG	CCTTCTGGGACATTGCTATCTGT
Nrtn	TGAGGACGAGGTGTCCTTCCT	AGCTCTTGCAGCGTGTGGTA
SP	GCAAAGCACAGTGATGAAGAAGC	TGAAAGCAGAACCAGGGGTAGC
Trka	AGAGTGGCCTCCGCTTTGT	CGCATTGGAGGACAGATTCA
Trkb	CCGGCTTAAAGTTTGTGGCTTAC	GGATCAGGTCAGACAAAGTCAAG
Trpv1	TTCCTGCAGAAGAGCAAGAAGC	CCCATTGTGCAGATTGAGCAT
Trpa1	GCAGGTGGAACTTCATACCAACT	CACTTTGCGTAAGTACCAGAGTGG

2.7 BACK-LABELING OF PANCREATIC AFFERENTS

To examine changes in pancreatic sensory afferent phenotype in PDAC mice throughout tumor development (ages 6-8, 10-12, and >16 weeks), pancreas-specific sensory neurons were back-labeled with 1,1'-dioctadecyl-3,3,3'3'-tetramethylindocarbocyanine perchlorate (DiI), a fluorescent lipophilic indocarbocynanine dye.

2.7.1 Animal surgery

All surgical procedures were performed under aseptic conditions and aseptic technique was used throughout. Anesthesia was initiated by inhaled 4% isoflurane and maintained with inhaled 2% isoflurane. As previously described [210,211,256], a laparotomy was performed to expose the

pancreas/tumor, and multiple injections of a total volume of 5µl of DiI (2% suspension in sterile saline; Invitrogen, Life Technologies, Grand Island, NY) were made. After the injections, abdominal muscles and overlying skin were sutured separately and mice were allowed to recover for 8-10 days following the surgery.

2.8 PRIMARY DRG CELL CULTURE AND CALCIUM IMAGING

2.8.1 DRG cell culture

Acute primary DRG cell cultures were prepared for calcium (Ca^{2+}) imaging as previously described [147,148,215,259–261]. Animals were euthanized by an overdose of inhaled isoflurane and transcardially perfused with 4°C calcium-/magnesium- free Hank's balanced salt solution (HBSS; Gibco, Life Technologies, Grand Island, NY). Bilateral thoracic DRG 9-12 were rapidly dissected into ice cold HBSS and then incubated in 60U papain (Worthington, Lakewood, NJ) in a solution of cysteine (1mg/3ml HBSS) and saturated $NaHCO_3$ for 10 minutes at 37°C. The solution was removed and replaced with 3ml HBSS with 12mg collagenase Type II (Worthington, Lakewood, NJ) and 14mg dispase Type II (Roche Diagnostics, Indianapolis, IN) for 20 minutes at 37°C. The collagenase/dispase solution was removed and replaced with 1ml Advanced DMEM/F12 media (Gibco, Life Technologies, Grand Island, NY) plus 10% fetal bovine serum (FBS; Gibco, Life Technologies, Grand Island, NY) and 1% Penicillin/Streptomycin (Pen/Strep; Gibco, Life Technologies, Grand Island, NY). Cells were spun at 1500g for 30 seconds, the pellet was resuspended in 550µl of fresh media and resuspended cells plated on laminin/poly-lysine coated coverslips (BD Biosciences, Bedford,

MA). The coverslips were incubated for 2 hours at 37°C then fed with Advanced DMEM/F12 media. Calcium imaging was performed 2.5-6 hours after plating.

2.8.2 Calcium imaging

Cells were loaded with Ca^{2+} indicator by incubation for 30 minutes in normal bath solution (NBS; HBSS, 1.4mM $CaCl_2$, and 0.9mM $MgSO_4$) containing 5mg/ml bovine serum albumin (BSA) and 2µM of the acetoxymethyl ester of fura-2 (Invitrogen, Life Technologies, Grand Island, NY) at 37°C. Coverslips were placed on an Olympus upright microscope stage with NBS at 30°C flowing at 5ml/minute. Perfusion rate was controlled with a gravity flow system (Warner VC65; Warner Instruments, Hamden, CT) and perfusate temperature maintained with a heated stage and in-line heating system (Warner PH1, SHM-6, TC344b; Warner Instruments, Hamden, CT). Drugs were delivered with a rapid-switching local perfusion system.

Firmly attached DiI^+-neurons were identified and selected as regions of interest using HCImage software (Hamamatsu Corporation, Sewickley, PA). Fields were first tested with a brief application of 50mM KCl (High K^+) and Ca^{2+} transients measured to identify responsive neurons. Ca^{2+} transients were measured as the ratio of absorbance at 340nm to absorbance at 380nm ($\Delta F_{340/380}$; Lambda DG4, Sutter Instrument, Novato, CA; Retiga 1300, QImaging, Burnaby, BC, Canada) with $\Delta F_{340/380} > 0.20$ considered a response (easily distinguished from optical noise of $\Delta F_{340/380} < 0.02$). Cells that were not responsive to High K^+ were not included in further analyses. Ca^{2+} transients were measured in response to application of either 1µM capsaicin (Sigma-Aldrich, St. Louis, MO) diluted in NBS from a stock solution of 10mM capsaicin in 1-methyl-2-pyrrolidinone or 100µM mustard oil (Sigma-Aldrich, St. Louis, MO)

diluted in NBS from 100mM mustard oil dissolved in 1-methyl-2-pyrrolidinone. These doses were chosen based on previous studies done in our laboratory showing responses of $\Delta F_{340/380}$ > 0.10 from the maximal number of responding cells [147,148,210,215,260,261].

In the protocol for each coverslip, cells were first tested with a 7 second application of High K^+ and allowed to recover to baseline (typically 5 minutes). Then, cells were tested for responses to either a 9-10 second capsaicin (1µM) application or 18-20 second mustard oil application and allowed to return to baseline (typically 10 minutes). The number of capsaicin or mustard oil responsive cells was calculated as a percentage of healthy (High K^+- responsive) cells and compared between PDAC and control afferents at each time point (6-8 weeks, 10-12 weeks, >16 weeks) using Chi square tests (SPSS Statistics). Ca^{2+} peak percent response to High K^+ [(Peak $\Delta F_{340/380}$ – Baseline $\Delta F_{340/380}$)/ Baseline $\Delta F_{340/380}$] for all responsive cells ($\Delta F_{340/380}$ > 0.20) was compared between PDAC and control pancreatic afferents at each time point using a two-way ANOVA. Within age comparisons between PDAC and control mice were performed using the Bonferroni correction (Matlab, MathWorks).

2.9 PANCREAS RNA ISOLATION AND QRT-PCR

Changes in growth factor and growth factor receptor gene expression in the pancreas of PDAC mice at 3-4, 6-8, 10-12, and >16 weeks of age were assessed using quantitative real time RT-PCR. The pancreas/tumor from animals deeply anesthetized with 0.1-0.2cc ketamine/xylazine was removed, immediately homogenized in 2mL Trizol reagent (Invitrogen, Life Technologies, Grand Island, NY), and frozen on dry ice. RNA was extracted using 400µl chloroform, precipitated in 800µl isopropanol overnight at -80°C, washed twice with 75% EtOH, and

resuspended in 100-200µl RNase-free water (Invitrogen, Life Technologies, Grand Island, NY). RNA samples were further purified using RNeasy columns (Qiagen, Valencia, CA). RNA samples were treated with DNAse and 1µg was reverse-transcribed using Superscript II. SYBR Green-labeled PCR amplification using Absolute QPCR SYBR Green ROX mix was done as described in **2.6 DRG RNA ISOLATION AND QUANTITATIVE REVERSE TRANSCRIPTION-PCR (qRT-PCR).** Primer sets for nerve growth factor (*Ngf*), artemin (*Artn*), glial cell line- derived neurotrophic factor (*Gdnf*), brain-derived neurotrophic factor (*Bdnf*), neurturin (*Nrtn*), tropomyosin-related kinase, type 1 and type 2 (*Trka* and *Trkb*), and glycosylphosphatidylinositol-linked receptor α1, α2, and α3 (*Gfrα1*, *Gfrα2*, and *Gfrα3*) were designed using ABI software or found in PrimerBank and are listed in Table 2. Primer sets for 60S ribosomal protein L13A (*Rpl13a*) were from a mouse housekeeping genes primer set (MHK-1; RealTimePrimers.com, Elkins Park, PA) and *Rpl13a* expression was used as a reference standard for analysis of gene expression in the pancreas (**Table 3**). Relative fold changes in RNA level was calculated using the $\Delta\Delta C_t$ method[257]. Significance was determined using Mann-Whitney U-tests (SPSS Statistics). Additional potential normalization genes from MHK-1[β-actin (*Actb*), β2-microglobulin (*B2m*), β-glucuronidase (*Gusb*), hypoxanthine phosphoribosyl-transferase1 (*Hprt1*), phosphoglycerokinase (*Pgk*), and cyclophilinA (*Ppia*)] were screened as potential reference standards and expression of each was found to be significantly increased in the pancreas of PDAC mice as compared to controls. Primer sets for MHK-1 transcripts are listed in **Table 3**.

Table 3. Primer sequences for murine normalization genes for qRT-PCR

Gene	Forward (5'→ 3')	Reverse (5'→ 3')
Actb	AAGAGCTATGAGCTGCCTGA	TACGGATGTCAACGTCACAC
B2m	GGCCTGTATGCTATCCAGAA	GAAAGACCAGTCCTTGCTGA
Gusb	AATGAGCCTTCCTCTGCTCT	AACTGGCTATTCAGCTGTGG
Hprt1	GCTGACCTGCTGGATTACAT	TTGGGGCTGTACTGCTTAAC
Pgk	GCAGATTGTTTGGAATGGTC	TGCTCACATGGCTGACTTTA
Ppia	AGCTCTGAGCACTGGAGAGA	GCCAGGACCTGTATGCTTTA
Rpl13a	ATGACAAGAAAAAGCGGATG	CTTTTCTGCCTGTTTCCGTA

2.10 PANCREATIC CANCER CELL LINES

Transcriptional profiling of human tumor-derived cell lines (MiaPaCa2 and Panc1; ATCC, Manassas, VA) and murine tumor-derived cell lines (Kpc1 and Kpc2) was carried out. Murine cell lines were derived from tumors from two different PDAC mice (*p48-Cre*; *LSL-Kras*^{G12D}*; p53*$^{Lox/Lox}$*)*, dissociated in the laboratory of Dr. Herbert J. Zeh III, chief of the Division of Gastrointestinal Surgical Oncology, UPMC[262], and cultured in RPMI media (Gibco, Life Technologies, Grand Island, NY) with 10% FBS and 1% Pen/Strep. MiaPaCa2 cells were cultured in MEM (Gibco, Life Technologies, Grand Island, NY) with 10% FBS, 1% Pen/Strep, and 2.5% horse serum (HS; Gibco, Invitrogen, Grand Island, NY). Panc1 cells were cultured in MEM with 10% FBS and 1% Pen/Strep. Cell lines were grown to confluence on a 100mm plate and RNA was collected in 1mL of Trizol reagent, extracted with 200µl chloroform, precipitated in 800µl isopropanol, rinsed with 75% EtOH, and reconstituted in RNase-free water. 5 µg of RNA from each cell line was treated with DNAse and 1µg of DNAsed RNA was reverse-transcribed using Superscript II. PCR amplification of 40ng of cDNA was done using GoTaq DNA polymerase (Promega, Madison, WI) and samples were separated by gel electrophoresis on a 2% agarose gel with ethidium bromide (0.5µg/ml), in TAE buffer. Primer sets for mouse *Ngf*,

Artn, *Gdnf*, *Bdnf*, *Nrtn*, *Trka*, *Gfrα3*, *Gfrα1*, *Trkb*, *Gfrα2*, and *Gapdh* are list in **Table 2**. Primer sets for human *NGF*, *ARTN*, *GDNF*, *BDNF*, *NRTN*, *TRKA*, *GFRα3*, *GFRα1*, *TRKB*, *GFRα2*, and *GAPDH* were designed using ABI software or found in PrimerBank and are listed in **Table 4**.

Table 4. Human primer sequences for RT-PCR

Gene	Forward (5'→ 3')	Reverse (5'→ 3')
ARTN	GCACCCCCATCTGCTCTTCC	CAGGCTGAGGTCGTGTGGAG
BDNF	TCCACCAGGTGAGAAGAGTGATG	TCACGCTCTCCAGAGTCCCATG
GAPDH	TGACAACTTTGGTATCGTGGAAGG	AGGCAGGGATGATGTTCTGGAG
GDNF	GGCAGTGCTTCCTAGAAGAGA	AAGACACAACCCCGGTTTTTG
GFRα1	CCAAAGGGAACAACTGCCTG	CGGTTGCAGACATCGTTGGA
GFRα2	CCAGCGAGTACACCTACCG	TCCTTGTCCTCATAGGAGCAG
GFRα3	GCCTGCTTGGACATCTATTGGA	CAGCCGGTCACACTTGTCAT
NGF	GGCAGACCCGCAACATTACT	CACCACCGACCTCGAAGTC
NRTN	CTCCGTGCTGTCCATCTG	CAGCTCCATCGCATCCG
TRKA	GTCAGCCACGGTGATGAAATC	CAGCACGTCACGTTCTTCCT
TRKB	ACCCGAAACAAACTGACGAGT	AGCATGTAAATGGATTGCCCA

3.0 RESULTS

3.1 DISEASE PROGRESSION

3.1.1 Observed course of illness

Neuroplastic changes associated with PDAC were studied using genetically engineered PDAC mice that express a conditional mutant *Kras* allele and a *Trp53* allele with *LoxP* sites under control of a pancreas-specific promoter (*Ptf1a-p48)* driving *Cre* (*p48-Cre*). In order to visualize pancreas-derived cells throughout the body, PDAC mice were crossed with a tdTomato reporter strain (*Gt(ROSA)26Sor*^{tdTomato}) to produce tPDAC mice. Beginning at postnatal day 28, all mice were weighed weekly to monitor for illness-related weight loss. However, no significant difference in weight between cancer mice and age- and sex-matched littermates was detected (**Figure 1**).

Along with weekly weight measurement, cancer mice were screened for the development of cancer-related sequelae such as abdominal distention due to ascites or jaundice secondary to biliary tree obstruction. Although age provided an approximation of disease progression in PDAC and tPDAC mice, significant variability in tumor size, tumor location, and sickness severity was observed, particularly in animals greater than 16 (> 16) weeks of age. Disease progression and sickness severity was therefore assessed using a hunching scale adapted from a

previous study of pancreatic acinar carcinoma in the mouse [223,224] described in **2.2 SICKNESS AND HUNCHING ASSESSMENT**. Animals were scored weekly starting at post-natal day 28 and the average age that a hunching score of 1 was first detected in PDAC mice was 10 weeks, which correlated with a PanIN-only stage of tumor development. A hunching score of 2 or 3 correlated with significant sickness and was detected as early as 19 weeks and as late as 26 weeks, at which point animals had significant tumor burden. A hunching score of 4 correlated with terminal disease and animals were euthanized.

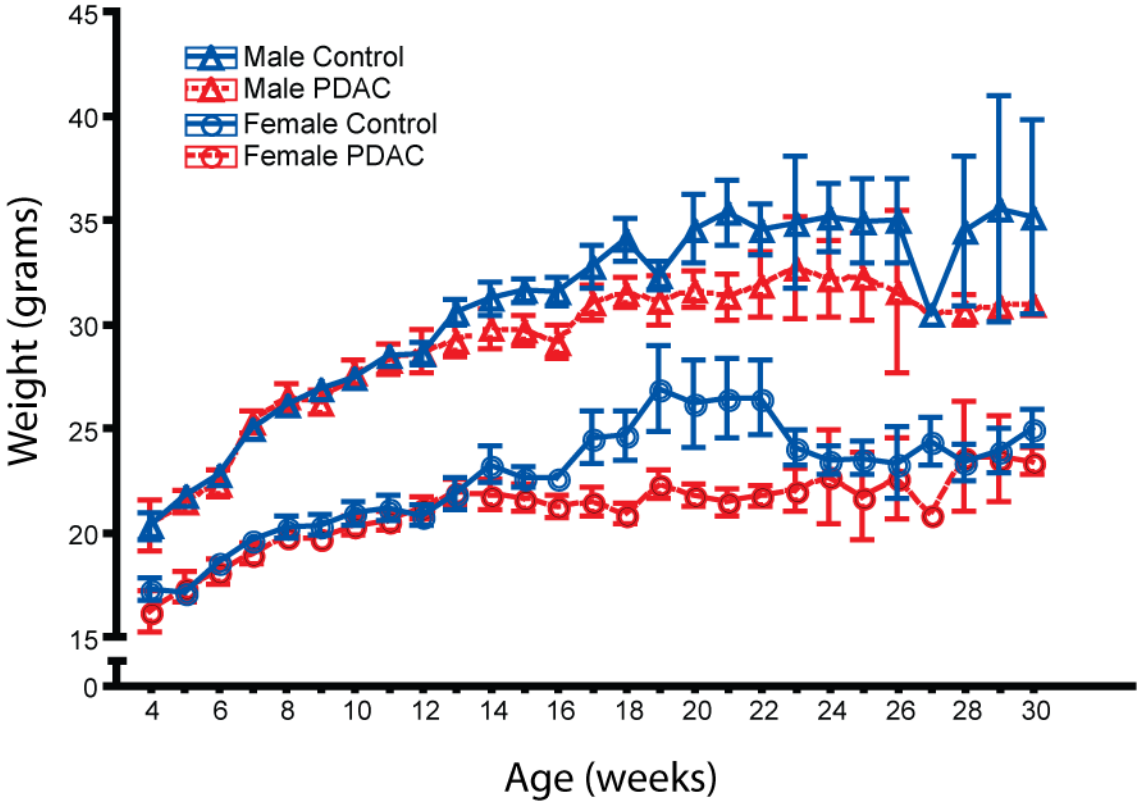

Figure 1. Weight gain in male and female PDAC and control mice

Weight increased in all groups with age and no significant difference in weight gain was observed between PDAC mice and age- and sex-matched littermate controls. The number of mice for each group ranged from 1 to 36 depending on age. Error bars represent SEM.

3.1.2 Gross anatomical changes

Although mutations in *Kras* and *Trp53* are present at birth in PDAC mice (including tPDAC mice), pancreata of PDAC and tPDAC mice at 3-4 and 6-8 weeks of age appeared grossly normal when resected for histological and RNA studies. At 10-12 weeks of age, the pancreas of some PDAC and tPDAC mice had a nodular appearance not evident in age-matched control mice (not shown). While disease course was variable among PDAC and tPDAC mice, large nodular tumors were observed in most mice by 16 weeks (**Figure 2**). The time to tumor development observed in our studies is consistent with prior reports using related mouse strains[89,117,254]. At later time points in disease progression (typically >20 weeks), local tumor spread to retroperitoneal structures, encasement or invasion of adjacent organs such as the duodenum, tumor invasion throughout peritoneum, and distant metastases to the liver and occasionally the lungs were grossly visible (**Figure 2B**). In many PDAC mice, dilatation of the common bile duct and/or gall bladder enlargement was evident, likely a result of tumor-related biliary tree obstruction (not shown).

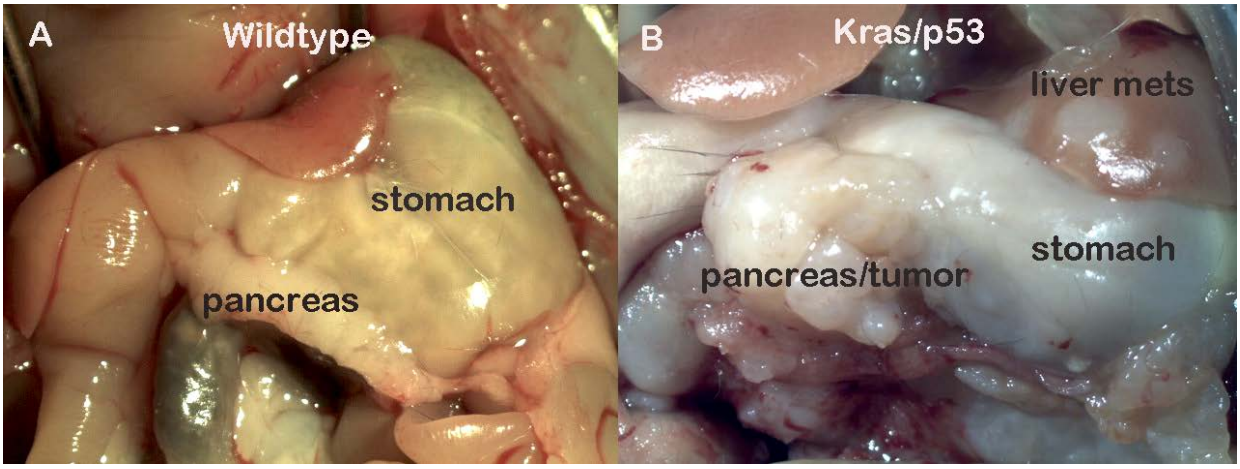

Figure 2. In situ appearance of advanced PDAC

The pancreas is located just below the stomach and first segment of the duodenum in control mice (A). A large, nodular, and fibrotic tumor is adherent to the stomach and duodenum and extends throughout the peritoneum in a 26.5 week-old PDAC mouse with advanced disease. Metastases to the liver (labeled liver mets) are grossly visible (B).

3.1.3 Histological changes associated with disease progression

At the time of weaning at postnatal day 21, the pancreas of PDAC mice appears histologically normal (**Figure 3A**). Pre-malignant pancreatic intraepithelial neoplasia (PanIN) lesions (typically scored as PanIN-1a or -1b), focal fibrosis, and occasionally acute pancreatitis are present in the pancreas of 6-8 week old PDAC mice (**Figure 3B**). By 10-12 weeks of age, multifocal PanIN lesions ranging from PanIN-1A to -3, more extensive focal fibrosis, chronic inflammation, and regions of pancreas with histological changes resembling descriptions of lobular atrophy in human PDAC tissue [77] are evident (**Figure 3C**). Typically, pancreatic ductal adenocarcinoma was histologically evident in the pancreas of PDAC mice by 16 weeks of age and a significant desmoplastic component of the tumor with was observed in many cases of advanced disease (**Figure 3D**). Chronic inflammation and extinction of the background pancreas was also observed in PDAC mice with advanced disease. Because the conditional mutant alleles are expressed in every cell of pancreatic origin, PDAC mice often displayed multifocal pancreatic disease. Therefore, PDAC mice had multiple regions of PanIN lesions at pre-malignant time points (6-8 and 10-12 weeks) and regions of both cancer and PanIN at later time points (>16 weeks). The presence of multifocal disease in this model likely contributed to the variability in disease course and survival time observed in PDAC and tPDAC mice.

In tPDAC mice, all cells of pancreatic origin are tdTomato$^+$ (**Figure 4**). As regions of fibrosis and acinar atrophy develop (6-8 weeks) and expand (10-12 and >16 weeks), regions of pancreas parenchyma are replaced with tdTomato negative stroma (**Figure 4B-D**). Metastatic tumor cells, also of pancreatic origin, in the liver and lung are also tdTomato$^+$ (**Figure 5**).

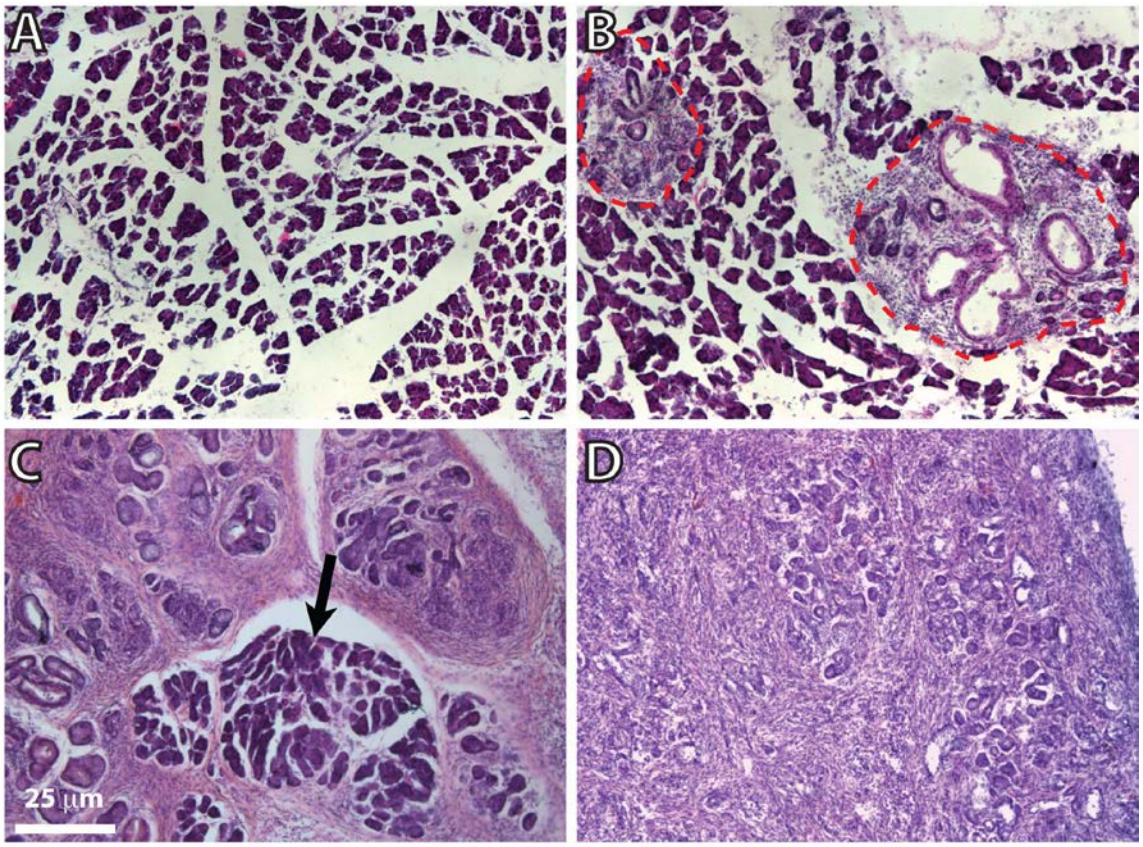

Figure 3. Histological changes in the pancreas of PDAC mice

Representative H&E stained sections of pancreas from PDAC mice demonstrate the progression from PanIN lesions and fibrosis to PDAC. The pancreas of PDAC mice appears histologically normal at 3-4 weeks of age (A). By 6-8 weeks of age, focal fibrosis and mild PanIN lesions (outlined by red dashed lines) are evident (B). Regions of healthy pancreas (arrow) are surrounded by extensive lobular fibrosis and multifocal PanIN lesions in PDAC mice at 10-12 weeks of age (C). Ductal adenocarcinoma with a large desmoplastic component is histologically evident in the pancreas of PDAC mice >16 weeks of age (D).

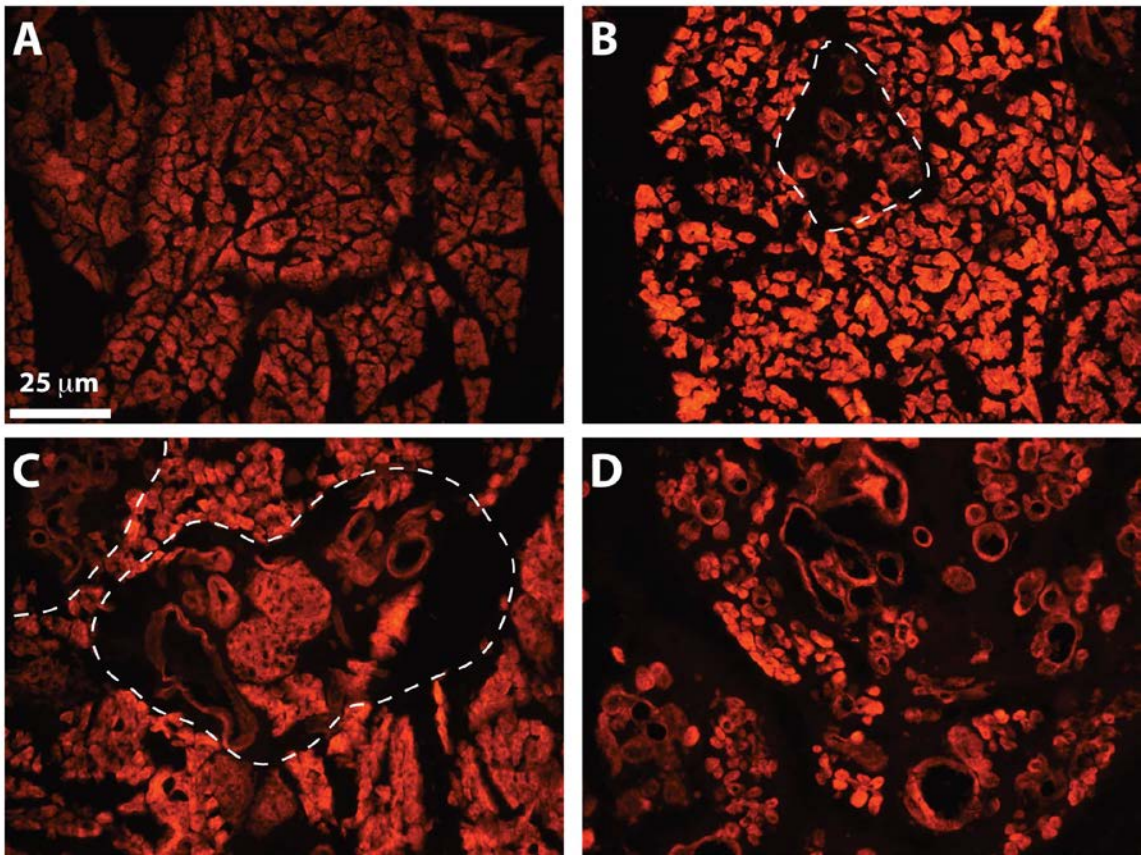

Figure 4. Changes in tdTomato expression in the pancreas of tPDAC mice

All cells of pancreatic origin express the red fluorescent protein tdTomato in tPDAC mice. However, regions of focal fibrosis (outlined by white dashed lines in B) that develop starting at 6-8 weeks of age (B) and expand into regions of lobular atrophy and fibrosis (outlined by white dashed lines in C) by 10-12 weeks of age (C) are tdTomato-negative. This leads to the progressive extinction of tdTomato fluorescence as background pancreas is replaced by desmoplastic reaction in tPDAC mice with advanced disease (D).

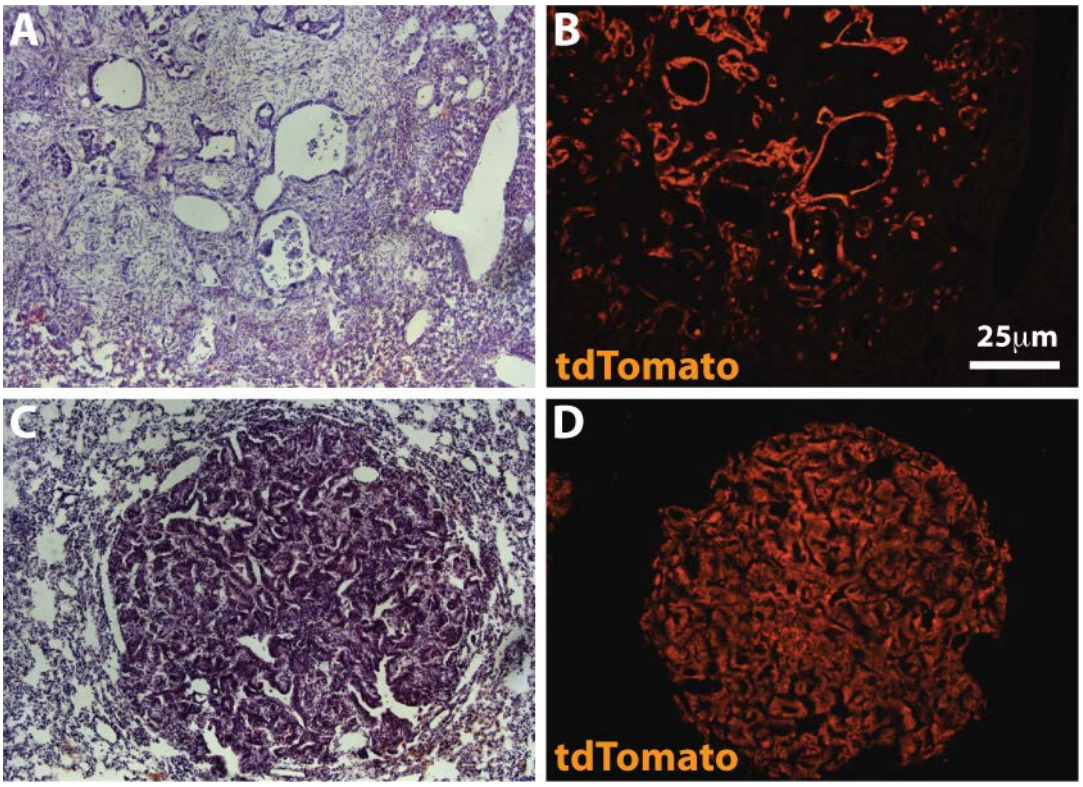

Figure 5. Metastatic disease in the liver and lung of tPDAC mice

H&E stained sections of liver (A) and lung (C) demonstrate the appearance of distance metastases present in some PDAC mice with advanced disease (>16 weeks of age). Metastatic tumor cells of pancreatic origin express tdTomato in the liver (B) and lung (D).

3.2 PAIN-RELATED BEHAVIOR

3.2.1 Decreased open-field exploratory activity

To assess the effects of PDAC-related pain on mouse behavior, we analyzed open-field exploratory activity throughout disease progression (7-31 weeks of age) using photoelectric monitoring. The change in horizontal movement along the floor of the behavior arena over time was not significantly different between PDAC and control mice (**Figures 6-9**). Measurements of horizontal movement included velocity of movement (Velocity; **Figure 6**), time spent moving (Move Time; **Figure 7**), distance travelled (Distance; **Figure 8**), and total number of movements (Moves; **Figure 9**). These behavior measurements were relatively consistent across animal age for both PDAC and control mice. In contrast, the change in vertical movement in which the animals are extending or rearing upward was significantly different between PDAC and control mice, with activity decreasing over time for many PDAC mice but not controls (**Figures 10-13**). Measurements of vertical movement included the number of vertical extensions (Extensions, p= 0.0014; **Figure 10**), the amount of time spent extending vertically (Time, p= 0.0006; **Figure 11**), distance travelled while extending vertically (Distance, 0.0099; **Figure 12**), and the number of movements made while extending vertically (Moves, p= 0.0311; **Figure 13**). Measurements of vertical movement include postural movements like rearing, but also included more subtle movements in which the mouse dorsiflexed its neck. One aspect that these vertical measurements have in common is elongation of the trunk, a movement that conflicts with the progressively hunched postures adopted by these animals as the disease progresses and with the pain-related hunching described in a mouse model of pancreatic acinar carcinoma [223,224].

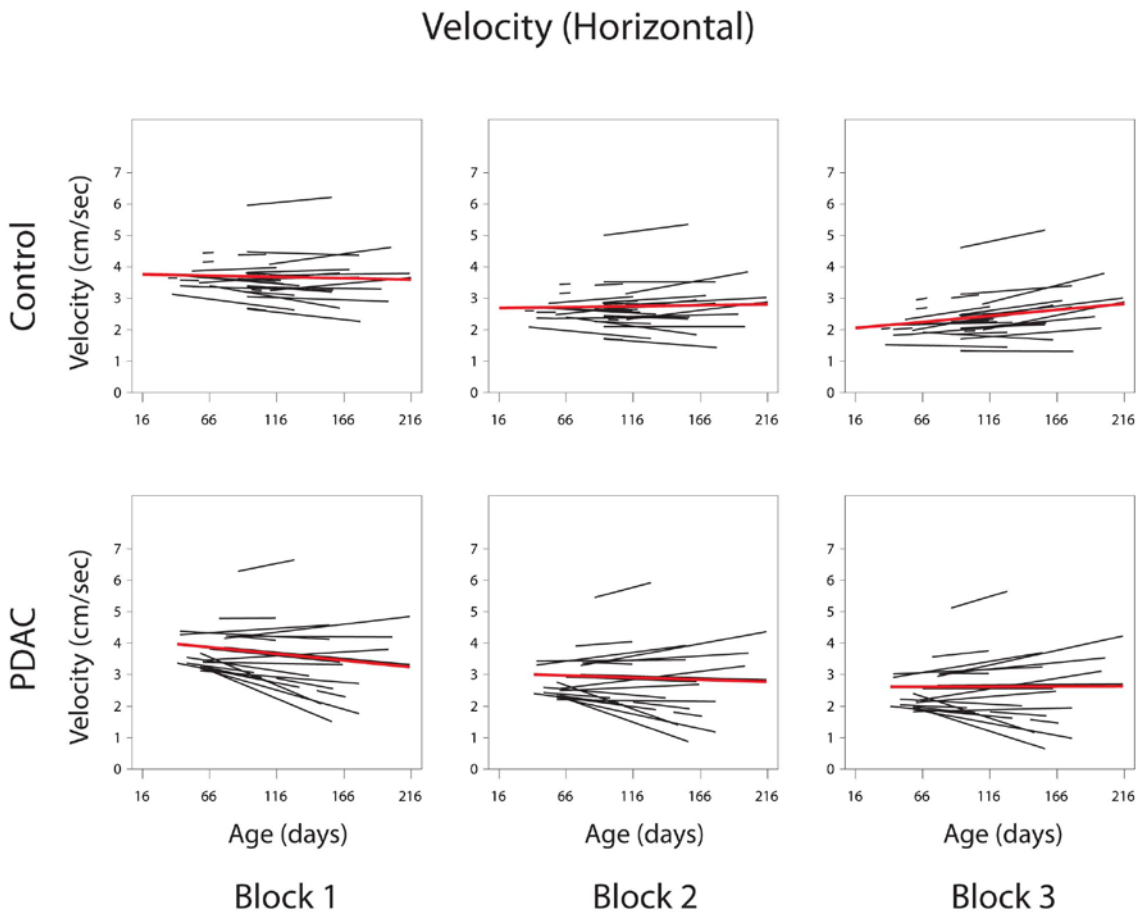

Figure 6. Velocity of horizontal movement by PDAC and control mice over time

The velocity of horizontal movements along the floor of the open-field testing arena was measured in PDAC and control mice over time. Data from the 15-minute testing period were divided into three 5-minute blocks (Blocks 1-3). Black lines represent the change in activity for individual animals over time and red lines represent the mean change in activity over time for the group. The change in behavior over time was relatively consistent across Blocks 1-3 and no significant difference in the change in velocity of horizontal movements over time was found between PDAC and control mice. Control n= 80, PDAC n= 66.

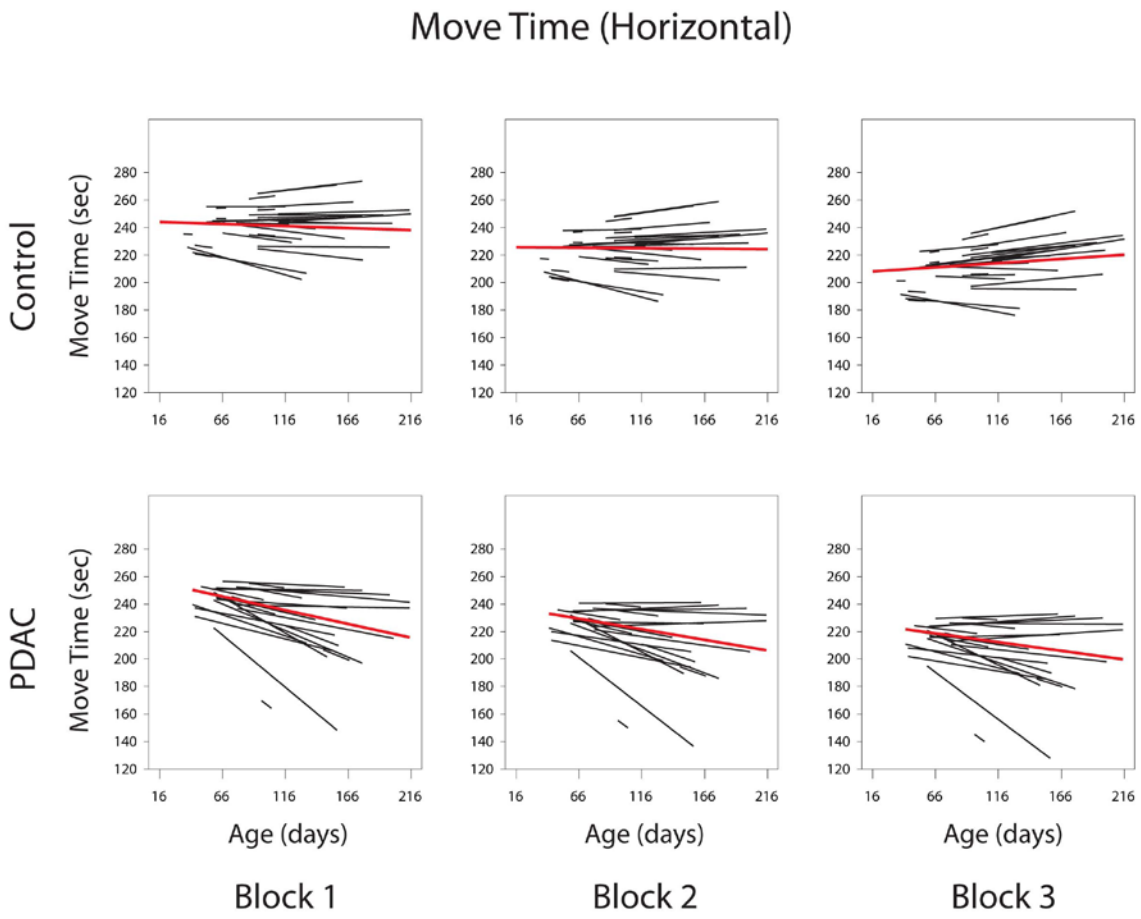

Figure 7. Time spent moving horizontally by PDAC and control mice over time

The time spent moving horizontally along the floor of the open-field testing arena was measured in PDAC and control mice over time. Data from the 15-minute testing period were divided into three 5-minute blocks (Blocks 1-3). Black lines represent the change in activity for individual animals over time and red lines represent the mean change in activity over time for the group. The change in behavior over time was relatively consistent across Blocks 1-3 and no significant difference in the change in time spent moving horizontally over time was found between PDAC and control mice. Control n= 80, PDAC n= 66.

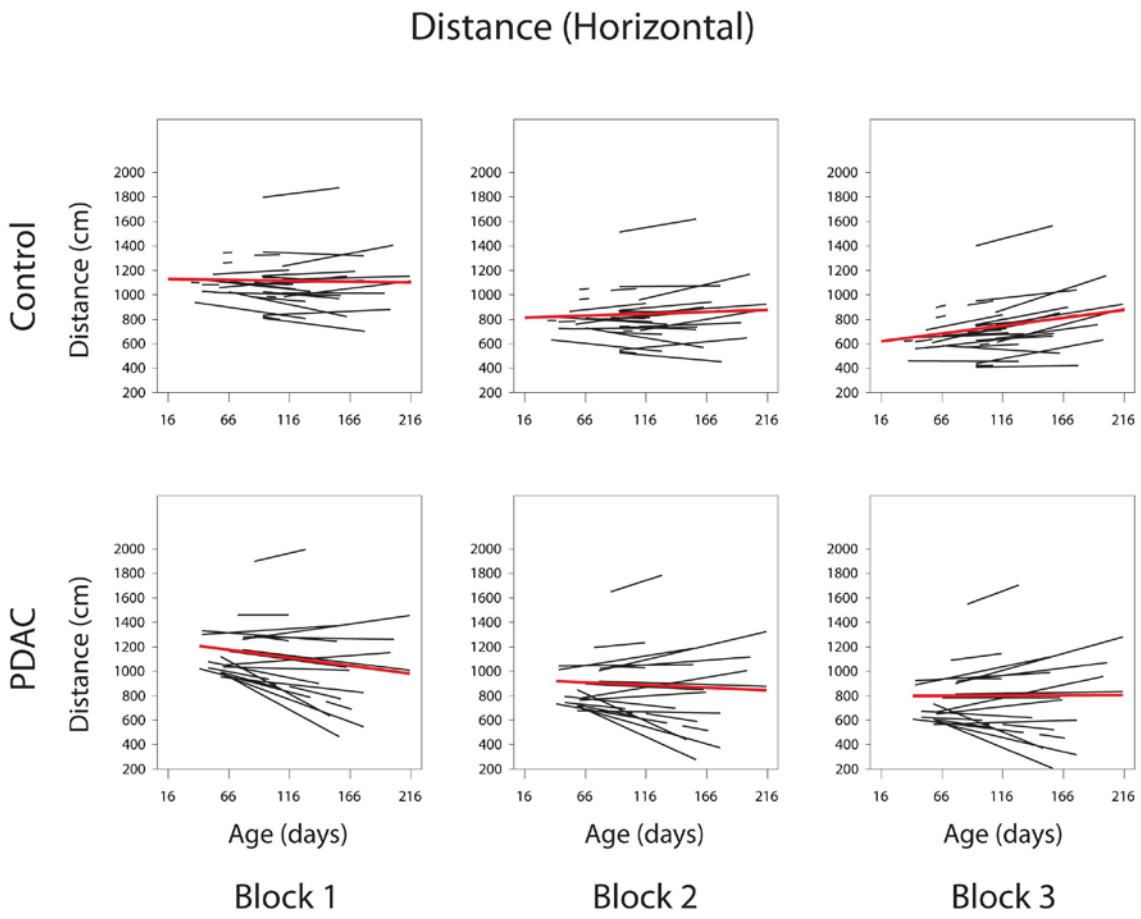

Figure 8. Distance travelled horizontally by PDAC and control mice over time

The distance travelled horizontally along the floor of the open-field testing arena was measured in PDAC and control mice over time. Data from the 15-minute testing period were divided into three 5-minute blocks (Blocks 1-3). Black lines represent the change in activity for individual animals over time and red lines represent the mean change in activity over time for the group. The change in behavior over time was relatively consistent across Blocks 1-3 and no significant difference in the change in distance travelled horizontally over time was found between PDAC and control mice. Control n= 80, PDAC n= 66.

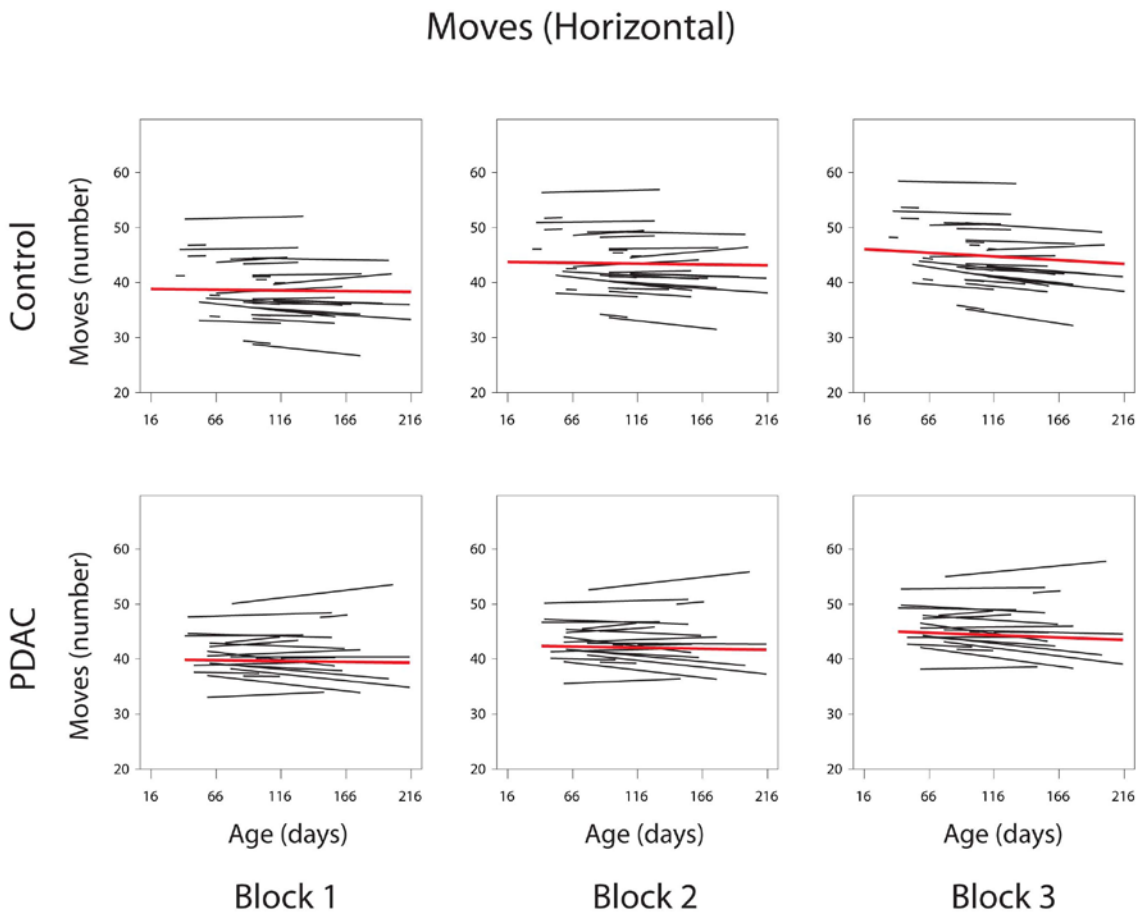

Figure 9. The number of horizontal movements by PDAC and control mice over time

The total number of horizontal movements along the floor of the open-field testing arena was measured in PDAC and control mice over time. Data from the 15-minute testing period were divided into three 5-minute blocks (Blocks 1-3). Black lines represent the change in activity for individual animals over time and red lines represent the mean change in activity over time for the group. The change in behavior over time was relatively consistent across Blocks 1-3 and no significant difference in the change in the number of horizontal movements over time was found between PDAC and control mice. Control n= 80, PDAC n= 66.

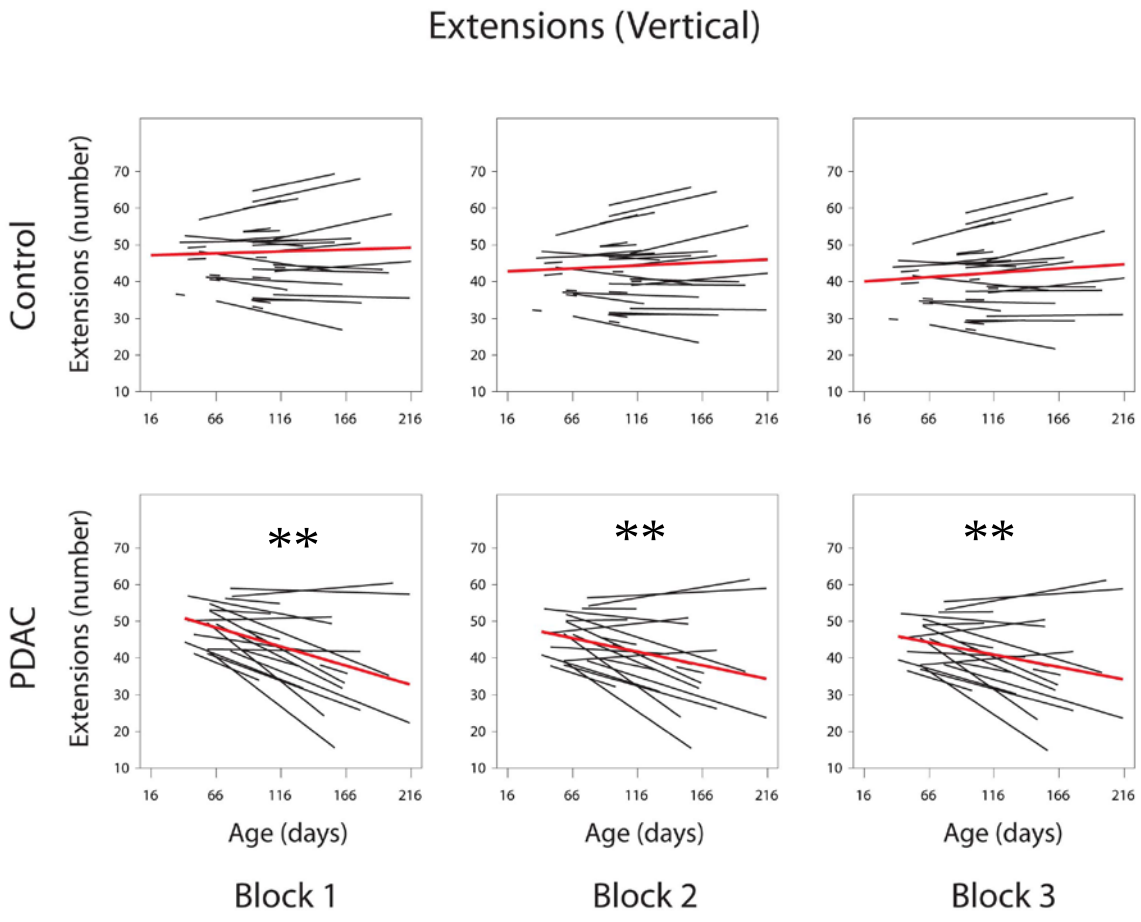

Figure 10. The number of vertical extensions made by PDAC mice decreases over time

The number of vertical extensions made was measured in PDAC and control mice over time. Data from the 15-minute testing period were divided into three 5-minute blocks (Blocks 1-3). Black lines represent the change in activity for individual animals over time and red lines represent the mean change in activity over time for the group. The change in behavior over time was relatively consistent across Blocks 1-3. There was a significant difference in the change in number of vertical extension made over time between PDAC and control mice. ** $p < 0.01$. Control n= 80, PDAC n= 66.

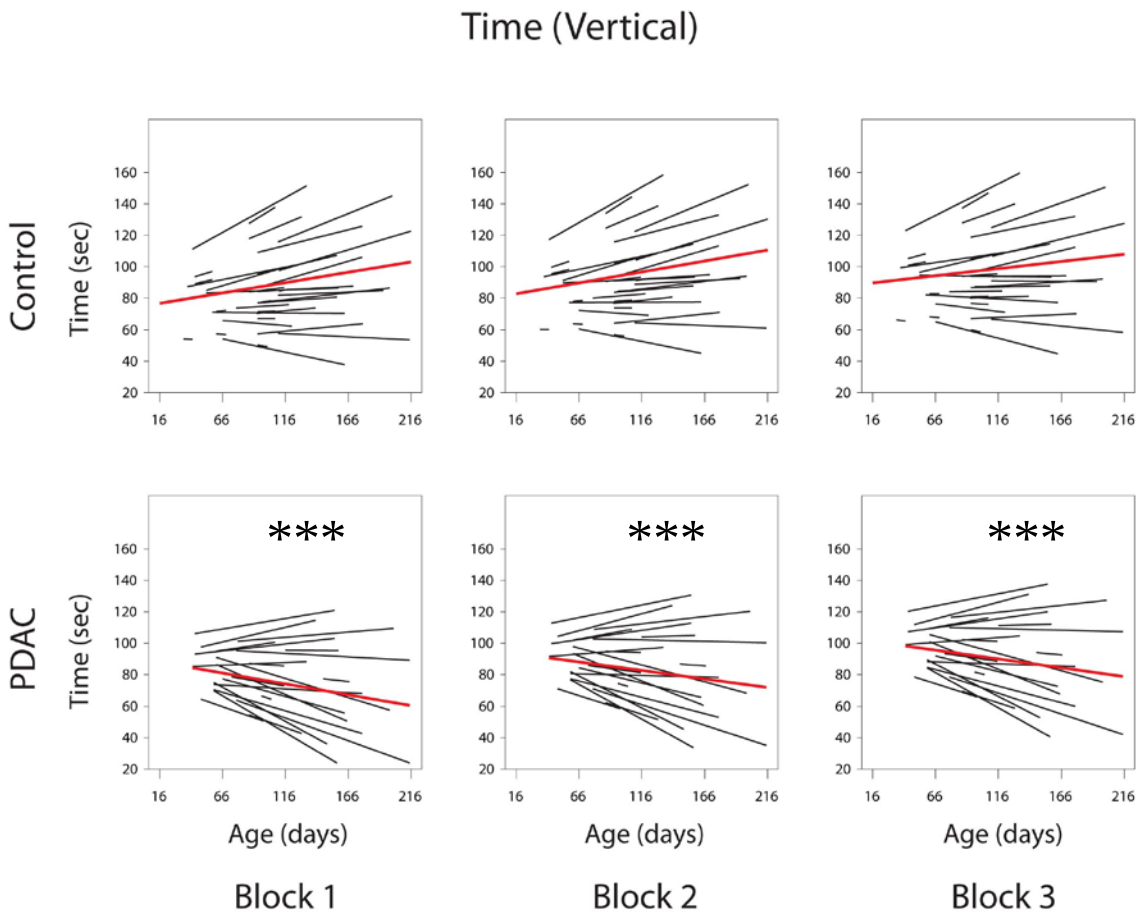

Figure 11. Time spent extending vertically decreases over time in PDAC mice

The amount of time spent extending vertically was measured in PDAC and control mice over time. Data from the 15-minute testing period were divided into three 5-minute blocks (Blocks 1-3). Black lines represent the change in activity for individual animals over time and red lines represent the mean change in activity over time for the group. The change in behavior over time was relatively consistent across Blocks 1-3. There was a significant difference in the change in the amount of time spent extending vertically over time between PDAC and control mice.

*** $p < 0.001$. Control n= 80, PDAC n= 66.

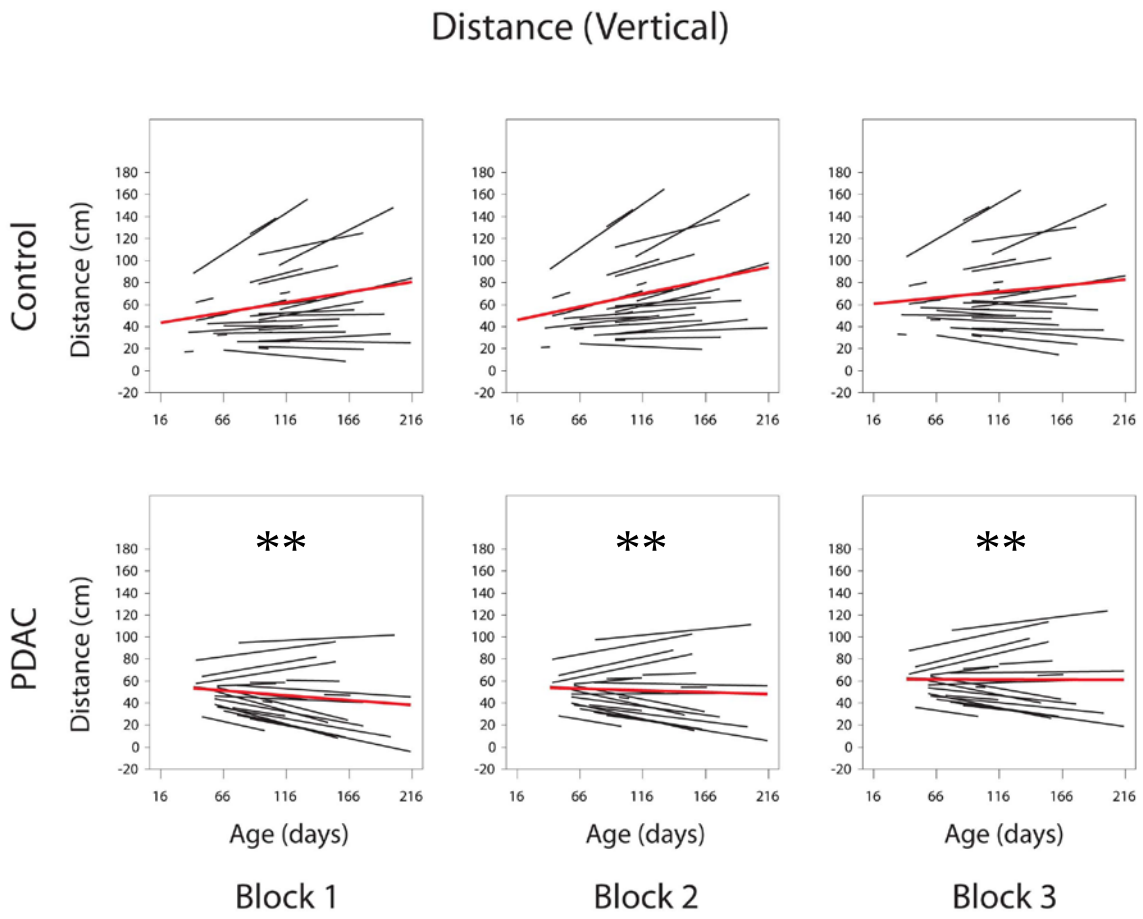

Figure 12. Distance travelled while extending vertically decreases over time in PDAC mice

The distance travelled while extending vertically was measured in PDAC and control mice over time. Data from the 15-minute testing period were divided into three 5-minute blocks (Blocks 1-3). Black lines represent the change in activity for individual animals over time and red lines represent the mean change in activity over time for the group. The change in behavior over time was relatively consistent across Blocks 1-3. There was a significant difference in the change in distance travelled while extending vertically over time between PDAC and control mice.

** $p < 0.01$. Control n= 80, PDAC n= 66.

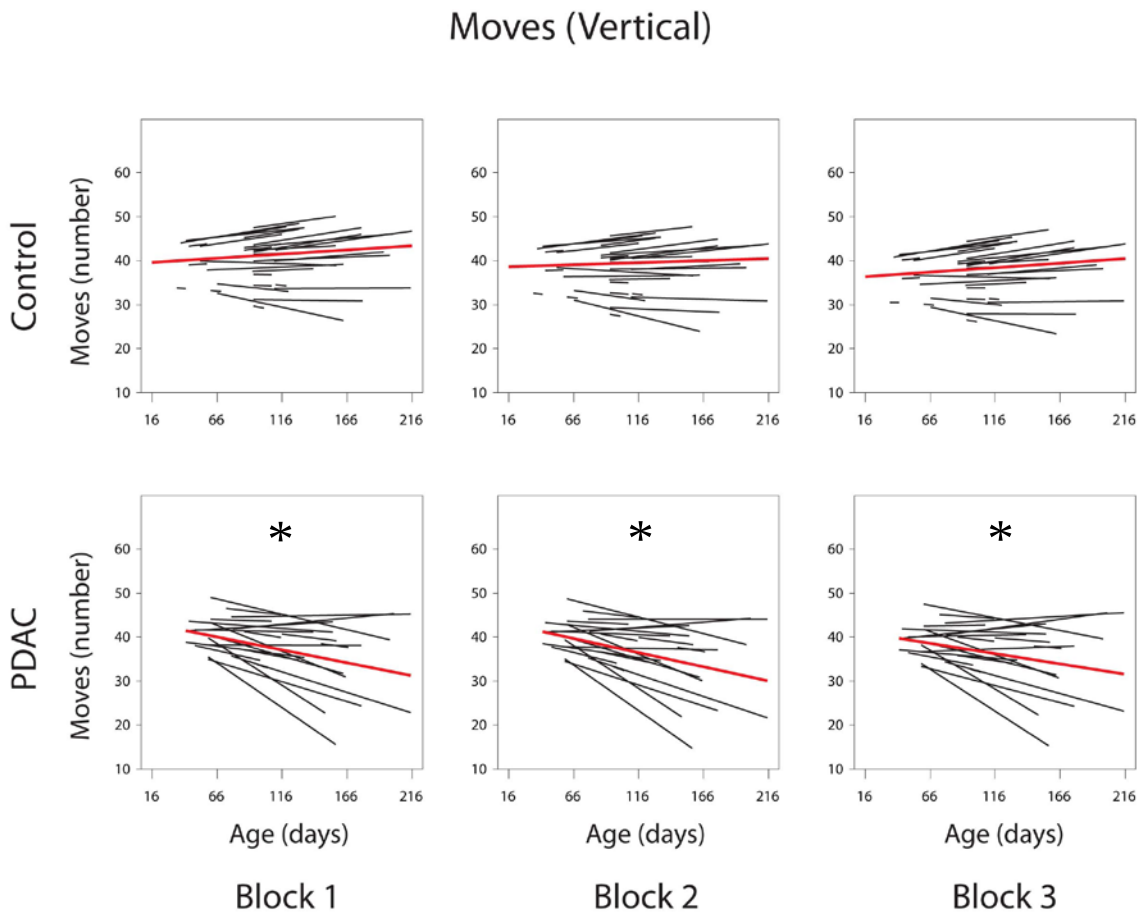

Figure 13. The number of movements made while extending vertically decreases over time in PDAC mice

The number of movements made while extending vertically was measured in PDAC and control mice over time. Data from the 15-minute testing period were divided into three 5-minute blocks (Blocks 1-3). Black lines represent the change in activity for individual animals over time and red lines represent the mean change in activity over time for the group. The change in behavior over time was relatively consistent across Blocks 1-3. There was a significant difference in the change in number of movements made while extending vertically over time between PDAC and control mice. *$p < 0.05$. Control n= 80, PDAC n= 66.

Behavior data were also binned into discreet age ranges corresponding to time points in disease progression (6-8 weeks, 10-12 weeks, and >16 weeks), however there was no significant effect of age or genotype nor was there a significant interaction for any of the horizontal movement measurements (**Table 5**) or vertical movement measurements (**Table 6**). When the data were filtered into discreet age ranges, the number of mice included in the analyses for each group was relatively small and may have made detection of significant effects difficult. Additionally, substantial variability in PDAC mouse behavior over time was observed in measurements of horizontal and vertical movements. This variability was most pronounced after 16 weeks of age and is likely related to the variable disease course observed in PDAC mice with cancer.

Table 5. Horizontal open-field exploratory activity in PDAC and control mice

Horizontal Behavior Measurements			
	6-8 weeks	**10-12 weeks**	**>16 weeks**
Velocity (cm/sec)	Control 2.66 ± 0.45 PDAC 2.68 ± 0.61	2.66 ± 1.26 3.22 ± 0.71	2.76 ± 0.71 3.00 ± 1.23
Move Time (sec)	220.56 ± 17.84 214.60 ± 17.16	227.11 ± 19.81 234.00 ± 18.90	229.38 ± 18.98 217.59 ± 39.17
Distance (cm)	813.30 ± 140.45 818.00 ± 176.86	814.96 ± 374.51 984.70 ± 215.29	844.31 ± 210.99 916.45 ± 367.54
Moves (number)	47.88 ± 9.31 48.20 ± 7.60	44.33 ± 8.85 40.14 ± 8.32	42.47 ± 8.69 43.48 ± 11.43

Measurements of horizontal open-field exploratory activity in PDAC (red) and control (blue) mice were analyzed at three different time points corresponding to stages of disease progression: 6-8 weeks, early PanIN stage; 10-12 weeks, moderate to severe PanIN stage; >16 weeks, PDAC stage. There were no significant differences between PDAC and control mice at any age. Data from the 15-minute testing period were divided into three 5-minutes blocks and data from Block 2 (mean ± standard deviation) are presented as representative. Control n= 16 (6-8 weeks), n= 9 (10-12 weeks), and n= 55 (>16 weeks). PDAC n= 5 (6-8 weeks), n= 7 (10-12 weeks), and n= 54 (>16 weeks).

Table 6. Vertical open-field exploratory activity in PDAC and control mice

Vertical Behavior Measurements				
		6-8 weeks	10-12 weeks	>16 weeks
Extensions (number)	Control	43.69 ± 12.41	48.78 ± 10.21	42.93 ± 13.28
	PDAC	42.40 ± 9.71	46.57 ± 8.30	42.39 ± 18.01
Time (sec)		94.75 ± 24.90	91.33 ± 16.87	96.62 ± 38.42
		89.80 ± 24.45	77.57 ± 13.60	87.48 ± 41.60
Distance (cm)		58.54 ± 22.16	40.12 ± 18.19	73.58 ± 69.91
		48.06 ± 19.61	36.20 ± 18.53	55.89 ± 45.12
Moves (number)		39.94 ± 7.06	44.22 ± 5.19	37.85 ± 8.82
		38.00 ± 6.74	40.57 ± 7.63	36.04 ± 12.80

Measurements of vertical open-field exploratory activity in PDAC (red) and control (blue) mice were analyzed at three different time points corresponding to stages of disease progression: 6-8 weeks, early PanIN stage; 10-12 weeks, moderate to severe PanIN stage; >16 weeks, PDAC stage. There were no significant differences between PDAC and control mice at any age. Data from the 15-minute testing period were divided into three 5-minutes blocks and data from Block 2 (mean ± standard deviation) are presented as representative. Control n= 16 (6-8 weeks), n= 9 (10-12 weeks), and n= 55 (>16 weeks). PDAC n= 5 (6-8 weeks), n= 7 (10-12 weeks), and n= 54 (>16 weeks).

3.2.2 Endogenous opioids in pain-related behavior

Open-field exploratory activity, specifically when involving movements that require reaching vertically, decreases with age in PDAC mice. We hypothesized that this change in behavior was reflective of PDAC-associated pain. A previous study of cancer pain in a mouse model of pancreatic acinar carcinoma demonstrated that mice with cancer treated with naloxone exhibited more pain-related behavior than mice treated with saline[224], suggesting that endogenous opioid signaling attenuates early cancer-related pain. To determine if a similar opioid-based mechanism occurs in PDAC mice, we tested whether blocking endogenous opioid signaling with naloxone treatment 30 minutes before behavior monitoring "un-masked" pain-related behavior in these mice. Mice were 17-31 weeks of age and PDAC mice had hunching scores of 1 or 2 at the time of testing. While open-field exploratory activity decreased substantially in some mice treated with naloxone (**Figures 14** and **15**), there was no significant difference between PDAC and control groups in the number of mice that demonstrated decreased activity for any of the behavior measurements. Neither age nor sex was significantly correlated with decreased exploratory activity following naloxone administration (data not shown). Percent change in behavior from baseline following naloxone administration was compared between PDAC and control mice, however no significant differences were observed in horizontal movement measurements (**Table 7**) or vertical movement measurements (**Table 8**).

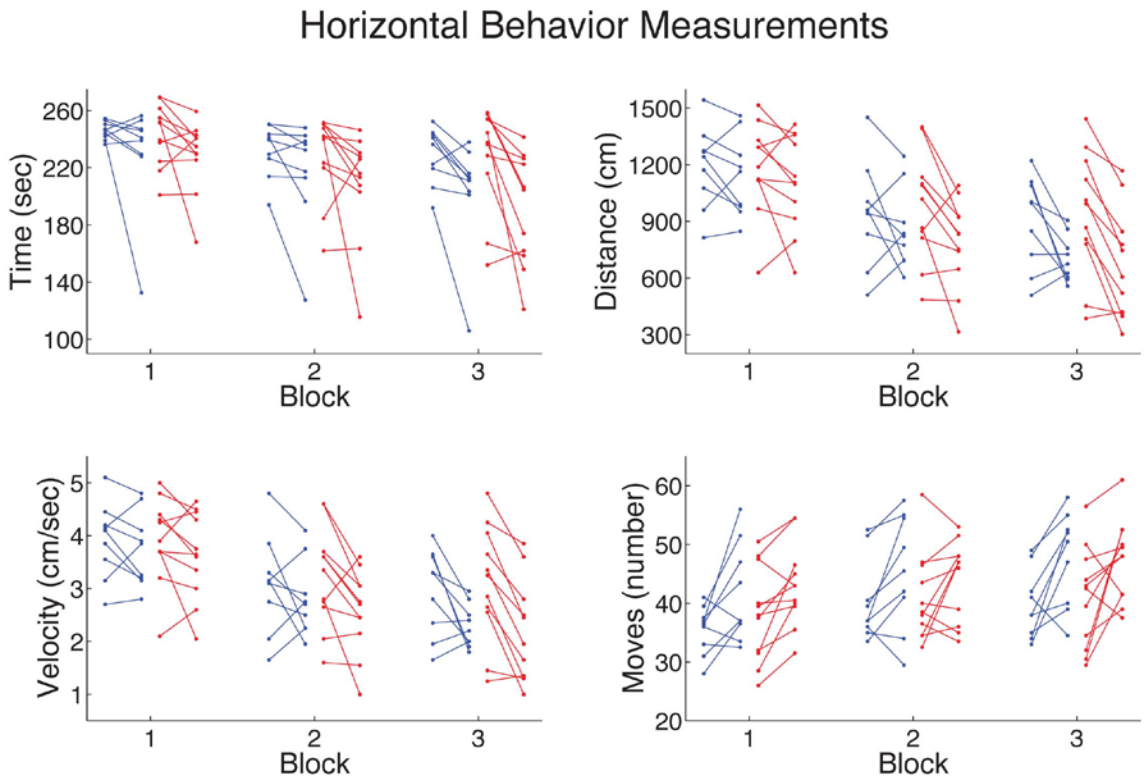

Figure 14. Effects of naloxone on horizontal open-field exploratory activity in PDAC and control mice

Horizontal open-field exploratory activity was measured at baseline, 23.5 hours later 4mg/kg naloxone was administered subcutaneously, and horizontal open-field exploratory activity was measured 30 minutes later (24 hours after baseline measurements were collected). Data from the two 15-minute testing periods were divided into three 5-minutes blocks, and change in behavior from baseline following naloxone treatment was relatively constant across time block. There was significant variability in post-naloxone behavior among control (blue) and PDAC (red) mice, however, there was no significant difference between the two groups in the number of mice demonstrating decreased horizontal behavior following naloxone treatment.

Control n= 9, PDAC n= 10

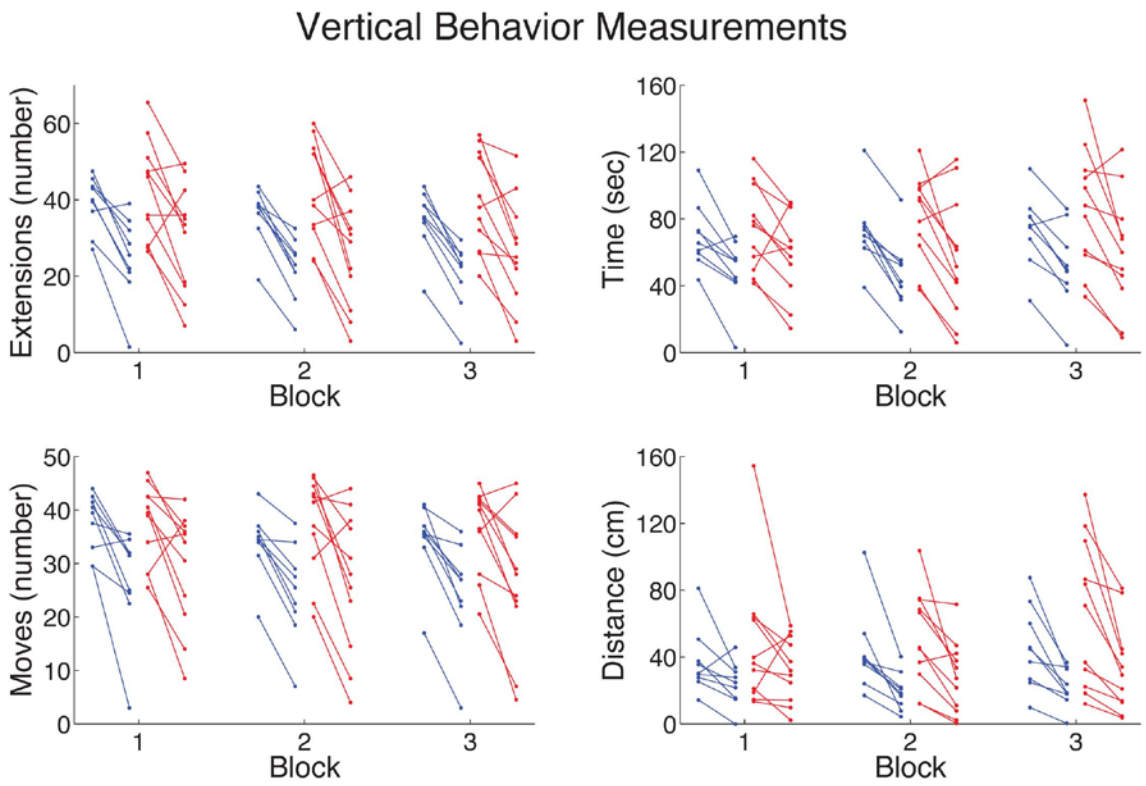

Figure 15. Effects of naloxone on vertical open-field exploratory activity in PDAC and control mice

Vertical open-field exploratory activity was measured at baseline, 23.5 hours later 4mg/kg naloxone was administered subcutaneously, and horizontal open-field exploratory activity was measured 30 minutes later (24 hours after baseline measurements were collected). Data from the two 15-minute testing periods were divided into three 5-minutes blocks, and change in behavior from baseline following naloxone treatment was relatively constant across time block. There was significant variability in post-naloxone behavior among control (blue) and PDAC (red) mice, however, there was no significant difference between the two groups in the number of mice demonstrating decreased vertical behavior following naloxone treatment.

Control n= 9, PDAC n= 10.

Table 7. Percent change in horizontal open-field exploratory activity after naloxone treatment

Horizontal Behavior Measurements				
		Block 1	**Block 2**	**Block 3**
Velocity (cm/sec)	Control	-3.39% ± 14.08	-4.27% ± 28.58	-17.24% ± 25.39
	PDAC	-5.92% ± 18.50	-17.36% ± 24.16	-28.85% ± 20.47
Move Time (sec)		-6.45% ± 14.92	-7.02% ± 11.96	-11.37% ± 14.23
		-5.50% ± 11.20	-8.00% ± 17.70	-15.39% ± 16.34
Distance (cm)		-3.28% ± 13.75	-3.71% ± 28.04	-16.18% ± 25.21
		-5.29% ± 18.69	-17.27% ± 23.60	-28.16% ± 20.64
Moves (number)		17.55% ± 20.35	12.93% ± 18.38	20.83% ± 20.91
		15.10% ± 16.69	9.18% ± 18.67	20.06% ± 28.53

Data from the 15-minute baseline and post-naloxone testing periods were divided into three 5-minute time blocks. Data presented are mean percent change score [(post-naloxone treatment – baseline)/baseline] ± standard deviation for control (blue) and PDAC (red) mice for each time block. There were no significant differences in percent change in behavior after naloxone treatment between the two groups for any of the horizontal behavior measurements.

Control n= 9, PDAC n= 10.

Table 8. Percent change in vertical open-field exploratory activity after naloxone treatment

Vertical Behavior Measurements				
		Block 1	Block 2	Block 3
Extensions (number)	Control	-38.56% ± 26.75	-41.28% ± 15.84	-44.20% ± 18.26
	PDAC	-28.33% ± 36.42	-41.05% ± 32.54	-36.24% ± 29.10
Time (sec)		-31.43% ± 28.15	-39.82% ± 18.27	-34.04% ± 24.88
		-19.14% ± 38.68	-35.68% ± 34.80	-33.54% ± 28.93
Distance (cm)		-33.72% ± 41.79	-53.57% ± 20.12	-51.82% ± 24.99
		-30.83% ± 33.63	-51.95% ± 33.92	-51.60% ± 20.35
Moves (number)		-29.39% ± 27.20	-29.44% ± 18.73	-33.07% ± 22.98
		-22.55% ± 28.95	-31.04% ± 31.63	-28.88% ± 29.63

Data from the 15-minute baseline and post-naloxone testing periods were divided into three 5-minute time blocks. Data presented are mean percent change score [(naloxone-treated – baseline activity)/baseline activity] ± standard deviation for control (blue) and PDAC (red) mice for each time block. There were no significant differences in percent change in behavior after naloxone treatment between the two groups for any of the vertical behavior measurements.

Control n= 9, PDAC n= 10.

3.3 TUMOR-NERVE INTERACTIONS

3.3.1 Neuroplastic changes

Neuroplastic changes are commonly described in sections of resected tumor from late-stage PDAC patients[136,263] and these changes in innervation frequently include perineural tumor invasion[129,130,132]. Transgenic mouse models of PDAC provide an excellent model in which to examine the temporal dynamics of changes in pancreas innervation and perineural invasion throughout PDAC disease progression. I therefore used the pan-neuronal marker PGP 9.5 to determine when changes in pancreatic nerve fibers occur in PDAC mice. At 6-8 weeks of age, tPDAC pancreata exhibited small areas of hyperinnervation not present in control pancreata (**Figure 16A-H**). These areas were restricted to regions containing fibrosis, acinar atrophy, and/or PanIN lesions, whereas innervation in histologically normal pancreas was similar to that of controls. In the pancreas of tPDAC mice at 10-12 weeks of age, there were significantly more lobules of pancreas with abnormal pathology and multifocal PanIN lesions ranging from PanIN1A to PanIN3, and increased hyperinnervation accompanied this expansion of pancreas pathology (**Figure 16I-L**).

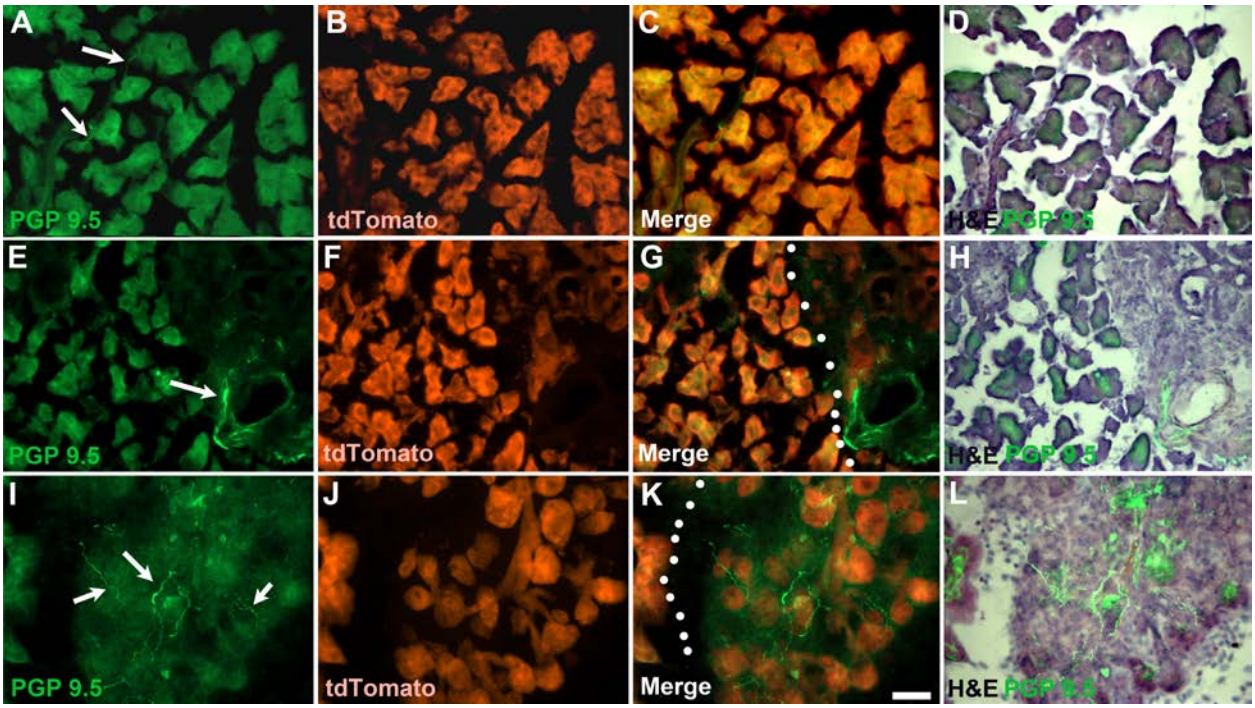

Figure 16. Distribution of PGP9.5- positive fibers during PDAC development

Only occasional thin PGP 9.5-positive fibers are observed (arrows) within the parenchyma of the pancreas (indicated by tdTomato expression) in control mice (A-D). By 6-8 weeks, numerous PGP-positive fibers (arrow) can be seen associated with blood vessels and dilated ducts in regions of focal fibrosis (E-H). Dotted lines indicate border between fibrotic region and normal appearing pancreas (G). Significant areas of fibrosis containing dense innervation by PGP-positive fibers are present in the pancreas of PDAC mice at 10-12 weeks (I-L). Dotted lines in (K) indicate region lobular fibrosis. Calibration bar = 50µm.

Large intrapancreatic nerve bundles in areas of hyperinnervation were observed in PDAC pancreata/tumors at >16 weeks of age (**Figure 17**). Hypertrophied nerves were often associated with areas of lobular fibrosis and acinar cell atrophy (**Figure 17D, H, L**). PGP^+ fibers were visualized extending from atrophied/aggregated islets (**Figure 17A-D**), near ducts and vasculature (**Figure 17E-K**), and adjacent to areas of PanIN lesions or tumor cells (**Figure 17I-L**). Hypertrophied fibers observed in the pancreas of older PDAC mice (10-12 and > 16 weeks) were $CGRP^+$ (**Figure 18**) and TH^+ (**Figure 19**), suggesting involvement of both sensory and sympathetic pancreatic nerves, respectively.

3.3.2 Perineural invasion in PDAC

Though documented in human PDAC[55], instances of intra- or extra-pancreatic perineural tumor invasion have not been previously described in transgenic mouse models of PDAC. Therefore, we used tPDAC mice to determine whether PNI or $tdTomato^+$ cells of pancreatic origin in local and distant sensory and sympathetic nerve ganglia could be detected. While intra-pancreatic PNI was not definitively observed, areas of focal fibrosis with hyperinnervation often featured branching of $PGP9.5^+$ fibers near the remaining $tdTomato^+$ cells, suggesting the tropism between the two. In one case, $tdTomato^+$ cells were present and appeared to be forming "pseudo ducts" inside the celiac ganglion (**Figure 20**), which was surrounded by a large tumor metastasis. In this case, many of the celiac ganglion cells were positive for $ATF3^+$, a marker of nerve injury only rarely expressed in control celiac ganglion cells (**Figure 20D-F**, arrows in **20D**).

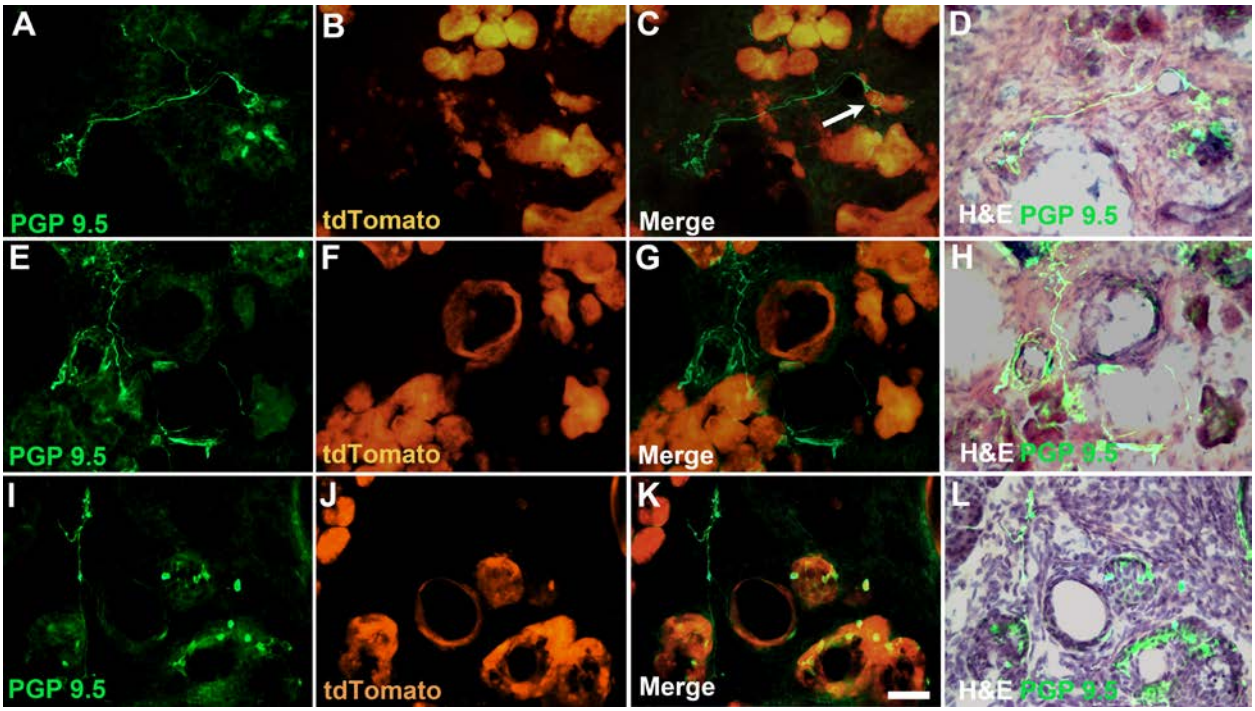

Figure 17. Examples of abnormal innervation in PDAC mice with identifiable tumors

Hypertrophied nerves with multiple branching fibers are present, primarily in regions with fibrosis and loss of acinar cells, as indicated by overlap of PGP 9.5 and loss of tdTomato-expressing cells. In some cases fiber bundles can be seen extending from atrophied/aggregated islets (A-D), associated with ducts or vasculature (E-H), and adjacent to areas of PanIN lesions or tumor cells (I-L). Arrow in (C) shows nerve fibers appearing to engulf tdTomato-positive cells. Calibration bar = 50µm

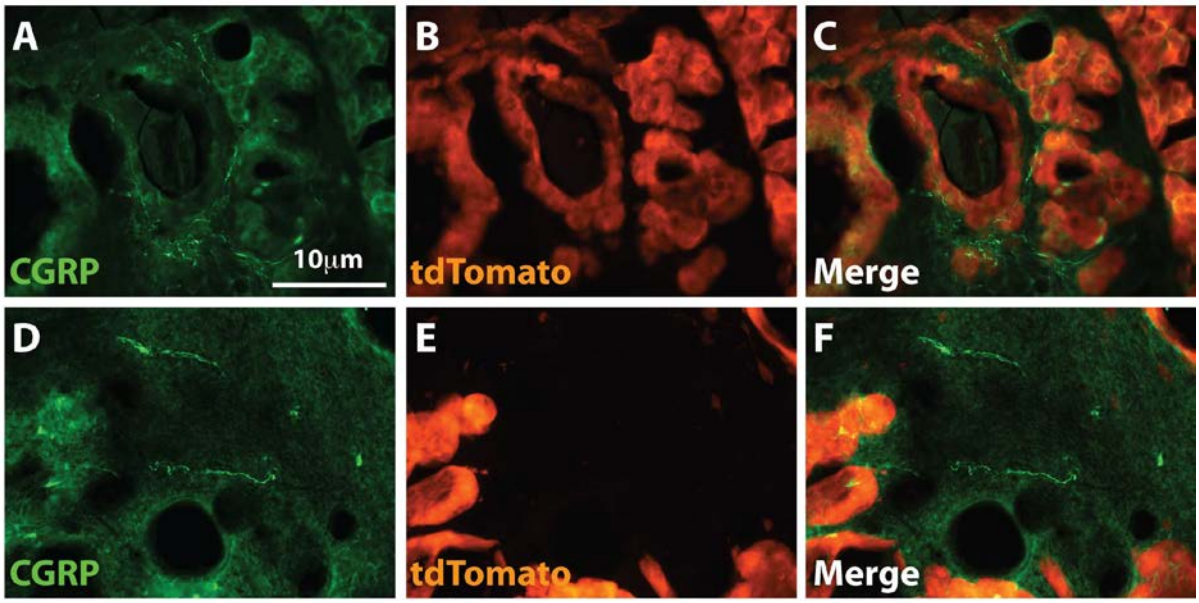

Figure 18. CGRP-positive nerve fibers in PDAC mice

Numerous CGRP-positive fibers are present in areas of pancreas with PanIN lesions and fibrosis in PDAC mice at 10-12 (A-C) and >16 (D-F) weeks of age.

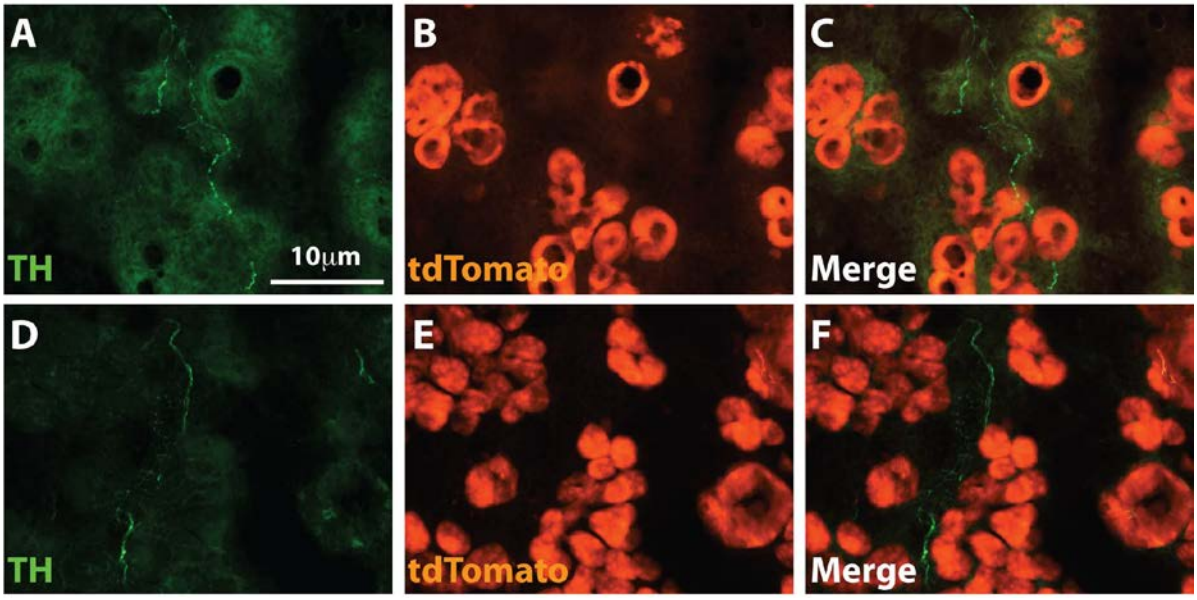

Figure 19. TH-positive nerve fibers in PDAC mice

Numerous TH-positive fibers are present in areas of pancreas with PanIN lesions and fibrosis in PDAC mice at 10-12 (A-C) and >16 (D-F) weeks of age.

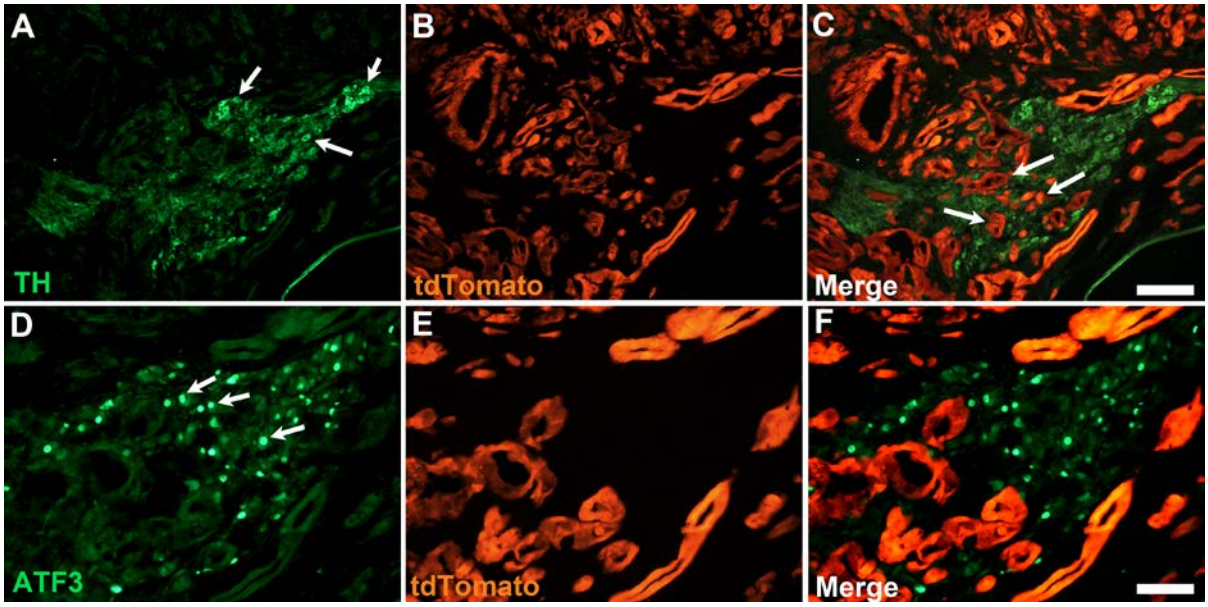

Figure 20. PDAC induces pathological changes in the celiac ganglion

Celiac ganglion neurons (arrows) immunostained with TH antibody (A). tdTomato staining reveals extensive tumor growth around and within (arrows in C) the borders of the celiac ganglion (B-C). The same celiac ganglion in (A-C) stained for expression of ATF3, a marker of neuronal injury (D-F). Numerous ATF3-positive neuronal nuclei are seen throughout the ganglion (arrows in D). Calibration bars A-C = 100μm; D-F = 50μm.

In a different tPDAC case, pancreas-derived cells invaded the dorsal T11 and T10 root ganglia (**Figure 21 B-E**). This migration of tumor cells into the DRG was associated with a metastatic tumor that surrounded the spinal cord at levels T9-T12 (**Figure 21A**), the levels of spinal cord that normally innervate the pancreas [256] Some pancreatic-derived cells in the DRG assumed complex morphology, exhibiting processes that could participate in cell-to-cell adhesion or chemotaxis (inset in **Figure 21E**). Despite the large number of tdTomato$^+$ cells present in the DRG, relatively few cells in the ipsi- or contralateral T10 and T11 DRG were ATF3$^+$ (data not shown).

3.3.3 Changes in sensory neuron gene expression

Changes in pancreatic innervation induced in mouse models of acute and chronic pancreatitis are associated with changes in gene expression in associated sensory ganglia[210,211]. We hypothesized that similar changes would be associated with the changes in pancreatic nerve fibers observed in PDAC mice. The relative expression of genes related to nociception, neurogenic inflammation, and nerve injury was therefore analyzed in the T9-12 DRG, the ganglia shown to receive the most pancreatic sensory input[256], of PDAC mice at ages 10-12 and >16 weeks. Similar to changes described in mouse models of pancreatitis, expression of *Trpa1* and *Trpv1* was significantly increased 1.74- and 1.36-fold, respectively, in the DRG of PDAC mice at >16 weeks of age ($p=0.013$ and $p=0.043$; **Table 9**). In 10-12 week old PDAC mice, there was a non-significant trend toward increased *Trpa1* expression (1.38-fold, $p=0.059$; **Table 9**).

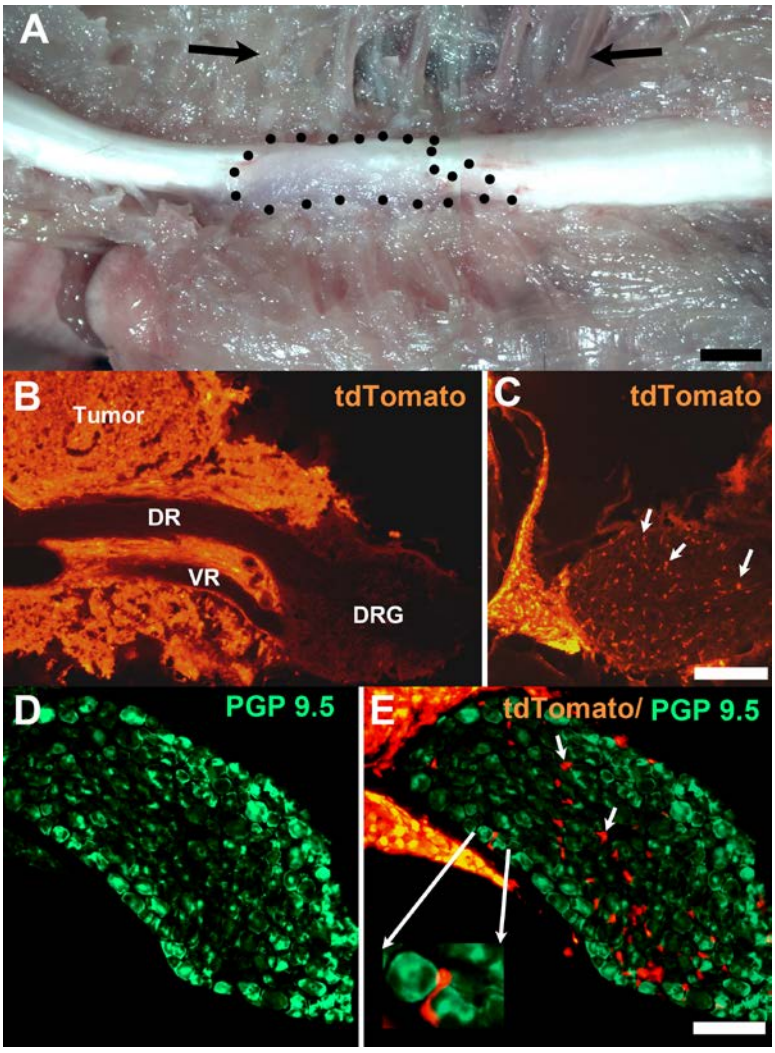

Figure 21. Pancreas-derived tumor surrounding the spinal cord at the vertebral levels giving rise to sensory innervation in the pancreas

Right and left arrows indicate T13 and T9 rib, respectively, demarcating the vertebral levels of the sensory ganglia that give rise to the majority of sensory innervation to the pancreas (A). Tumor, indicated by tdTomato expression, surrounds both dorsal (DR) and ventral (VR) roots of the right T11 DRG (B). No tdTomato-positive cells are seen in this DRG. Left T11 DRG containing numerous tdTomato-positive cells, presumably representing migrating tumor cells associated with the tumor formation (C). Left T10 DRG stained with PGP 9.5 (D). Merged

photomicrograph showing numerous tdTomato-positive cells interspersed between PGP 9.5-positive DRG neurons (E). tdTomato-positive cells were only seen in T10 and T11 DRG on the left side (C&E). Insert in (E) shows a tdTomato–positive cell appearing to migrate between two DRG neurons. Calibration bars A = 2mm; B&C = 100µm; C&D = 50µm.

In rodent models of pancreatitis, TRPV1 and TRPA1 channels are implicated in neurogenic inflammation and release of neuropeptides such as CGRP and SP in the pancreas[210,211,214,216,218] (reviewed in[137,207]). In line with this mechanism, the DRG of PDAC mice at both 10-12 and >16 weeks of age also exhibited increased levels of *Cgrp* mRNA (1.36- and 1.27- fold, respectively (p=0.043 and p=0.029; **Table 9**). In contrast, *SP* expression in the DRG was not significantly different between PDAC and control mice at 10-12 weeks and only a non-significant trend toward increased expression in PDAC DRG was apparent at >16 weeks of age (1.44-fold, p= 0.081; **Table 9**). Similarly, expression of *Atf3*, a marker of nerve injury, was not significantly different between control and PDAC DRG at 10-12 weeks, but a non-significant trend toward increased expression was evident at >16 weeks of age (1.92-fold, p= 0.059; **Table 9**). In contrast, expression of the voltage-gated channels $Na_v1.8$ and $K_v4.3$ was not significantly different in the DRG of control and PDAC mice at either age (**Table 9**).

Table 9. Changes in sensory ganglia gene expression in PDAC mice

Gene	10-12 weeks	>16 weeks
Atf3	1.22 (p=0.950)	1.92^ (p=0.059)
Cgrp	1.36***** (p=0.043)	1.27***** (p=0.029)
K_v4.3	0.99 (p=0.573)	1.00 (p=1.000)
Na_v1.8	1.12^ (p=0.081)	1.19 (p=0.282)
SP	1.11 (p=0.662)	1.44^ (p=0.081)
Trpv1	1.42 (p=0.142)	1.36***** (p=0.043)
Trpa1	1.38^ (p=0.059)	1.74***** (p=0.013)

Expression of genes related to injury, nociception, and neurogenic inflammation in DRG T9-12 of PDAC mice. Data are normalized using *Gapdh* as a reference standard and presented as fold change in expression relative to age-matched controls. Control n= 6, PDAC n= 8 for both age groups. *p< 0.05; ^ denotes a non-significant trend

3.3.4 Changes in evoked calcium transients in pancreatic sensory afferents

Increased expression of *Trpv1* and *Trpa1* in pancreatic afferents in mouse models of acute and chronic pancreatitis were associated with an increased number of pancreatic afferents responding to application of TRP agonists, enhanced Ca^{2+} transients in pancreatic afferents in response to TRP channel agonists, and increased peak response to application of 50mM KCl[210,211]. To determine if a similar change in TRP channel activation is associated with PDAC, pancreatic afferents in PDAC mice and controls were back-labeled with 1,1'-dioctadecyl-3,3,3'3'-tetramethylindocarbocyanine perchlorate (DiI) and 8-10 days later, DRG T9-12 were removed bilaterally and dissociated to generate primary DRG cultures for Ca^{2+} imaging analyses as described in **2.8 PRIMARY DRG CELL CULTURE AND CALCIUM IMAGING**. Evoked Ca^{2+} transients in response to 50mM KCl (High K^+) were measured in DiI^+ cells and those not responding to High K^+ ($\Delta F_{340/380} < 0.20$) application were excluded from further analyses. The percentage of pancreatic afferents responding to application of either the TRPV1 agonist capsaicin (1μM) or the TRPA1 agonist mustard oil (100μM) was measured for both PDAC and control mice at 6-8, 10-12, and >16 weeks of age. The number of cells responding to either agonist ($\Delta F_{340/380} < 0.20$) was not significantly different between cancer and control pancreas-specific sensory neurons at any time point (**Table 10**). However, analysis of peak percent change in $\Delta F_{340/380}$ from baseline following application of High K^+ in pancreatic afferents of PDAC mice compared to control afferents revealed a significant age effect ($F= 14.14$, $p<0.05$) and a significant interaction between age and genotype ($F= 3.02$, $p<0.05$). Bonferroni post-tests revealed a non-significant trend toward increased peak percent change in $\Delta F_{340/380}$ from baseline in pancreatic neurons from PDAC mice at 10-12 weeks of age compared to pancreatic afferents from age-matched controls ($p<0.07$; **Figure 22**).

Table 10. Percentage of pancreas-specific afferents responding to TRP channel agonists

	Capsaicin (1μM)		
	6-8 weeks	**10-12 weeks**	**>16 weeks**
Percent Responders	Control 43.06% ± 17.77 (27)	32.35% ± 12.49 (38)	64.77% ± 14.40 (33)
	PDAC 63.34% ± 18.56 (27)	58.39% ± 11.52 (51)	62.63% ± 17.63 (40)
	Mustard Oil (100μM)		
	6-8 weeks	**10-12 weeks**	**>16 weeks**
Percent Responders	Control 66.00% ± 9.64 (33)	45.18% ± 19.08 (35)	47.23% ± 23.74 (28)
	PDAC 85.55% ± 7.23 (54)	71.00% ± 8.27 (64)	73.03% ± 17.06 (36)

Mean percentage (± standard error of the mean) of pancreas-specific afferents from control (blue) or PDAC (red) mice responding ($\Delta F_{340/380} < 0.20$) to brief application of capsaicin (1μM) or mustard oil (100μM). Number of cells in each group indicated in parentheses. There were no significant differences in percentage of cells responding to either agonist between PDAC and control groups at any time point in PDAC development.

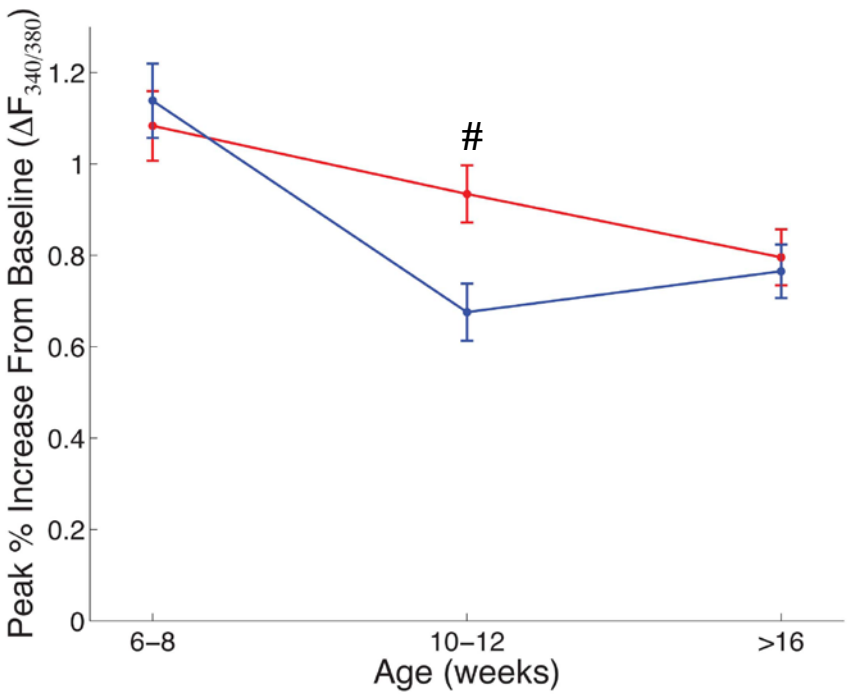

Figure 22. Changes in evoked calcium transients in pancreatic sensory afferents

Average peak percent change in $\Delta F_{340/380}$ from baseline following application High K^+ for control (blue) and PDAC (red) pancreatic afferents. Control n= 66 cells (6-8), n= 76 cells (10-12), and n= 73 cells (>16). PDAC n= 78 cells (6-8), n= 97 cells (10-12), and 58 cells (>16). Error bars represent standard error of the mean. # non-significant trend, $p<0.07$.

3.4 NEUROTROPHIC FACTOR EXPRESSION IN PDAC

3.4.1 Changes in neurotrophic factor expression in the pancreas of PDAC mice

Previous studies have associated increased neurotrophic growth factor expression with PDAC-induced neuronal hypertrophy, perineural invasion and PDAC-related pain[155–158,162] (reviewed in[119,120,191]). Furthermore, increased neurotrophic factor expression during development or following inflammation has been shown to induce nerve sprouting and sensitization of primary sensory afferents as well as sympathetic efferents[145–149,260]. To determine if changes occur in neurotrophic factors and their receptors during tumor development and progression, pancreas RNA collected from PDAC and control mice was analyzed at 3-4, 6-8, 10-12, and >16 weeks of age. There were no significant differences in expression of *Ngf*, *Gdnf*, *Bdnf*, *Artn*, *Nrtn* or their receptors between PDAC and control mice at 3-4 weeks of age (**Figure 23** and only *Gfrα2*, the receptor for *Nrtn*, was significantly increased (3.74 fold; p=0.008) in the pancreas of PDAC mice at 6-8 weeks (**Figure 23**). In the 10-12 week age group, *Ngf*, *Trkb*, *Nrtn*, and *Gfrα2* were significantly increased (2.25-, 2.18-, 1.39-, and 3.42-fold, respectively; p= 0.007, p= 0.012, p=0.028, and p= 0.028) in the pancreas of PDAC mice (**Figure 23**). In the pancreas of PDAC mice >16 weeks of age, *Ngf*, *Trka*, *Gdnf*, and *Gfrα2* were significantly increased (3.6-, 29.9-, 7.11-, and 4.02-fold, respectively; p= 0.03, p= 0.001, p= 0.023, and p= 0.024; **Figure 23**). In contrast, *Gfrα3* expression in the pancreas of >16 weeks old PDAC mice was significantly decreased (4.30-fold; p= 0.009; **Figure 23**).

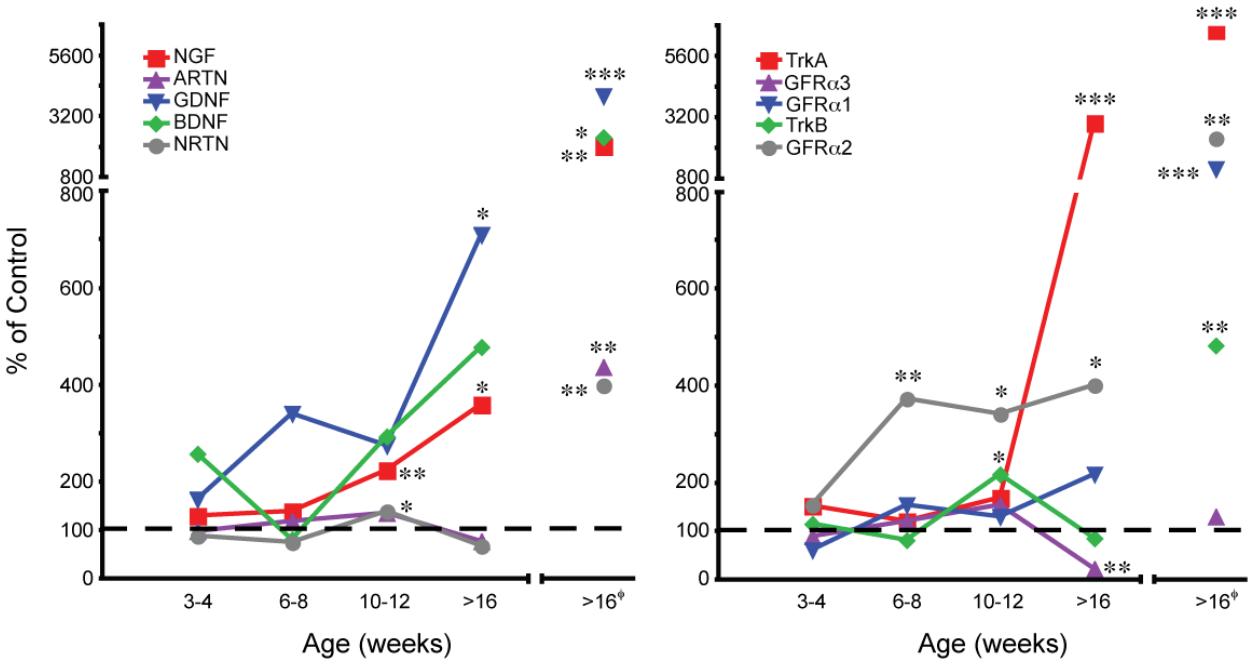

Figure 23. Increased neurotrophic factor and neurotrophic factor receptor expression in the pancreas of PDAC mice

Expression of neurotrophic factors and neurotrophic factor receptors in the pancreas of PDAC mice was measured at 3-4, 6-8, 10-12, and >16 weeks of age, normalized using *Rpl13a* as a reference standard, and presented as the percent expression of age-matched controls. Control n= 4 (3-4 weeks), n= 4 (6-8), n=5 (10-12), and n=6 (>16). PDAC n= 6 (3-4), n=7 (6-8), n=7 (10-12), and n=10 (>16). *p<0.05; **p<0.01; ***p<0.001. Data from >16 weeks old mice are also presented as the percent expression of controls normalized to the amount of cDNA amplified (>16Φ) and using this method of comparison, expression all neurotrophic factors and neurotrophic factor receptors except *Gfrα3* is significantly increased, p<0.01.

For the transcriptional analyses above, gene expression was normalized to the housekeeping gene *Rpl13a*, which did not significantly change in PDAC mice at 3-4, 6-8, and 10-12 weeks of age. However, expression of *Rpl13a* was increased 3-fold in the pancreas of PDAC mice >16 weeks of age, as was the expression of seven other housekeeping genes (5- to 15-fold; **Table 11**). These changes suggest that as the tumor replaces normal pancreas parenchyma, fundamental changes in the tissue, including increases in rapidly dividing cells, occur producing an mRNA signature unique to PDAC. It should also be mentioned that if mRNA expression is normalized based on the initial amount of cDNA amplified, larger and statistically significant changes in gene expression occur in all growth factors and receptors, except *Gfrα3* (**Figure 23**). Thus, regardless of the method used, significant changes in growth factor and receptor mRNA occur, indicating that as cancer progresses, the pancreas produces a milieu that resembles the pro-growth environment experienced by the peripheral nervous system during development.

Table 11. Changes in housekeeping gene expression in the pancreas of PDAC mice

Gene	>16 weeks
Actb	15.24
B2m	14.75
Gapdh	14.14
Gusb	5.23
Hprt1	5.29
Pgk	4.92
Ppia	5.00
Rpl13a	3.10

Expression of housekeeping genes in the pancreas of PDAC mice >16 weeks of age normalized to the amount of cDNA amplified and presented as fold change in expression relative to age-matched controls. N=4 for control and PDAC.

3.4.2 Neurotrophic factor and neurotrophic factor receptor expression in PDAC cell lines

A variety of cell types including tumor cells, infiltrating immune cells, and cells in the stromal compartment of the tumor could each contribute to the observed changes in growth factor and growth factor receptor expression in the pancreas of PDAC mice. Previous studies of human tumor cell lines have demonstrated that many express a variety of growth factors and receptors, suggesting that PDAC cells represent a significant source and target of released intrapancreatic neurotrophic factors. To address the contribution of PDAC cells to changes in growth factor expression, RNA from two cell lines created from dissociated tumors of PDAC mice (Kpc1 and Kpc2) was analyzed to assess tumor-specific neurotrophic factor and neurotrophic factor receptor expression. Reverse transcriptase-PCR analysis showed that the Kpc1 and Kpc2 lines express *Ngf*, *Artn*, *Gdnf*, *Nrtn*, and *Gfrα2* (**Figure 24**). The Kpc2 line also expresses *Gfrα3* and *Gfrα1* (**Figure 24**). The Kpc expression profile is quite similar to that of the two human tumor cell lines, Panc1 and MiaPaCa2, which express *ARTN*, *BDNF*, *TRKA*, *GFRα3*, and *GFRα2* (**Figure 24**). Panc1 also expresses *NGF*, *GFRα1* and *TRKB* while MiaPaCa2 also expresses *GDNF* (**Figure 24**). These findings indicate that the growth factor-enriched environment of the pancreas during PDAC is generated, at least in part, from PDAC cells. In addition, the development and progression of PDAC may be driven by both autocrine activation of growth factor receptors by growth factors released by tumor cells, and by paracrine activation of growth factor receptors by growth factors and inflammatory mediators released by stromal cells and/or infiltrating immune cells.

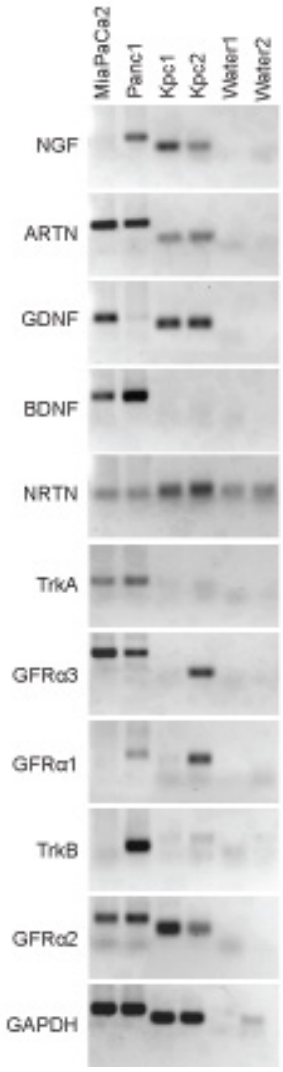

Figure 24. Neurotrophic factor and neurotrophic factor receptor expression in PDAC cell lines

RT-PCR analysis of gene expression in two murine PDAC cell lines (Kpc1 and Kpc2) and two human PDAC cell lines (MiaPaCa2 and Panc1).

4.0 DISCUSSION

4.1 DISEASE PROGRESSION IN PDAC MICE PARALLELS HUMAN PDAC

4.1.1 PDAC-related illness

In patients with PDAC, common presenting signs and symptoms include jaundice, abdominal or epigastric pain, and weight loss[1,3,42,62,65](reviewed in[66–68]). As the disease progresses, patients may develop additional cancer sequelae such as anorexia, hepatomegaly, diabetes, cachexia, Courvoisier's sign, presence of an abdominal mass, ascites, duodenal obstruction, and delayed gastric emptying[3,62,69,73](reviewed in[39]). In PDAC and tPDAC mice, several of the same signs were observed as tumor growth progressed. Specifically, jaundice, bloody abdominal ascites, encasement of the duodenum, and enlarged gall bladder were all observed in the PDAC mouse cohort. While PDAC mice generally weighed less than age-matched controls across all ages, no significant weight loss was observed. In some cases, the development of abdominal ascites could have masked weight loss and/or cachexia associated with the cancer. At later stages of the disease, PDAC mice adopt a rounded-back hunched posture that is likely related to the development of PDAC pain and may be analogous to PDAC patients who report that lying in a curled or fetal position reduces pain[3].

The cohort of PDAC mice used for these studies resembles a clinical cohort of patients in that the collection of signs observed and the time course of disease progression were highly variable, particularly at later stages of disease. Like human PDAC, some of the observed variability is likely due to differences in the genetic profiles of tumors in PDAC mice. While all PDAC mice have mutations in *Kras* and loss of *Trp53* expression, it is possible that additional mutations accumulate throughout tumor development and progression, influencing the observed disease course and tumor-related pathology.

Unfortunately, early detection of PDAC is uncommon and often patients present with either locally invasive disease or distant metastases and are therefore not candidates for surgical resection[1,38]. Local tumor spread typically includes retroperitoneal structures such as the aorta or superior mesenteric vessels as well as adjacent organs such as the duodenum[1,38], while metastatic disease in PDAC most frequently affects the liver, peritoneum, and lungs (reviewed in[39,74]). In PDAC mice, metastases to the peritoneum and liver were also most commonly observed, with occasional metastases to the lung. This suggests common mechanisms could underlie metastatic spread in human and mouse PDAC. This commonality has particular importance for study the of tumor-nerve interactions as perineural tumor invasion is thought to be an important mode of disease spread.

4.1.2 Tumor development and histology

The studies of this dissertation focused on the neuroplastic changes that occur during the development and progression of cancer. Most cases of PDAC are thought to arise from pre-malignant PanIN lesions that progress from low-grade dysplasia (PanIN-1A) to high-grade

dysplasia (PanIN-3) to invasive carcinoma[75,76] (reviewed in[74]). In transgenic mouse models of PDAC similar to the one used in this study, histological analysis of the pancreas of PDAC mice throughout tumor development demonstrates a progression from PanIN to PDAC[117,243]. In this study, PanIN-1 lesions were evident in the pancreas of PDAC mice as early as 6-8 weeks of age, PanIN-2 or -3 lesions were present by 10-12 weeks of age, and PDAC typically developed by 16 weeks of age. An important distinction between mouse and human PDAC is the multifocal nature of disease in PDAC mice. Because the pancreas-specific mutations expressed in PDAC mice are in all cells of pancreatic origin, multifocal PanIN lesions and multiple tumor loci develop in PDAC mice. Other PDAC features such as lobular atrophy, similar to what has been described in the pancreas of patients at high risk of developing PDAC[77], and the dense, stromal fibrosis or desmoplastic reaction prominent in human PDAC were also observed in the pancreas of PDAC mice. Overall, tumor development in PDAC mice closely models human PDAC, providing a useful tool to examine the development of cancer-related neuroplastic changes.

4.2 CANCER-RELATED PAIN IN MICE PARALLELS PAIN IN HUMAN PDAC

4.2.1 PDAC pain presents in late stages of disease

Abdominal or epigastric pain is a common presenting symptom in patients with PDAC, however this frequently correlates with late stage disease[1,3] (reviewed in[66–68]). The late onset of symptoms such as pain largely explains why early detection of pancreatic cancer is rare. Pain is also one of the most commonly reported symptoms in PDAC patients, with up to 80% of patients reporting pain by end stage disease[136]. Interestingly, patient report of pain is not correlated with

tumor size or tumor location, but is associated with depression[71,72], decreased quality of life[71,72], and worse prognosis[68,136]. This suggests that PDAC-related pain is not due solely to tumor mass and that pathological mechanisms underlying tumor development and progression affect pancreatic afferents as well. A better understanding of early neuroplastic changes in the pancreas during early stages of PDAC would provide valuable insight into mechanisms underlying cancer pain, which could lead to novel treatment strategies that improve the quality of life in PDAC patients.

As experienced by patients with PDAC, pain-related behavior was observed in PDAC mice with increasing age and at later stages of disease. Hunching behavior was evident at 10-12 weeks, when moderate to severe PanIN lesions, but not PDAC were present. However, decreased open-field exploratory activity, particularly with regard to vertical movements, were not observed until later time points (> 16 weeks of age), when PDAC mice have a significant tumor burden. With disease progression, PDAC mice adopt increasingly hunched postures when moving within their home cage, which is consistent with the decline in vertical movement measurements over with increased age. While it is possible that the changes in exploratory activity are related purely to illness severity, the specificity of decreased activity only in vertical movements, which require the animals to extend their abdomens, but not in the horizontal movements where a hunched posture can be maintained, suggests increased desire to alleviate abdominal pain or discomfort. The observation that pain-related behavior is most evident late in PDAC mice, after the progression from PanIN to PDAC, is consistent with previous studies of PDAC pain using a genetic mouse model of acinar carcinoma[223,224]. These finding suggest that the early, relatively restricted neuroplastic changes observed in tPDAC mice at pre-cancer stages are insufficient to cause pain, as measured by changes in animal posture and movement behavior.

Widespread hyperinnervation and associated changes in sensory afferent phenotype observed in tPDAC mice with PDAC may be necessary for detectable changes PDAC-related pain behavior.

4.2.2 Endogenous mechanisms may attenuate PDAC-related pain

The use of opioid analgesics may provide palliation for some patients with PDAC-related pain and a previous study of pain in a mouse model of pancreatic acinar carcinoma demonstrated reversal of pain-related hunching and vocalizations in mice following treatment with morphine[223,224]. Furthermore, treatment with the CNS-penetrant opioid receptor antagonist naloxone to block endogenous opioid signaling "unmasked" pain-related hunching and vocalizations in this mouse model of acinar carcinoma[224]. This suggests a role for opioid-dependent mechanisms in modulation of PDAC-related pain. In our study, we observed naloxone-induced attenuation of open-field exploratory activity in some PDAC mice, but a significant difference between cancer and control groups was not measured. There was significant variability in response to naloxone treatment among PDAC mice, consistent with the varied disease course and survival time of the study cohort. Given that some variability in response to naloxone was observed in control mice as well, experimental factors such as uniform injection of the full naloxone dose and habituation to the behavior box due to repeated testing in a 24-hour period could have also affected the observed behavior. Differences in tumor burden, the genetic profile of the tumor, and the presence of local or distant metastases, or the presence or tumor-related sequelae such as bile duct obstruction could each contribute to differential responses to naloxone treatment among PDAC mice. Additionally, there are patients with PDAC who never report cancer pain. Therefore, there could be clinically important differences

between mice that develop PDAC-related pain early and are affected by naloxone treatment, and mice who develop pain at advanced stages of disease and are not affected by naloxone treatment early.

4.3 CHANGES IN PANCREAS INNERVATION IN PDAC OCCUR EARLY IN DISEASE PROGRESSION

4.3.1 Hyperinnervation in mouse and human PDAC

Tumor-nerve interactions and hypertrophied nerve bundles in resected human PDAC tissue have been well documented[118–121,136]. Hypertrophied nerve bundles are correlated with increased pain severity[136] and may also provide an anatomical substrate for the extensive perineural tumor invasion observed in the disease. A previous study of pancreatic innervation in a mouse model of acinar carcinoma also demonstrated increased nerve density involving both sensory and sympathetic nerve fibers[223].

Innervation of the pancreas/tumor of tPDAC mice >16 weeks old was highly variable depending on the region of tumor examined. In desmoplastic regions of the tumor with extinction of the background pancreas there were relatively few PGP9.5$^+$ nerve fibers. These regions contrasted with areas of hyperinnervation where disorganized, torturous nerve fibers, similar in appearance to newly- sprouted nerve fibers, and hypertrophied fiber bundles were associated with tdTomato-positive cells. These areas of hyperinnervation exhibited CGRP$^+$ sensory fibers and TH$^+$ sympathetic fibers.

Studies of neuroplastic changes in human PDAC are limited to a relatively small window in the late stages of disease in which most patients are diagnosed. Having established that similar changes in pancreas and tumor innervation occur in PDAC mice at late stages of disease, it is reasonable to suggest that a similar process underlies the development of hyperinnervation in human and mouse PDAC during early, pre-malignant stages. The parallels in PanIN to PDAC progression in mouse and human PDAC described above in **4.1.2 Tumor development and histology** support this assertion. Understanding the mechanisms that underlie the development of PDAC-related hyperinnervation may provide new targets for intervention to prevent such changes, which could attenuate both PDAC-related pain as well as disease progression.

4.3.2 Hyperinnervation related to PDAC begins in pre-malignant stages of tumor development in PDAC mice

We hypothesized that PDAC-related changes in pancreas innervation observed in advanced stages of human and mouse PDAC are not simply a consequence of the tumor, but rather represent a reciprocal relationship between the cancer and the peripheral nervous system that begins early in tumor development. Because pre-malignant time periods are difficult to study in human PDAC, studies of neuroplastic changes in PDAC mice can provide valuable insight into the relationship between pancreas innervation and tumor progression. As early as 6-8 weeks of age, areas of hyperinnervation are evident in the pancreas of tPDAC mice, typically in regions of focal fibrosis containing mild PanIN lesions. At 10-12 weeks, the expansion of focal fibrosis and progression from mild to moderate or severe PanIN are accompanied by increased innervation and, in some cases, large fiber bundles. The appearance of hyperinnervation at these pre-

malignant time points suggests that early changes in the microenvironment affect pancreatic nerves, potentially recruiting them as participants in disease progression.

It is unknown whether the initial changes in the pancreas that result in the formation of PanIN lesions directly impact nerve fibers or whether cells in the microenvironment begin to express factors that may act on local pancreatic afferents. The development of focal fibrosis and PanIN lesion formation could involve a variety of growth factors and cytokines and could also result in a microenvironment that is ischemic or acidic relative to normal pancreas. Furthermore, it is possible that early changes in the microenvironment that drive pancreatic hyperinnervation also affect sensory afferent phenotype; resulting in sensitized afferents that could contribute to PDAC-pain and promote the transition from mild to severe PanIN and/or the expansion of fibrosis through neurogenic inflammation.

4.4 CHANGES IN NEUROTROPHIC FACTOR AND NEUROTROPHIC FACTOR RECEPTOR EXPRESSION IN THE PANCREAS OF PDAC MICE OCCUR EARLY

4.4.1 Neurotrophic factors in PDAC

Studies from this laboratory and others have shown that neurotrophic factors enhance sprouting and sensitization of primary sensory afferents and sympathetic neurons in adult systems[145–154]. Inflammatory mediators and growth factors identified in resected PDAC specimens are known to produce nerve hypertrophy, enhance neuron excitability, and promote perineural invasion[136,155–158,162,263]. Multiple neurotrophic factors and their receptors have been implicated in human PDAC; increased GDNF, GFRα1, NGF, TRKA, ARTN, and GFRα3 have

been described in human PDAC tissue[155–161]. In particular, increased NGF and ARTN is significantly correlated with nerve hypertrophy in human PDAC[155,156]. *In vitro*, isolated myenteric plexuses exposed to extracts from human PDAC tissue exhibit increased neurite density compared to normal medium and this effect can be blocked by depletion of NGF or ARTN from the tumor extract[156,168]. Increased NGF and TRKA in PDAC also correlates with patient report of pain[119,157,159], suggesting that intrapancreatic neurotrophic factor expression in PDAC promotes peripheral nerve sprouting and sensitizes pancreatic sensory afferents.

PDAC cell lines have been shown to express a variety of growth factor receptors including *TRKA, TRKB, GFRα1, GFRα2,* and *GFRα3,* suggesting that neurotrophic factors in the tumor microenvironment also influence tumor cells[119]. Increased NGF, TRKA, and GDNF in human PDAC tissue is significantly correlated with the degree of peripheral nerve invasion[157,158,160] and *in vitro,* ARTN, GDNF, and NGF promote invasive behavior of human PDAC cell lines[155,161,173–175]. Thus, neurotrophic factor expression in PDAC has a key role in the reciprocal relationship between the tumor and peripheral nervous system.

In PDAC mice >16 weeks of age, changes in expression of neurotrophic factors and neurotrophic factor receptors are similar to those described in human PDAC, with significant increases in *Ngf, Trka, Gdnf, and Gfrα2* and a significant decrease in *Gfrα3*. Because *Gfrα3* is expressed by vascular smooth muscle cells, its decrease may reflect the relatively avascular nature of the tumor. However, in contrast to human studies, *Artn* expression is not significantly increased when normalized to the least-changed housekeeping gene, *Rpl13a*. Significant increases in expression of normalization genes were observed in PDAC mice with advanced tumors, suggesting that the pancreas/tumor of older PDAC is quite different from that of age-matched control mice. This result is consistent with extinction of background pancreas observed

in some PDAC mice with advanced disease. An alternative normalization procedure, based on the amount of cDNA amplified, was also employed to obtain a more complete picture of neurotrophic factor levels in the tumor. In this comparison, we find that *Ngf*, *Trka*, *Gdnf*, *Artn*, *Bdnf*, *Nrtn*, and their receptors, except *Gfrα3*, were significantly increased in the tumors of PDAC mice when compared to control pancreas. Therefore, neurotrophic factor signaling in PDAC likely plays a prominent role in shaping tumor innervation and the tumor microenvironment in both human and murine PDAC.

4.4.2 Changes in neurotrophic factor expression begin in pre-malignant stages of tumor development in PDAC mice

In tPDAC mice, the presence of hyperinnervation in regions of the pancreas at 6-8 and 10-12 weeks of ages suggests that a neurotrophic factor-rich, "pro-growth" microenvironment is present at pre-malignant stages of PDAC development. While only *Gfrα2* is significantly increased at 6-8 weeks, the regions of PanIN and associated fibrosis in the pancreas are relatively small at this time point; making detection of changes in neurotrophic factor expression within the whole pancreas difficult. It is possible, however, that undetected local changes in growth factors in the microenvironment surrounding the developing PanIN lesions could affect nearby pancreatic afferents. At 10-12 weeks, when more PanIN lesions, lobular pathology, and regions of hyperinnervation are present, *Ngf*, *Trkb*, *Nrtn*, and *Gfrα2* mRNA levels are significantly increased in the pancreas of PDAC mice compared to controls. Increased growth factor and growth factor receptor expression in the pancreas at these pre-malignant time points could be coming from tumor precursor cells in the PanIN lesions, infiltrating immune cells, or local stromal cells such as stellate cells.

Regardless of the source, changes in neurotrophic factor signaling in the pancreas that begin prior to the development of cancer are predicted to have both direct and indirect effects on tumor progression from PanIN to PDAC. Given that tumor cells express a variety of growth factor receptors, it is possible that tumor precursor cells could also express neurotrophic factor receptors and be directly affected by increased neurotrophic factors in the pancreas. Additionally, exposure to neurotrophic factors could induce nerve sprouting/hypertrophy in pancreatic afferents as well as sensitize them, resulting in increased activation and neurogenic inflammation. Activated afferents have been shown to release a variety of pro-inflammatory molecules such as CGRP, SP, and ATP that could drive neurogenic inflammation localized to the regions of the pancreas containing PanIN, fibrosis, and hyperinnervation. Thus, neurotrophic factors in the pancreas can indirectly drive disease progression through sensitization of pancreatic afferents.

4.5 PERINEURAL TUMOR INVASION IN MOUSE PDAC

4.5.1 Perineural invasion is a common and important component of PDAC

Previous studies have shown that intrapancreatic PNI is present in up to 100% of PDAC cases (reviewed in[118,128,129]). Intra- and extra-pancreatic perineural invasion correlate with worse disease prognosis, post-operative recurrence, and decreased survival time[52–57,130–133]. Both PDAC-related pain and local tumor spread to retroperitoneal structures are thought to be related to perineural tumor invasion[52,134–136] (reviewed in[119]). Thus, PNI in PDAC represents an important component of the disease that, if blocked, could result in significant improvement in

morbidity and mortality. Unfortunately, little is known about the mechanisms underlying the development of PNI in human PDAC and previous studies of PNI have relied upon *in vitro* co-culture assays or xenograft models[139,155–158,160–162,168,169,172,173,175–178,230–232,235,264,265]. Therefore, we employed pancreas-specific lineage tracing using tPDAC mice to determine whether intra- or extra-pancreatic PNI occurs in murine PDAC.

4.5.2 Perineural invasion occurs in PDAC mice

Intrapancreatic PNI was difficult to definitively detect in tPDAC mice at any age, but PGP9.5$^+$ fibers in regions of PanIN, fibrosis, or PDAC appeared to have an affinity for or tropism toward tdTomato$^+$ cells. Extra-pancreatic invasion of local and distant nerve ganglia was found in some cases. The celiac ganglion of one tPDAC mouse was encased by a large tumor metastasis and tdTomato$^+$ cells were present inside the ganglion. This suggests that tumor cells migrated from the pancreas along sympathetic nerves that synapse in the celiac ganglion or the sensory afferents that run through it; similar to what may occur in locally advanced human PDAC. In a different tPDAC mouse, tdTomato$^+$ cells were discovered inside the T10 and T11 DRG and tumor encasement of the spinal cord was grossly visible from T9-T12, again suggesting tumor cell migration along sensory afferents leading to metastatic spread.

In addition to providing a mode of extra-pancreatic tumor spread, PNI also involves damage to peripheral nerves that could trigger changes in gene expression in autonomic and sensory afferents. In the case of the observed celiac ganglion PNI described above, many celiac ganglion neurons express ATF3, a marker for nerve injury. Such injured neurons could have gene expression profiles similar to what is observed during peripheral nerve regeneration after injury including upregulation of growth factor receptors. Invading tumor cells found in the

dorsal root and celiac ganglia also represent a potential source of growth factors, cytokines, and other factors that could alter neuron gene expression and excitability, leading to pain. Therefore, PNI could contribute to the development of PDAC pain via physical damage of peripheral afferents as well as changes in nociception-related genes.

How or why tumor cells invade and move along peripheral nerve fibers is not well understood and the use of lineage tracing to identify pancreatic cells invading peripheral ganglia could provide significant insight into this process, not only for PDAC, but also for other cancers in which PNI is prominent. *In vitro* studies and xenograft models of PNI in PDAC suggest that perineural invasion and tumor migration along nerves requires a variety of secreted factors in the environment promoting mutual tropism as well as expression of particular genes in tumor cells such as adhesion molecules[128,264]. One possibility is that nerves are drawn toward the tumor via neurotrophic factor signaling and subsequently activated. Sensitized pancreatic afferents, in turn, secrete molecules such as glutamate, which are used by the tumor to promote growth or migration[266]. Neurotrophic factors in the tumor microenvironment could also increase tumor cell migration or invasion by inducing gene expression changes via neurotrophic factor receptor activation and signaling. Another possibility is that de-differentiated PDAC tumor cells assume a neuronal-like phenotype and the similarity between tumor cells and pancreatic afferents drive mutual tropism between the two[85,128]. *In vitro*, transcription profiling in high-invasion and low-invasion human pancreatic cancer cells lines suggests that there may be a particular genetic profile associated with PNI that could reveal targets for blocking or attenuating the process[264]. Therefore, future studies in which tumor cells that participate in PNI *in vivo* are isolated and transcriptionally profiled may critical insight necessary for understanding the mechanisms underlying tumor nerve interactions in PDAC and other cancers.

4.6 NEUROPLASTIC CHANGES IN THE PANCREAS OF PDAC MICE ALTER DRG PHENOTYPE

4.6.1 Sensitization of DRG neurons in PDAC

Neuroplastic changes frequently described in PDAC are similar to changes observed in inflammatory pancreatitis. Pancreatitis is associated with increased growth factor expression[167], hypertrophied nerve bundles[136,167] and sensitized pancreatic afferents, all of which are thought to increase pancreatitis-related pain[136,185]. In rodent models of pancreatitis, pancreatic sensory afferents upregulate non-specific cation channels, such as TRPV1 and TRPA1, and demonstrate hypersensitivity[210,211,214]. Given that chronic inflammation is also a component of PDAC, we hypothesized that similar changes in pancreatic sensory afferents would occur in PDAC mice.

In the DRG of PDAC mice >16 weeks of age, expression of *Trpv1* and *Trpa1* is significantly increased and at 10-12 weeks of age, there is a non-significant trend toward increased *Trpa1* expression. We would expect to see changes in the DRG similar to what has been described in pancreatitis at pre-cancer stages of PDAC progression, when there is often acute or chronic inflammation in the pancreas. However, the number of DRG neurons in the T9-T12 ganglia that innervate the pancreas is relatively small and based on the limited distribution of hyperinneravation at early time points, only a subset of pancreatic afferents is likely affected early. Therefore, when analyzing whole DRG gene expression, it could be difficult to detect early changes in a relatively small number of neurons.

Changes in TRP agonist evoked calcium transients in pancreas-specific DRG neurons, backlabeled with DiI, were examined using $Ca2^{+}$ imaging. Despite the increase in *Trpv1* and *Trpa1* expression in DRG T9-T12 of PDAC mice, there were no significant differences between

PDAC mice and controls in the number of DiI^+ cells responding to application of the of either the TRPV1 agonist capsaicin, or the TRPA1 agonist mustard oil. Increased expression of *Trpv1* and *Trpa1* in whole DRG could be due to either an increased number of cells expressing the ion channels, or due to higher levels of expression in cells already expressing the ion channels. The Ca^+ imaging results would suggest the latter. Pancreatic afferent neurons in PDAC mice did demonstrate significantly higher peaks in evoked calcium transients in response to administration of a 50mM KCl solution. Therefore, exposure to neurotrophic factors in the pancreas could drive both changes in TRP channel expression as well as changes in DRG neuron activation.

4.6.2 Neurogenic inflammation and PDAC disease progression

The observed changes in pancreatic afferent phenotype could underlie both the development of PDAC-related pain as well as drive neurogenic inflammation as has been previously described in rodent models of pancreatitis. Activation of TRPV1 in pancreatic afferents has been shown to drive neurogenic inflammation in the pancreas through release of peptides such as CGRP and SP, and importantly, blocking this process attenuates pain and inflammation[210,211,214,216,218] (reviewed in[137,191,207]). *Cgrp* expression is significantly increased in the DRG of PDAC mice > 16 weeks of age and there is a non-significant trend toward increased *SP* expression, suggesting that a similar process of peripheral afferent activation and neurogenic inflammation occurs in PDAC. The process of afferent sensitization and the development of neurogenic inflammation may begin at pre-malignant stages of disease progression as increased expression of *Cgrp* was in the DRG from PDAC mice at 10-12 weeks of age.

Chronic pancreatitis is associated with significantly increased the risk of pancreatic malignancy[13–17,37] and pancreatic inflammation has been shown to promote disease progression

and metastases in mouse models of PDAC[107–111,117]. Even a small population of sensitized pancreatic afferents localized to areas of PanIN and fibrosis at pre-tumor stages could drive neurogenic inflammation similar to what has been described in animal models of pancreatitis, and thereby contribute to or accelerate the progression from PanIN to PDAC.

4.7 SUMMARY

Early detection of PDAC is uncommon and little is known about how the nervous system might impact the transition from healthy pancreas to a pre-malignant PanIN stage to PDAC. Here we demonstrate that neuroplastic changes associated with human PDAC are also observed in a transgenic mouse model of PDAC. The similarities between the murine model of PDAC used in these studies and human PDAC are summarized in **Table 12**. Importantly, I have found that these changes begin at a pre-cancerous stage of disease, implying an active role of the nervous system in disease progression. Furthermore, we demonstrated changes in sensory afferents including higher peak evoked calcium transients and increased expression of TRP channels as well as peptides associated with the generation of neurogenic inflammation.

In conclusion, early neuroplastic changes in the pancreas are important not only for the subsequent development of PDAC-related pain, but also for driving disease progression from pre-malignant stages to cancer via sensory afferent sensitization and neurogenic inflammation (**Figure 25**). Given that prominent PNI and tumor-nerve interactions have been described in a number of malignancies, interventions targeting the peripheral nervous system represent a novel tumor treatment strategy for variety of cancers, including PDAC.

Table 12. Comparison of murine and human PDAC

	PDAC Mice	Human PDAC	Is Murine Model Useful?
Histological Progression	-PanIN to PDAC -Multiple tumor loci	-PanIN to PDAC -Single tumor locus	Progression from pre-cancer lesions to malignancy in murine model closely parallels human disease. However the multiple tumor loci in the pancreas of PDAC mice could result in earlier detection of disease-related symptoms (e.g., pain) and pathology (e.g., inflammation).
Tumor Sequelae	-Jaundice -Bloody abdominal ascites -Enlarged gall bladder and/or common bile duct	-Jaundice -Anorexia -Weight loss -Cachexia -Abdominal ascites -Courvoisier's sign -Gastric outlet obstruction/ delayed gastric emptying -Nausea/vomiting -Diarrhea	Some signs associated with human PDAC, such as jaundice and abdominal ascites, are observed in PDAC mice. However, many of the symptoms such as anorexia and nausea/vomiting cannot be assessed. Additionally, weight loss and cachexia were not observed in PDAC mice, suggesting this murine model is not useful for studying these PDAC sequelae.
Common Metastases	-Liver -Peritoneum -Lung	-Liver -Peritoneum -Lung	A similar pattern of metastases is observed in PDAC mice and human PDAC, suggesting PDAC mice are a useful for studying disease dissemination.
Neuroplastic Changes	-Hyperinnervation beginning at PanIN-only stage	-Increased neural density -Neuritis	Similar neuroplastic changes are observed in murine and human PDAC suggesting that PDAC mice are a useful model for studying changes in pancreatic innervation throughout PDAC development and progression.
Neurotrophic Factors (and receptors)	-Increased neurotrophic factor expression beginning at PanIN-only stage -Expression of neurotrophic factors in murine PDAC cell lines	-Increased neurotrophic factor expression in PDAC tissue -Expression of neurotrophic factors in human PDAC cell lines	Similar profiles of neurotrophic factor expression are observed in the pancreas of PDAC mice and human PDAC tissue. Both murine and human PDAC cell lines express a variety of neurotrophic factors and receptors. This suggests neurotrophic factors play an important role in the tumor microenvironment and PDAC mice are a useful model for studying that role.
PNI	-Present in extra-pancreatic ganglia	-Present in intra-pancreatic nerves -Present in extra-pancreatic nerve plexuses	Although intra-pancreatic PNI was not definitively observed in PDAC mice, the presence of extra-pancreatic PNI suggests similar modes of tumor spread along nerves in PDAC mice and human PDAC. Thus, PDAC mice are a useful model for studying tumor-nerve interactions including PNI.
Pain	-Hunching observed at PanIN-only stages could represent early, pain associated with pre-malignant lesions -Pain-related behavior is observed after the development of PDAC	-Pain is a common symptoms at presentation and becomes more prevalent/severe with disease progression	Pain-related postural changes may be present at pre-cancer stages in PDAC mice but not in human PDAC. However, the development of pain-related behavior changes after PDAC is present in PDAC mice suggests that this murine model will be useful for studying tumor-nerve interactions that underlie the development of PDAC pain.

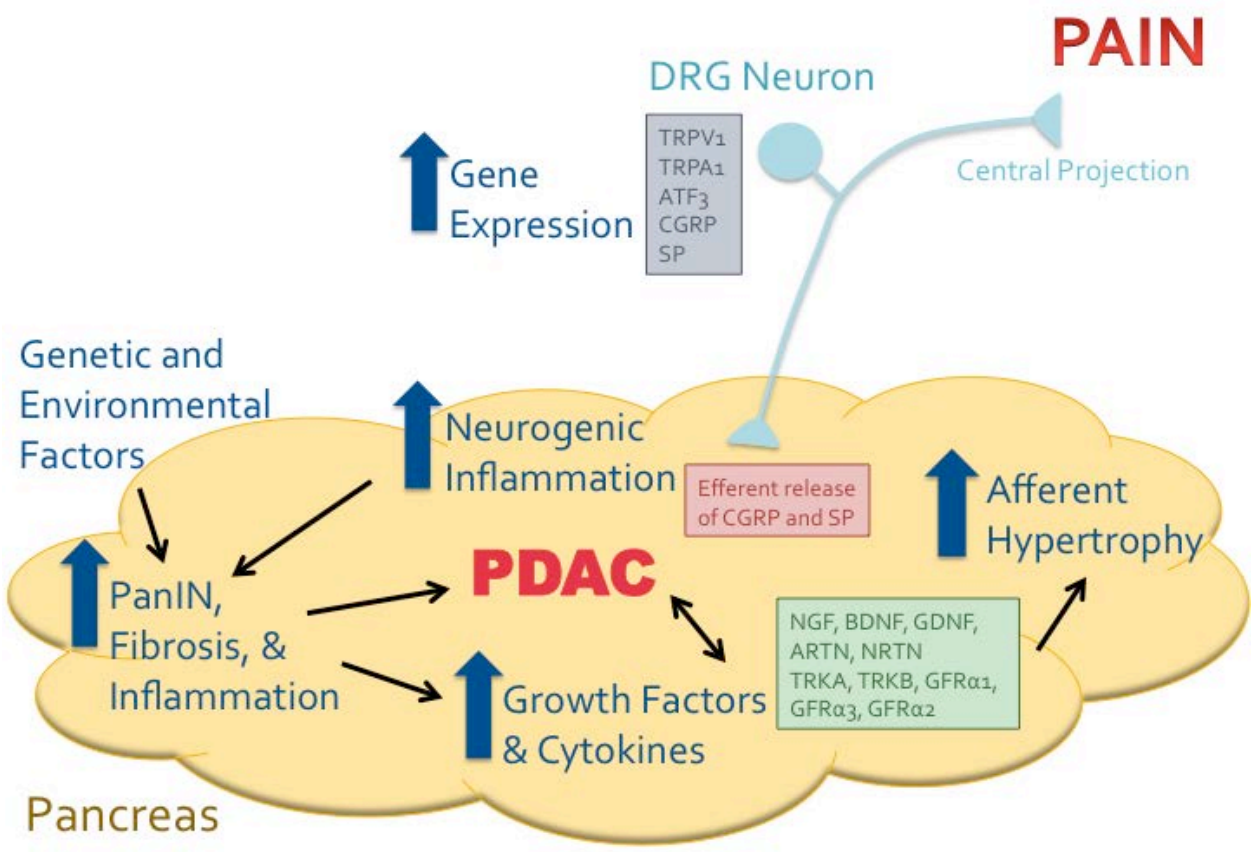

Figure 25. Afferent sensitization, pain, and neurogenic inflammation in PDAC

Genetic and environmental factors contribute to the development of PanIN lesions, fibrosis, and inflammation that can result in PDAC. During PDAC development, increased production of neurotrophic factors and cytokines in the pancreas sensitize pancreatic afferents, leading to changes in pancreatic innervation and altered gene expression in dorsal root ganglia (DRG) neurons. Increased expression of nociception-related genes such as TRPV1 and TRPA1 increase the excitability of pancreatic afferent neurons causing pain. These changes contribute to increased release of CGRP and SP, neuropeptides that underlie neurogenic inflammation in the pancreas, driving disease progression from precancerous PanIN lesions to PDAC.

4.8 FUTURE DIRECTIONS

In future studies I will directly test the hypothesis that blocking neurotrophic factor signaling in the pancreas of PDAC mice will prevent or attenuate changes in pancreatic afferent phenotype and PDAC-related pain by inhibiting neurotrophic factor signaling by injection of antibodies that bind neurotrophic factors such as NGF[214,226,232–234,241] or by treatment with a small molecule TRK inhibitor[231]. We predict that blocking neurotrophic factor signaling in the pancreas will prevent changes in gene expression in pancreatic afferents, and attenuate PDAC-related pain. Blocking afferent sensitization should also prevent neurogenic inflammation in the pancreas and delay the development and/or progression of tumor growth in PDAC mice. We will further examine the role of neurogenic inflammation in the development and progress of PDAC using two additional strategies targeting pancreatic afferents: treatment with TRP channel antagonists that have been shown to be effective in attenuating inflammation and pain associated with acute and chronic pancreatitis[210,211] and denervation of sensory afferents via neonatal capsaicin treatment[216,221,267,268].

It is possible that use of these strategies may block afferent sensitization, PDAC-related pain, and neurogenic inflammation, but not influence tumor development or progression in PDAC mice. This would suggest that peripheral nervous system participation is not required for disease progression, however it would not rule out its contribution to the disease. Furthermore, prevention of PDAC-related pain in PDAC mice using either of the first two strategies could lead to new strategies for treating cancer pain in patients with PDAC that may significantly improve quality of life.

5.0 BIBLIOGRAPHY

1. American Cancer Society Cancer Facts & Figures 2013. *Atlanta: American Cancer Society* (2013).
2. Klimstra, D. S. Nonductal neoplasms of the pancreas. *Modern pathology* **20 Suppl 1**, S94–112 (2007).
3. Porta, M. *et al.* Exocrine pancreatic cancer: symptoms at presentation and their relation to tumour site and stage. *Clinical & translational oncology* **7**, 189–97 (2005).
4. Sohn, T. A. *et al.* Resected Adenocarcinoma of the Pancreas 616 Patients : Results , Outcomes , and Prognostic Indicators. *Journal of gastrointestinal surgery* **4**, 567–579 (2000).
5. Silverman, D. T. *et al.* Why Do Black Americans Have a Higher Risk of Pancreatic Cancer than White Americans. *Epidemiology* **14**, 45–54 (2003).
6. Iodice, S., Gandini, S., Maisonneuve, P. & Lowenfels, A. B. Tobacco and the risk of pancreatic cancer: a review and meta-analysis. *Langenbeck's archives of surgery / Deutsche Gesellschaft für Chirurgie* **393**, 535–45 (2008).
7. Arslan, A. A. *et al.* Anthropometric Measures, Body Mass Index, and Pancreatic Cancer. *Archives of Internal Medicine* **170**, 791–802 (2010).
8. Aune, D. *et al.* Body mass index, abdominal fatness and pancreatic cancer risk: a systematic review and non-linear dose-response meta-analysis of prospective studies. *Annals of oncology* **23**, 843–52 (2012).
9. Tramacere, I. *et al.* Alcohol drinking and pancreatic cancer risk: a meta-analysis of the dose-risk relation. *International journal of cancer.* **126**, 1474–86 (2010).
10. Huxley, R., Ansary-Moghaddam, a, Berrington de González, a, Barzi, F. & Woodward, M. Type-II diabetes and pancreatic cancer: a meta-analysis of 36 studies. *British journal of cancer* **92**, 2076–83 (2005).
11. Stevens, R. J., Roddam, a W. & Beral, V. Pancreatic cancer in type 1 and young-onset diabetes: systematic review and meta-analysis. *British Journal of Cancer* **96**, 507–509 (2007).
12. Chari, S. T. *et al.* Pancreatic cancer-associated diabetes mellitus: prevalence and temporal association with diagnosis of cancer. *Gastroenterology* **134**, 95–101 (2008).
13. Raimondi, S., Lowenfels, A. B., Morselli-Labate, A. M., Maisonneuve, P. & Pezzilli, R. Pancreatic cancer in chronic pancreatitis; aetiology, incidence, and early detection. *Best practice & research. Clinical gastroenterology* **24**, 349–58 (2010).
14. Whitcomb, D. C. & Pogue-Geile, K. Pancreatitis as a risk for pancreatic cancer. *Gastroenterology Clinics of North America* **31**, 663–678 (2002).

15. Whitcomb, D. C., Applebaum, S. & Martin, S. P. Hereditary pancreatitis and pancreatic carcinoma. *Annals of the New York Academy of Sciences* **880**, 201–9 (1999).
16. Lowenfels, A. B. *et al.* Pancreatitis and the risk of pancreatic cancer. *New England Journal of Medicine* **328**, 1433–7 (1993).
17. Whitcomb, D. C. Inflammation and Cancer V. Chronic pancreatitis and pancreatic cancer. *American journal of physiology. Gastrointestinal and liver physiology* **287**, G315–9 (2004).
18. Permuth-Wey, J. & Egan, K. M. Family history is a significant risk factor for pancreatic cancer: results from a systematic review and meta-analysis. *Familial cancer* **8**, 109–17 (2009).
19. Petersen, G. M. *et al.* Pancreatic cancer genetic epidemiology consortium. *Cancer epidemiology, biomarkers & prevention* **15**, 704–10 (2006).
20. Vincent, A., Herman, J., Schulick, R., Hruban, R. H. & Goggins, M. Pancreatic cancer. *Lancet* **378**, 607–20 (2011).
21. Shi, C., Hruban, R. H. & Klein, A. P. Familial Pancreatic Cancer. *Archives of pathology & laboratory medicine* **133**, 365–374 (2009).
22. Olson, S. H. & Kurtz, R. C. Epidemiology of pancreatic cancer and the role of family history. *Journal of surgical oncology* **107**, 1–7 (2013).
23. Grover, S. & Syngal, S. Hereditary pancreatic cancer. *Gastroenterology* **139**, 1076–80, 1080.e1–2 (2010).
24. Couch, F. J. *et al.* The prevalence of BRCA2 mutations in familial pancreatic cancer. *Cancer epidemiology, biomarkers & prevention* **16**, 342–6 (2007).
25. Murphy, K. M. *et al.* Evaluation of Candidate Genes MAP2K4 , MADH4 , ACVR1B , and BRCA2 in Familial Pancreatic Cancer : Deleterious BRCA2 Mutations in 17 %. *Cancer Research* **62**, 3789–3793 (2002).
26. Goggins, M. *et al.* Germline BRCA2 Gene Mutations in Patients with Apparently Sporadic Pancreatic Carcinomas. *Cnacner Research* **56**, 5360–5364 (1996).
27. Thompson, D. & Easton, D. F. Cancer Incidence in BRCA1 mutation carriers. *Journal of the National Cancer Institute* **94**, 1358–65 (2002).
28. Iqbal, J. *et al.* The incidence of pancreatic cancer in BRCA1 and BRCA2 mutation carriers. *British journal of cancer* **107**, 2005–9 (2012).
29. Lal, G. *et al.* Inherited Predisposition to Pancreatic Adenocarcinoma : Role of Family History and Germ-Line p16 , BRCA1 , and BRCA2 Mutations. *Cancer Research* **60**, 409–416 (2000).
30. Lynch, H. T., Fusaro, R. M., Lynch, J. F. & Brand, R. Pancreatic cancer and the FAMMM syndrome. *Familial cancer* **7**, 103–12 (2008).
31. Goldstein, A. M. *et al.* Increased risk of pancreatic cancer in melanoma-prone kindreds with p16INK4 mutations. *The New England journal of medicine* **333**, 1433–7 (1995).
32. Van Lier, M. G. F. *et al.* High cancer risk in Peutz-Jeghers syndrome: a systematic review and surveillance recommendations. *The American journal of gastroenterology* **105**, 1258–64; author reply 1265 (2010).
33. Kastrinos, F. *et al.* Risk of pancreatic cancer in families with Lynch syndrome. *JAMA* **302**, 1790–5 (2009).
34. Su, G. H. *et al.* Germline and somatic mutations of the STK11/LKB1 Peutz-Jeghers gene in pancreatic and biliary cancers. *The American journal of pathology* **154**, 1835–40 (1999).

35. Roberts, N. J. *et al.* ATM mutations in patients with hereditary pancreatic cancer. *Cancer discovery* **2**, 41–6 (2012).
36. Whitcomb, D. C. *et al.* Hereditary pancreatitis is caused by a mutation in the cationic trypsinogen gene. *Nature Genetics* **14**, 141–145 (1996).
37. Rebours, V. *et al.* Risk of pancreatic adenocarcinoma in patients with hereditary pancreatitis: a national exhaustive series. *The American journal of gastroenterology* **103**, 111–9 (2008).
38. Bilimoria, K. Y. *et al.* Validation of the 6th edition AJCC Pancreatic Cancer Staging System: report from the National Cancer Database. *Cancer* **110**, 738–44 (2007).
39. Hidalgo, M. Pancreatic cancer. *The New England journal of medicine* **362**, 1605–17 (2010).
40. Kato, K. *et al.* Prognostic factors for survival after extended pancreatectomy for pancreatic head cancer: influence of resection margin status on survival. *Pancreas* **38**, 605–12 (2009).
41. Franko, J., Hugec, V., Lopes, T. L. & Goldman, C. D. Survival Among Pancreaticoduodenectomy Patients Treated for Pancreatic Head Cancer <1 or 2 cm. *Annals of surgical oncology* **20**, 357–61 (2013).
42. Manabe, T. *et al.* Small Carcinoma of the Pancreas. Clinical and Pathologic evaluation of 17 Patients. *Cancer* **62**, 135–141 (1988).
43. Tsuchiya, R. *et al.* Collective review of small carcinomas of the pancreas. *Annals of surgery* **203**, 77–81 (1986).
44. National Comprehensive Cancer Network *NCCN Clinical Practice Guidelines in Oncology (NCCN Guidelines®) Pancreatic Adenocarcinoma, Version 1.2013*. (2013).
45. Yeo, C. J. *et al.* Pancreaticoduodenectomy for cancer of the head of the pancreas. 201 Patients. *Annals of surgery* **221**, 721–733 (1995).
46. Hernandez, J. M. *et al.* CA 19-9 velocity predicts disease-free survival and overall survival after pancreatectomy of curative intent. *Journal of gastrointestinal surgery* **13**, 349–53 (2009).
47. Berger, A. C. *et al.* Postresection CA 19-9 predicts overall survival in patients with pancreatic cancer treated with adjuvant chemoradiation: a prospective validation by RTOG 9704. *Journal of clinical oncology* **26**, 5918–22 (2008).
48. Lim, J. E., Chien, M. W. & Earle, C. C. Prognostic factors following curative resection for pancreatic adenocarcinoma: a population-based, linked database analysis of 396 patients. *Annals of surgery* **237**, 74–85 (2003).
49. Nitecki, S. S., Sarr, M. G., Colby, T. V & Van Heerden, J. A. Long-Term Survival After Resection for Ductal Adenocarcinoma of the Pancreas. Is it Really Improving? *Annals of surgery* **221**, 59–66 (1995).
50. Helm, J. *et al.* Histologic characteristics enhance predictive value of American Joint Committee on Cancer staging in resectable pancreas cancer. *Cancer* **115**, 4080–9 (2009).
51. Botsis, T. & Anagnostou, V. K. Cancer Informatics Modeling prognostic Factors in Resectable pancreatic Adenocarcinomas. *Cancer Informatics* 281–291
52. Murakami, Y. *et al.* Prognostic impact of para-aortic lymph node metastasis in pancreatic ductal adenocarcinoma. *World journal of surgery* **34**, 1900–7 (2010).
53. Garcea, G. *et al.* Tumour characteristics predictive of survival following resection for ductal adenocarcinoma of the head of pancreas. *European journal of surgical oncology* **33**, 892–7 (2007).

54. Chen, J. W. C. *et al.* Predicting patient survival after pancreaticoduodenectomy for malignancy: histopathological criteria based on perineural infiltration and lymphovascular invasion. *HPB* **12**, 101–8 (2010).
55. Mitsunaga, S. *et al.* Detail Histologic Analysis of Nerve Plexus Invasion in Invasive Ductal Carcinoma of the Pancreas and Its Prognostic Impact. *American journal of surgical pathology* **31**, 1636–1644 (2007).
56. Ozaki, H. *et al.* The prognostic significance of lymph node metastasis and intrapancreatic perineural invasion in pancreatic cancer after curative resection. *Surgery today* **29**, 16–22 (1999).
57. Sudo, T. *et al.* Prognostic impact of perineural invasion following pancreatoduodenectomy with lymphadenectomy for ampullary carcinoma. *Digestive diseases and sciences* **53**, 2281–6 (2008).
58. Willett, C. G., Lewandrowski, K., Warshaw, a L., Efird, J. & Compton, C. C. Resection margins in carcinoma of the head of the pancreas. Implications for radiation therapy. *Annals of surgery* **217**, 144–8 (1993).
59. Abrams, R. A. Radiotherapy in the adjuvant management of pancreatic adenocarcinoma: is it helpful? *Expert Review of Gastroenterology and Hepatology* 149 (2012).
60. Evans, D. B. *et al.* Preoperative gemcitabine-based chemoradiation for patients with resectable adenocarcinoma of the pancreatic head. *Journal of clinical oncology* **26**, 3496–502 (2008).
61. Alter, C. L. Palliative and supportive care of patients with pancreatic cancer. *Seminars in oncology* **23**, 229–40 (1996).
62. Singh, S. M., Longmire Jr, W. P. & Reber, H. A. Surgical Palliation for Pancreatic Cancer. *Annals of surgery* **212**, 132–139 (1990).
63. Gourgou-Bourgade, S. *et al.* Impact of FOLFIRINOX compared with gemcitabine on quality of life in patients with metastatic pancreatic cancer : results from the PRODIGE 4 / ACCORD 11 randomized trial. *Journal of Clinical Oncology* **31**, 23–9 (2013).
64. Rothenberg, M. L. *et al.* A phase II trial of gemcitabine in patients with 5-FU-refractory pancreas cancer. *Annals of Oncology* **7**, 347–353 (1996).
65. Holly, E. a, Chaliha, I., Bracci, P. M. & Gautam, M. Signs and symptoms of pancreatic cancer: a population-based case-control study in the San Francisco Bay area. *Clinical gastroenterology and hepatology* **2**, 510–7 (2004).
66. Modolell, I., Guarner, L. & Malagelada, J. R. Vagaries of clinical presentation of pancreatic and biliary tract cancer. *Annals of Oncology* **10**, S82–S84 (1999).
67. Warshaw, A. L. & Fernandez-del Castillo, C. Pancreatic Carcinoma. *The New England journal of medicine* **326**, 455–465 (1992).
68. Kalser, M. H., Barkin, J. & MacIntyre, J. M. Pancreatic Cancer. Assessment of Prognosis by Clinical Presentation. *Cancer* **56**, 397–402 (1985).
69. Barkin, J. S., Goldberg, R. I., Sfakianakis, G. N. & Levi, J. Pancreatic carcinoma is associated with delayed gastric emptying. *Digestive diseases and sciences* **31**, 265–7 (1986).
70. Holland, J. C. *et al.* Comparative Psychological Disturbance in Patients with Pancreatic and Gastric Cancer. *American journal of Psychiatry* **143**, 982–986 (1986).
71. Jia, L. *et al.* Investigation of the incidence of pancreatic cancer-related depression and its relationship with the quality of life of patients. *Digestion* **82**, 4–9 (2010).

72. Kelsen, D. P. *et al.* Pain and depression in patients with newly diagnosed pancreas cancer. *Journal of clinical oncology* **13**, 748–55 (1995).
73. Perez, M. M., Newcomer, a D., Moertel, C. G., Go, V. L. & Dimagno, E. P. Assessment of weight loss, food intake, fat metabolism, malabsorption, and treatment of pancreatic insufficiency in pancreatic cancer. *Cancer* **52**, 346–52 (1983).
74. Hezel, A. F., Kimmelman, A. C., Stanger, B. Z., Bardeesy, N. & Depinho, R. a Genetics and biology of pancreatic ductal adenocarcinoma. *Genes & development* **20**, 1218–49 (2006).
75. Andea, A., Sarkar, F. & Adsay, V. N. Clinicopathological correlates of pancreatic intraepithelial neoplasia: a comparative analysis of 82 cases with and 152 cases without pancreatic ductal adenocarcinoma. *Modern pathology* **16**, 996–1006 (2003).
76. Hruban, R. H. *et al.* Pancreatic intraepithelial neoplasia: a new nomenclature and classification system for pancreatic duct lesions. *The American journal of surgical pathology* **25**, 579–86 (2001).
77. Brune, K. *et al.* Multifocal neoplastic precursor lesions associated with lobular atrophy of the pancreas in patients having a strong family history of pancreatic cancer. *The American journal of surgical pathology* **30**, 1067–76 (2006).
78. Detlefsen, S., Sipos, B., Feyerabend, B. & Klöppel, G. Pancreatic fibrosis associated with age and ductal papillary hyperplasia. *Virchows Archiv : an international journal of pathology* **447**, 800–5 (2005).
79. Fernández-del Castillo, C. & Adsay, N. V. Intraductal papillary mucinous neoplasms of the pancreas. *Gastroenterology* **139**, 708–13, 713.e1–2 (2010).
80. Jimenez, R. E. *et al.* Sequential accumulation of K-ras mutations and p53 overexpression in the progression of pancreatic mucinous cystic neoplasms to malignancy. *Annals of surgery* **230**, 501–9; discussion 509–11 (1999).
81. Wasif, N. *et al.* Impact of tumor grade on prognosis in pancreatic cancer: should we include grade in AJCC staging? *Annals of surgical oncology* **17**, 2312–20 (2010).
82. Hruban, R. H. *et al.* K-ras Oncogene Activation in Adenocarcinoma of the Human Pancreas A Study of 82 Carcinomas Using a Combination of Mutant-Enriched Polymerase Chain Reaction Analysis and Allele-Specific Oligonucleotide Hybridization. *American journal of pathology* **143**, 545–554 (1993).
83. Jones, S. *et al.* Core signaling pathways in human pancreatic cancers revealed by global genomic analyses. *Science* **321**, 1801–6 (2008).
84. Almoguera, C. *et al.* Most human carcinomas of the exocrine pancreas contain mutant c-K-ras genes. *Cell* **53**, 549–54 (1988).
85. Biankin, A. V *et al.* Pancreatic cancer genomes reveal aberrations in axon guidance pathway genes. *Nature* **491**, 399–405 (2012).
86. Wittinghofer, A., Scheffzek, K. & Ahmadian, M. R. The interaction of Ras with GTPase-activating proteins. *FEBS Letters* **410**, 63–67 (1997).
87. Z'graggen, K. *et al.* Prevalence of activating K-ras mutations in the evolutionary stages of neoplasia in intraductal papillary mucinous tumors of the pancreas. *Annals of surgery* **226**, 491–8; discussion 498–500 (1997).
88. Moskaluk, C. A., Hruban, R. H. & Kern, S. E. p16 and K-ras Gene Mutations in the Intraductal Precursors of Human Pancreatic Adenocarcinoma. **57**, 2140–2143 (1997).
89. Hingorani, S. R. *et al.* Preinvasive and invasive ductal pancreatic cancer and its early detection in the mouse. *Cancer cell* **4**, 437–50 (2003).

90. Collins, M. A. *et al.* Oncogenic Kras is required for both the initiation and maintenance of pancreatic cancer in mice. *The Journal of Clinical Investigation* **122**, 639–653 (2012).
91. Caldas, C. *et al.* Frequent somatic mutations and homozygous deletions of the p16 (MTS1) gene in pancreatic adenocarcinoma. *Nature Genetics* **8**, 27–32 (1994).
92. Schutte, M. *et al.* Abrogation of the Rb/p16 Tumor-suppressive Pathway in Virtually All Pancreatic Carcinomas. *Cancer Research* **57**, 3126–3130 (1997).
93. Redston, M. S. *et al.* p53 Mutations in Pancreatic Carcinoma and Evidence of Common Involvement of Homocopolymer Tracts in DNA Microdeletions. *Cancer Research* **54**, 3025–3033 (1994).
94. Hahn, S. a *et al.* DPC4, a candidate tumor suppressor gene at human chromosome 18q21.1. *Science* **271**, 350–3 (1996).
95. Rozenblum, E. *et al.* Tumor-suppressive Pathways in Pancreatic Carcinoma. *Cancer Research* **57**, 1731–1734 (1997).
96. Derynck, R. & Zhang, Y. E. Smad-dependent and Smad- independent pathways in TGF-beta family signalling. *Nature* **425**, 577–584 (2003).
97. Goggins, M. *et al.* Genetic Alterations of the Transforming Growth Factor β Receptor Genes in Pancreatic and Biliary Adenocarcinomas. *Cancer Research* **58**, 5329–5332 (1998).
98. Farrow, B., Albo, D. & Berger, D. H. The role of the tumor microenvironment in the progression of pancreatic cancer. *The Journal of surgical research* **149**, 319–28 (2008).
99. Mihaljevic, A. L., Michalski, C. W., Friess, H. & Kleeff, J. Molecular mechanism of pancreatic cancer--understanding proliferation, invasion, and metastasis. *Langenbeck's archives of surgery* **395**, 295–308 (2010).
100. Chu, G. C., Kimmelman, A. C., Hezel, A. F. & DePinho, R. a Stromal biology of pancreatic cancer. *Journal of cellular biochemistry* **101**, 887–907 (2007).
101. Evans, A. & Costello, E. The role of inflammatory cells in fostering pancreatic cancer cell growth and invasion. *Frontiers in physiology* **3**, 270 (2012).
102. Steele, C. W. *et al.* Exploiting inflammation for therapeutic gain in pancreatic cancer. *British journal of cancer* 997–1003 (2013).doi:10.1038/bjc.2013.24
103. Farrow, B. & Evers, B. M. Inflammation and the development of pancreatic cancer. *Surgical oncology* **10**, 153–69 (2002).
104. Kuraishy, A., Karin, M. & Grivennikov, S. I. Tumor promotion via injury- and death-induced inflammation. *Immunity* **35**, 467–77 (2011).
105. Löhr, M., Maisonneuve, P. & Lowenfels, a B. K-Ras mutations and benign pancreatic disease. *International journal of pancreatology* **27**, 93–103 (2000).
106. Rivera, J. a *et al.* Analysis of K-ras oncogene mutations in chronic pancreatitis with ductal hyperplasia. *Surgery* **121**, 42–9 (1997).
107. Carrière, C., Young, A. L., Gunn, J. R., Longnecker, D. S. & Korc, M. Acute pancreatitis markedly accelerates pancreatic cancer progression in mice expressing oncogenic Kras. *Biochemical and biophysical research communications* **382**, 561–5 (2009).
108. Carrière, C., Young, A. L., Gunn, J. R., Longnecker, D. S. & Korc, M. Acute pancreatitis accelerates initiation and progression to pancreatic cancer in mice expressing oncogenic Kras in the nestin cell lineage. *PloS one* **6**, e27725 (2011).
109. Guerra, C. *et al.* Chronic pancreatitis is essential for induction of pancreatic ductal adenocarcinoma by K-Ras oncogenes in adult mice. *Cancer cell* **11**, 291–302 (2007).

110. Guerra, C. *et al.* Pancreatitis-induced inflammation contributes to pancreatic cancer by inhibiting oncogene-induced senescence. *Cancer cell* **19**, 728–39 (2011).
111. Fukuda, A. *et al.* Stat3 and MMP7 Contribute to Pancreatic Ductal Adenocarcinoma Initiation and Progression. *Cancer cell* **19**, 441–55 (2011).
112. Bachem, M. G. *et al.* Pancreatic carcinoma cells induce fibrosis by stimulating proliferation and matrix synthesis of stellate cells. *Gastroenterology* **128**, 907–921 (2005).
113. Tang, D. *et al.* Persistent activation of pancreatic stellate cells creates a microenvironment favorable for the malignant behavior of pancreatic ductal adenocarcinoma. *International journal of cancer* **132**, 993–1003 (2013).
114. Masamune, A., Watanabe, T., Kikuta, K. & Shimosegawa, T. Roles of pancreatic stellate cells in pancreatic inflammation and fibrosis. *Clinical gastroenterology and hepatology* **7**, S48–54 (2009).
115. Erkan, M. *et al.* The activated stroma index is a novel and independent prognostic marker in pancreatic ductal adenocarcinoma. *Clinical gastroenterology and hepatology* **6**, 1155–61 (2008).
116. Olive, K. P. *et al.* Inhibition of Hedgehog signaling enhances delivery of chemotherapy in a mouse model of pancreatic cancer. *Science* **324**, 1457–61 (2009).
117. Rhim, A. D. *et al.* EMT and dissemination precede pancreatic tumor formation. *Cell* **148**, 349–61 (2012).
118. Liu, B. & Lu, K.-Y. Neural invasion in pancreatic carcinoma. *Hepatobiliary & pancreatic diseases international* **1**, 469–76 (2002).
119. Bapat, A. a, Hostetter, G., Von Hoff, D. D. & Han, H. Perineural invasion and associated pain in pancreatic cancer. *Nature reviews. Cancer* **11**, 695–707 (2011).
120. Liebig, C., Ayala, G., Wilks, J. a, Berger, D. H. & Albo, D. Perineural invasion in cancer: a review of the literature. *Cancer* **115**, 3379–91 (2009).
121. Demir, I. E. *et al.* Neural Invasion in Pancreatic Cancer: The Past, Present and Future. *Cancers* **2**, 1513–1527 (2010).
122. Marchesi, F., Piemonti, L., Mantovani, A. & Allavena, P. Molecular mechanisms of perineural invasion, a forgotten pathway of dissemination and metastasis. *Cytokine & growth factor reviews* **21**, 77–82 (2010).
123. Cozzi, G. *et al.* Perineural invasion as a predictor of extraprostatic extension of prostate cancer: A systematic review and meta-analysis. *Scandinavian journal of urology* 1–6 (2013).doi:10.3109/21681805.2013.776106
124. Harnden, P. *et al.* The prognostic significance of perineural invasion in prostatic cancer biopsies: a systematic review. *Cancer* **109**, 13–24 (2007).
125. Mendenhall, W. M. *et al.* Cutaneous head and neck basal and squamous cell carcinomas with perineural invasion. *Oral oncology* **48**, 918–22 (2012).
126. King, T. *et al.* Contribution of afferent pathways to nerve injury-induced spontaneous pain and evoked hypersensitivity. *Pain* **152**, 1997–2005 (2011).
127. Binmadi, N. O. & Basile, J. R. Perineural invasion in oral squamous cell carcinoma: a discussion of significance and review of the literature. *Oral oncology* **47**, 1005–10 (2011).
128. Ceyhan, G. O. *et al.* Neural invasion in pancreatic cancer: a mutual tropism between neurons and cancer cells. *Biochemical and biophysical research communications* **374**, 442–7 (2008).
129. Pour, P. M., Bell, R. H. & Batra, S. K. Neural invasion in the staging of pancreatic cancer. *Pancreas* **26**, 322–5 (2003).

130. Hirai, I. *et al.* Perineural invasion in pancreatic cancer. *Pancreas* **24**, 15–25 (2002).
131. Chatterjee, D. *et al.* Perineural and intraneural invasion in posttherapy pancreaticoduodenectomy specimens predicts poor prognosis in patients with pancreatic ductal adenocarcinoma. *The American journal of surgical pathology* **36**, 409–17 (2012).
132. Takahashi, T., Ishikura, H. & Motohara, T. Perineural Invasion by Ductal Adenocarcinoma of the Pancreas. *Journal of Surgical Oncology* 164–170 (1997).
133. Takahashi, H. *et al.* Perineural invasion and lymph node involvement as indicators of surgical outcome and pattern of recurrence in the setting of preoperative gemcitabine-based chemoradiation therapy for resectable pancreatic cancer. *Annals of surgery* **255**, 95–102 (2012).
134. Kayahara, M., Nakagawara, H., Kitagawa, H. & Ohta, T. The nature of neural invasion by pancreatic cancer. *Pancreas* **35**, 218–23 (2007).
135. Kanda, M. *et al.* Pattern of lymph node metastasis spread in pancreatic cancer. *Pancreas* **40**, 951–5 (2011).
136. Ceyhan, G. O. *et al.* Pancreatic neuropathy and neuropathic pain--a comprehensive pathomorphological study of 546 cases. *Gastroenterology* **136**, 177–186.e1 (2009).
137. Liddle, R. a & Nathan, J. D. Neurogenic inflammation and pancreatitis. *Pancreatology* **4**, 551–9; discussion 559–60 (2004).
138. Li, X. *et al.* Neurotransmitter Substance P Mediates Pancreatic Cancer Perineural Invasion via NK-1R in Cancer Cells. *Molecular cancer research* **11**, 294–302 (2013).
139. Marchesi, F. *et al.* The chemokine receptor CX3CR1 is involved in the neural tropism and malignant behavior of pancreatic ductal adenocarcinoma. *Cancer research* **68**, 9060–9 (2008).
140. Ben, Q.-W. *et al.* Positive expression of L1-CAM is associated with perineural invasion and poor outcome in pancreatic ductal adenocarcinoma. *Annals of surgical oncology* **17**, 2213–21 (2010).
141. Swanson, B. J. *et al.* MUC1 is a counter-receptor for myelin-associated glycoprotein (Siglec-4a) and their interaction contributes to adhesion in pancreatic cancer perineural invasion. *Cancer research* **67**, 10222–9 (2007).
142. Airaksinen, M. S. & Saarma, M. The GDNF family: signalling, biological functions and therapeutic value. *Nature reviews. Neuroscience* **3**, 383–94 (2002).
143. Huang, E. J. & Reichardt, L. F. Neurotrophins: Roles in Neuronal Development and Function. *Annual Review Neuroscience* **24**, 677–736 (2001).
144. Huang, E. J. & Reichardt, L. F. Trk receptors: roles in neuronal signal transduction. *Annual review of biochemistry* **72**, 609–42 (2003).
145. Molliver, D. C., Lindsay, J., Albers, K. M. & Davis, B. M. Overexpression of NGF or GDNF alters transcriptional plasticity evoked by inflammation. *Pain* **113**, 277–84 (2005).
146. Wang, S., Elitt, C. M., Malin, S. a & Albers, K. M. Effects of the neurotrophic factor artemin on sensory afferent development and sensitivity. *Sheng li xue bao : [Acta physiologica Sinica]* **60**, 565–70 (2008).
147. Elitt, C. M. *et al.* Artemin overexpression in skin enhances expression of TRPV1 and TRPA1 in cutaneous sensory neurons and leads to behavioral sensitivity to heat and cold. *The Journal of neuroscience* **26**, 8578–87 (2006).
148. Elitt, C. M., Malin, S. a, Koerber, H. R., Davis, B. M. & Albers, K. M. Overexpression of artemin in the tongue increases expression of TRPV1 and TRPA1 in trigeminal afferents

and causes oral sensitivity to capsaicin and mustard oil. *Brain research* **1230**, 80–90 (2008).
149. Malin, S. a & Davis, B. M. Postnatal roles of glial cell line-derived neurotrophic factor family members in nociceptors plasticity. *Sheng li xue bao : [Acta physiologica Sinica]* **60**, 571–8 (2008).
150. Shu, X. & Mendell, L. M. Nerve growth factor acutely sensitizes the response of adult rat sensory neurons to capsaicin. *Neuroscience letters* **274**, 159–62 (1999).
151. Shu, X. & Mendell, L. M. Acute Sensitization by NGF of the Response of Small-Diameter Sensory Neurons to Capsaicin. *Journal of neurophysiology* **86**, 2931–2938 (2001).
152. Ciobanu, C., Reid, G. & Babes, A. Acute and chronic effects of neurotrophic factors BDNF and GDNF on responses mediated by thermo-sensitive TRP channels in cultured rat dorsal root ganglion neurons. *Brain research* **1284**, 54–67 (2009).
153. Malik-Hall, M., Dina, O. a & Levine, J. D. Primary afferent nociceptor mechanisms mediating NGF-induced mechanical hyperalgesia. *The European journal of neuroscience* **21**, 3387–94 (2005).
154. Schmutzler, B. S., Roy, S. & Hingtgen, C. M. Glial cell line-derived neurotrophic factor family ligands enhance capsaicin-stimulated release of calcitonin gene-related peptide from sensory neurons. *Neuroscience* **161**, 148–56 (2009).
155. Ceyhan, G. O. *et al.* The neurotrophic factor artemin promotes pancreatic cancer invasion. *Annals of surgery* **244**, 274–81 (2006).
156. Ceyhan, G. O. *et al.* Nerve growth factor and artemin are paracrine mediators of pancreatic neuropathy in pancreatic adenocarcinoma. *Annals of surgery* **251**, 923–31 (2010).
157. Zhu, B. Z. *et al.* Nerve growth factor expression correlates with perineural invasion and pain in human pancreatic cancer. *Journal of Clinical Oncology* **17**, 2419–2428 (1999).
158. Ma, J., Jiang, Y., Jiang, Y., Sun, Y. & Zhao, X. Expression of nerve growth factor and tyrosine kinase receptor A and correlation with perineural invasion in pancreatic cancer. *Journal of gastroenterology and hepatology* **23**, 1852–9 (2008).
159. Dang, C., Zhang, Y., Ma, Q. & Shimahara, Y. Expression of nerve growth factor receptors is correlated with progression and prognosis of human pancreatic cancer. *Journal of gastroenterology and hepatology* **21**, 850–8 (2006).
160. Duan, L., Hu, X., Feng, D., Lei, S. & Hu, G. GPC-1 may serve as a predictor of perineural invasion and a prognosticator of survival in pancreatic cancer. *Asian journal of surgery / Asian Surgical Association* **36**, 7–12 (2013).
161. Gil, Z. *et al.* Paracrine regulation of pancreatic cancer cell invasion by peripheral nerves. *Journal of the National Cancer Institute* **102**, 107–18 (2010).
162. Zeng, Q. *et al.* The Relationship between Over-expression of Glial Cell-derived Neurotrophic Factor and Its RET Receptor with Progression and Prognosis of Human Pancreatic Cancer. *Journal of International Medical Research* **36**, 656–664 (2008).
163. Takamido, S. *et al.* Intrapancreatic axonal hyperbranching of dorsal root ganglia neurons in chronic pancreatitis model rats and its relation to pancreatic pain. *Pancreas* **33**, 268–79 (2006).
164. Zhu, Z. W., Friess, H., Wang, L., Zimmermann, a & Büchler, M. W. Brain-derived neurotrophic factor (BDNF) is upregulated and associated with pain in chronic pancreatitis. *Digestive diseases and sciences* **46**, 1633–9 (2001).

165. Friess, H. *et al.* Nerve Growth Factor and Its High-Affinity Receptor in Chronic Pancreatitis. *Annals of surgery* **230**, 615–624 (1999).
166. Di Sebastiano, P. *et al.* Immune cell infiltration and growth-associated protein 43 expression correlate with pain in chronic pancreatitis. *Gastroenterology* **112**, 1648–55 (1997).
167. Ceyhan, G. O. *et al.* The neurotrophic factor artemin influences the extent of neural damage and growth in chronic pancreatitis. *Gut* **56**, 534–44 (2007).
168. Demir, I. E. *et al.* The microenvironment in chronic pancreatitis and pancreatic cancer induces neuronal plasticity. *Neurogastroenterology and motility* **22**, 480–90, e112–3 (2010).
169. Li, J. & Ma, Q. Hyperglycemia promotes the perineural invasion in pancreatic cancer. *Medical hypotheses* **71**, 386–9 (2008).
170. Li, J. *et al.* Relationship between neural alteration and perineural invasion in pancreatic cancer patients with hyperglycemia. *PloS one* **6**, e17385 (2011).
171. Sahin, I. H. *et al.* Association of diabetes and perineural invasion in pancreatic cancer. *Cancer medicine* **1**, 357–62 (2012).
172. Sclabas, G. M. *et al.* Overexpression of tropomysin-related kinase B in metastatic human pancreatic cancer cells. *Clinical cancer research* **11**, 440–9 (2005).
173. Zhu, Z. *et al.* Nerve growth factor and enhancement of proliferation, invasion, and tumorigenicity of pancreatic cancer cells. *Molecular carcinogenesis* **35**, 138–47 (2002).
174. Bakst, R. L. *et al.* Radiation impairs perineural invasion by modulating the nerve microenvironment. *PloS one* **7**, e39925 (2012).
175. Cavel, O. *et al.* Endoneurial macrophages induce perineural invasion of pancreatic cancer cells by secretion of GDNF and activation of RET tyrosine kinase receptor. *Cancer research* **72**, 5733–43 (2012).
176. Okada, Y. *et al.* Experimental implication of celiac ganglionotropic invasion of pancreatic-cancer cells bearing c-ret proto-oncogene with reference to glial-cell-line-derived neurotrophic factor (GDNF). *International journal of cancer* **81**, 67–73 (1999).
177. Okada, Y. *et al.* Nerve growth factor stimulates MMP-2 expression and activity and increases invasion by human pancreatic cancer cells. *Clinical & experimental metastasis* **21**, 285–92 (2004).
178. Veit, C. *et al.* Activation of Phosphatidylinositol 3-Kinase and Extracellular Signal-Regulated Kinase Is Required for Glial Cell Line-Derived Neurotrophic Factor-Induced Migration and Invasion of Pancreatic Carcinoma Cells Activation of Phosphatidylinositol 3-Kinase and. *Cancer research* **64**, 5291–5300 (2004).
179. Mantyh, P. W., Clohisy, D. R., Koltzenburg, M. & Hunt, S. P. Molecular mechanisms of cancer pain. *Nature reviews. Cancer* **2**, 201–9 (2002).
180. Mantyh, P. W. Cancer pain and its impact on diagnosis, survival and quality of life. *Nature reviews. Neuroscience* **7**, 797–809 (2006).
181. Portenoy, R. K. & Lesage, P. Management of cancer pain. *Lancet* **353**, 1695–700 (1999).
182. Barreto, S. G. & Saccone, G. T. P. Pancreatic nociception--revisiting the physiology and pathophysiology. *Pancreatology* **12**, 104–12 (2012).
183. Di Sebastiano, P., Di Mola, F. F., Bockman, D. E., Friess, H. & Büchler, M. W. Chronic pancreatitis: the perspective of pain generation by neuroimmune interaction. *Gut* **52**, 907–11 (2003).

184. Von Gunten, C. F. Pathophysiology of pain in cancer. *Journal of pediatric hematology/oncology* **33 Suppl 1**, S12–8 (2011).
185. Ceyhan, G. O., Demir, I. E., Maak, M. & Friess, H. Fate of nerves in chronic pancreatitis: Neural remodeling and pancreatic neuropathy. *Best practice & research. Clinical gastroenterology* **24**, 311–22 (2010).
186. Noble, M. & Gress, F. G. Techniques and results of neurolysis for chronic pancreatitis and pancreatic cancer pain. *Current gastroenterology reports* **8**, 99–103 (2006).
187. Bradley, E. L. & Bem, J. Nerve blocks and neuroablative surgery for chronic pancreatitis. *World journal of surgery* **27**, 1241–8 (2003).
188. Arcidiacono, P. G., Calori, G., Carrara, S., McNicol, E. D. & Testoni, P. A. Celiac plexus block for pancreatic cancer pain in adults. *Cochrane database of systematic reviews (Online)* **3**, CD007519 (2011).
189. Olesen, S. S. *et al.* Descending inhibitory pain modulation is impaired in patients with chronic pancreatitis. *Clinical gastroenterology and hepatology* **8**, 724–30 (2010).
190. Demir, I. E., Tieftrunk, E., Maak, M., Friess, H. & Ceyhan, G. O. Pain mechanisms in chronic pancreatitis: of a master and his fire. *Langenbeck's archives of surgery* **396**, 151–60 (2011).
191. Ceyhan, G. O., Michalski, C. W., Demir, I. E., Müller, M. W. & Friess, H. Pancreatic pain. *Best practice & research. Clinical gastroenterology* **22**, 31–44 (2008).
192. Schmidt, B. L., Hamamoto, D. T., Simone, D. A. & Wilcox, G. L. Mechanisms of cancer pain. *Molecular Interventions* **10**, 164–178 (2010).
193. Sommer, C. & Kress, M. Recent findings on how proinflammatory cytokines cause pain: peripheral mechanisms in inflammatory and neuropathic hyperalgesia. *Neuroscience letters* **361**, 184–7 (2004).
194. Ren, K. & Dubner, R. Interactions between the immune and nervous systems in pain. *Nature medicine* **16**, 1267–1276 (2010).
195. Feng, Q. X. *et al.* Astrocytic activation in thoracic spinal cord contributes to persistent pain in rat model of chronic pancreatitis. *Neuroscience* **167**, 501–9 (2010).
196. Qian, N.-S. *et al.* Spinal toll like receptor 3 is involved in chronic pancreatitis-induced mechanical allodynia of rat. *Molecular pain* **7**, 15 (2011).
197. Zhang, R.-X. *et al.* Spinal glial activation in a new rat model of bone cancer pain produced by prostate cancer cell inoculation of the tibia. *Pain* **118**, 125–36 (2005).
198. Hidaka, K. *et al.* Central glial activation mediates cancer-induced pain in a rat facial cancer model. *Neuroscience* **180**, 334–43 (2011).
199. Li, X. *et al.* Stage-dependent anti-allodynic effects of intrathecal Toll-like receptor 4 antagonists in a rat model of cancer induced bone pain. *The journal of physiological sciences* **63**, 203–9 (2013).
200. Hu, J.-H., Wu, M.-Y., Tao, M. & Yang, J.-P. Changes in protein expression and distribution of spinal CCR2 in a rat model of bone cancer pain. *Brain research* **1509**, 1–7 (2013).
201. Doré-Savard, L. *et al.* Behavioral, medical imaging and histopathological features of a new rat model of bone cancer pain. *PloS one* **5**, e13774 (2010).
202. Hald, A., Nedergaard, S., Hansen, R. R., Ding, M. & Heegaard, A.-M. Differential activation of spinal cord glial cells in murine models of neuropathic and cancer pain. *European journal of pain* **13**, 138–45 (2009).

203. Liu, S. *et al.* Tibia tumor-induced cancer pain involves spinal p38 mitogen-activated protein kinase activation via TLR4-dependent mechanisms. *Brain research* **1346**, 213–23 (2010).
204. D'Haese, J. G., Demir, I. E., Friess, H. & Ceyhan, G. O. Fractalkine/CX3CR1: why a single chemokine-receptor duo bears a major and unique therapeutic potential. *Expert opinion on therapeutic targets* **14**, 207–19 (2010).
205. Ceyhan, G. O. *et al.* Neural fractalkine expression is closely linked to pain and pancreatic neuritis in human chronic pancreatitis. *Laboratory investigation* **89**, 347–61 (2009).
206. Demir, I. E. *et al.* Perineural mast cells are specifically enriched in pancreatic neuritis and neuropathic pain in pancreatic cancer and chronic pancreatitis. *PloS one* **8**, e60529 (2013).
207. Liddle, R. a The role of Transient Receptor Potential Vanilloid 1 (TRPV1) channels in pancreatitis. *Biochimica et biophysica acta* **1772**, 869–78 (2007).
208. Fernandes, E. S., Fernandes, M. a & Keeble, J. E. The functions of TRPA1 and TRPV1: moving away from sensory nerves. *British journal of pharmacology* **166**, 510–21 (2012).
209. Dhaka, A., Viswanath, V. & Patapoutian, A. Trp ion channels and temperature sensation. *Annual review of neuroscience* **29**, 135–61 (2006).
210. Schwartz, E. S. *et al.* Synergistic Role of TRPV1 and TRPA1 in Pancreatic Pain and Inflammation. *Gastroenterology* 1283–1291 (2010).doi:10.1053/j.gastro.2010.12.033
211. Schwartz, E. S. *et al.* TRPV1 and TRPA1 Antagonists Prevent the Transition of Acute to Chronic Inflammation and Pain in Chronic Pancreatitis. *The Journal of neuroscience* **33**, 5603–11 (2013).
212. Xu, G.-Y., Winston, J. H., Shenoy, M., Yin, H. & Pasricha, P. J. Enhanced excitability and suppression of A-type K+ current of pancreas-specific afferent neurons in a rat model of chronic pancreatitis. *American journal of physiology. Gastrointestinal and liver physiology* **291**, G424–31 (2006).
213. Xu, G.-Y. *et al.* Transient receptor potential vanilloid 1 mediates hyperalgesia and is up-regulated in rats with chronic pancreatitis. *Gastroenterology* **133**, 1282–92 (2007).
214. Zhu, Y. *et al.* Nerve Growth Factor Modulates TRPV1 Expression and Function and Mediates Pain in Chronic Pancreatitis. *Gastroenterology* **141**, 370–7 (2011).
215. Malin, S. a *et al.* Glial cell line-derived neurotrophic factor family members sensitize nociceptors in vitro and produce thermal hyperalgesia in vivo. *The Journal of neuroscience* **26**, 8588–99 (2006).
216. Nathan, J. D. *et al.* Primary sensory neurons: a common final pathway for inflammation in experimental pancreatitis in rats. *American journal of physiology. Gastrointestinal and liver physiology* **283**, G938–46 (2002).
217. Noble, M. D., Romac, J., Vigna, S. R. & Liddle, R. a A pH-sensitive, neurogenic pathway mediates disease severity in a model of post-ERCP pancreatitis. *Gut* **57**, 1566–71 (2008).
218. Romac, J. M. J., McCall, S. J., Humphrey, J. E., Heo, J. & Liddle, R. a Pharmacologic disruption of TRPV1-expressing primary sensory neurons but not genetic deletion of TRPV1 protects mice against pancreatitis. *Pancreas* **36**, 394–401 (2008).
219. Li, C. *et al.* Anatomical and functional characterization of a duodeno-pancreatic neural reflex that can induce acute pancreatitis. *American journal of physiology. Gastrointestinal and liver physiology* **304**, G490–500 (2013).
220. Hutter, M. M. *et al.* Transient receptor potential vanilloid (TRPV-1) promotes neurogenic inflammation in the pancreas via activation of the neurokinin-1 receptor (NK-1R). *Pancreas* **30**, 260–5 (2005).

221. Ikeura, T. *et al.* Effects of sensory denervation by neonatal capsaicin administration on experimental pancreatitis induced by dibutyltin dichloride. *Medical molecular morphology* **40**, 141–9 (2007).
222. Tevethia, M. J., Bonneau, R. H., Griffith, J. W. & Mylin, L. A simian virus 40 large T-antigen segment containing amino acids 1 to 127 and expressed under the control of the rat elastase-1 promoter produces pancreatic acinar carcinomas in transgenic mice. *Journal of virology* **71**, 8157–66 (1997).
223. Lindsay, T. H. *et al.* Pancreatic cancer pain and its correlation with changes in tumor vasculature, macrophage infiltration, neuronal innervation, body weight and disease progression. *Pain* **119**, 233–46 (2005).
224. Sevcik, M. a *et al.* Endogenous opioids inhibit early-stage pancreatic pain in a mouse model of pancreatic cancer. *Gastroenterology* **131**, 900–10 (2006).
225. Duan, K.-Z. *et al.* Targeting A-type K(+) channels in primary sensory neurons for bone cancer pain in a rat model. *Pain* **153**, 562–74 (2012).
226. Jimenez-Andrade, J. M. *et al.* Pathological sprouting of adult nociceptors in chronic prostate cancer-induced bone pain. *The Journal of neuroscience* **30**, 14649–56 (2010).
227. Kaan, T. K. Y. *et al.* Systemic blockade of P2X3 and P2X2/3 receptors attenuates bone cancer pain behaviour in rats. *Brain : a journal of neurology* **133**, 2549–64 (2010).
228. Niiyama, Y., Kawamata, T., Yamamoto, J., Omote, K. & Namiki, A. Bone cancer increases transient receptor potential vanilloid subfamily 1 expression within distinct subpopulations of dorsal root ganglion neurons. *Neuroscience* **148**, 560–72 (2007).
229. Pan, H.-L., Zhang, Y.-Q. & Zhao, Z.-Q. Involvement of lysophosphatidic acid in bone cancer pain by potentiation of TRPV1 via PKCε pathway in dorsal root ganglion neurons. *Molecular pain* **6**, 85 (2010).
230. Schweizerhof, M. *et al.* Hematopoietic colony-stimulating factors mediate tumor-nerve interactions and bone cancer pain. *Nature medicine* **15**, 802–7 (2009).
231. Ghilardi, J. R. *et al.* Administration of a tropomyosin receptor kinase inhibitor attenuates sarcoma-induced nerve sprouting , neuroma formation and bone cancer pain Administration of a tropomyosin receptor kinase inhibitor attenuates sarcoma-induced nerve sprouting , neuroma fo. *Molecular Pain* **6**, 1–12 (2010).
232. Jimenez-Andrade, J. M., Ghilardi, J. R., Castañeda-Corral, G., Kuskowski, M. a & Mantyh, P. W. Preventive or late administration of anti-NGF therapy attenuates tumor-induced nerve sprouting, neuroma formation, and cancer pain. *Pain* **152**, 2564–74 (2011).
233. Mantyh, W. G. *et al.* Blockade of nerve sprouting and neuroma formation markedly attenuates the development of late stage cancer pain. *Neuroscience* (2010).doi:10.1016/j.neuroscience.2010.08.056
234. Sevcik, M. a *et al.* Anti-NGF therapy profoundly reduces bone cancer pain and the accompanying increase in markers of peripheral and central sensitization. *Pain* **115**, 128–41 (2005).
235. Wacnik, P. W. *et al.* Functional interactions between tumor and peripheral nerve: morphology, algogen identification, and behavioral characterization of a new murine model of cancer pain. *The Journal of neuroscience* **21**, 9355–66 (2001).
236. Wacnik, P. W. *et al.* Tumor-induced mechanical hyperalgesia involves CGRP receptors and altered innervation and vascularization of DsRed2 fluorescent hindpaw tumors. *Pain* **115**, 95–106 (2005).

237. Geis, C. *et al.* Evoked pain behavior and spinal glia activation is dependent on tumor necrosis factor receptor 1 and 2 in a mouse model of bone cancer pain. *Neuroscience* **169**, 463–74 (2010).
238. Wacnik, P. W., Eikmeier, L. J., Simone, D. a, Wilcox, G. L. & Beitz, a J. Nociceptive characteristics of tumor necrosis factor-alpha in naive and tumor-bearing mice. *Neuroscience* **132**, 479–91 (2005).
239. Cain, D. M. *et al.* Functional interactions between tumor and peripheral nerve: changes in excitability and morphology of primary afferent fibers in a murine model of cancer pain. *The Journal of neuroscience* **21**, 9367–76 (2001).
240. Lam, D. K., Dang, D., Zhang, J., Dolan, J. C. & Schmidt, B. L. Novel animal models of acute and chronic cancer pain: a pivotal role for PAR2. *The Journal of neuroscience* **32**, 14178–83 (2012).
241. Ye, Y. *et al. Nerve growth factor links oral cancer progression, pain, and cachexia. Molecular cancer therapeutics* **10**, 1667–76 (2011).
242. Ding, Y., Cravero, J. D., Adrian, K. & Grippo, P. Modeling pancreatic cancer in vivo: from xenograft and carcinogen-induced systems to genetically engineered mice. *Pancreas* **39**, 283–92 (2010).
243. Tuveson, D. a & Hingorani, S. R. Ductal pancreatic cancer in humans and mice. *Cold Spring Harbor symposia on quantitative biology* **70**, 65–72 (2005).
244. Westphalen, C. B. & Olive, K. P. Genetically engineered mouse models of pancreatic cancer. *Cancer journal (Sudbury, Mass.)* **18**, 502–10 (2012).
245. Morris, J. P., Wang, S. C. & Hebrok, M. KRAS, Hedgehog, Wnt and the twisted developmental biology of pancreatic ductal adenocarcinoma. *Nature reviews. Cancer* **10**, 683–95 (2010).
246. Hruban, R. H. *et al.* Pathology of genetically engineered mouse models of pancreatic exocrine cancer: consensus report and recommendations. *Cancer research* **66**, 95–106 (2006).
247. Guerra, C. & Barbacid, M. Genetically engineered mouse models of pancreatic adenocarcinoma. *Molecular oncology* **7**, 232–247 (2013).
248. Nagy, a Cre recombinase: the universal reagent for genome tailoring. *Genesis* **26**, 99–109 (2000).
249. Jackson, E. L. *et al.* Analysis of lung tumor initiation and progression using conditional expression of oncogenic K-ras. *Genes & development* **15**, 3243–8 (2001).
250. Tuveson, D. a *et al.* Endogenous oncogenic K-ras(G12D) stimulates proliferation and widespread neoplastic and developmental defects. *Cancer cell* **5**, 375–87 (2004).
251. Kawaguchi, Y. *et al.* The role of the transcriptional regulator Ptf1a in converting intestinal to pancreatic progenitors. *Nature genetics* **32**, 128–34 (2002).
252. Aguirre, A. J. *et al.* Activated Kras and Ink4a/Arf deficiency cooperate to produce metastatic pancreatic ductal adenocarcinoma. *Genes & development* **17**, 3112–26 (2003).
253. Bardeesy, N. *et al.* Smad4 is dispensable for normal pancreas development yet critical in progression and tumor biology of pancreas cancer. *Genes & Development* **20**, 3130–3146 (2006).
254. Bardeesy, N. *et al.* Both p16(Ink4a) and the p19(Arf)-p53 pathway constrain progression of pancreatic adenocarcinoma in the mouse. *Proceedings of the National Academy of Sciences of the United States of America* **103**, 5947–52 (2006).

255. Marino, S., Vooijs, M., Gulden, H. Van Der, Jonkers, J. & Berns, A. cerebellum Induction of medulloblastomas in p53-null mutant mice by somatic inactivation of Rb in the external granular layer cells of the cerebellum. *Genes & Development* **14**, 994–1004 (2000).
256. Fasanella, K. E., Christianson, J. a, Chanthaphavong, R. S. & Davis, B. M. Distribution and neurochemical identification of pancreatic afferents in the mouse. *The Journal of comparative neurology* **509**, 42–52 (2008).
257. Livak, K. J. & Schmittgen, T. D. Analysis of relative gene expression data using real-time quantitative PCR and the 2(-Delta Delta C(T)) Method. *Methods* **25**, 402–8 (2001).
258. Wang, X., Spandidos, A., Wang, H. & Seed, B. PrimerBank: a PCR primer database for quantitative gene expression analysis, 2012 update. *Nucleic acids research* **40**, D1144–9 (2012).
259. Malin, S. a, Davis, B. M. & Molliver, D. C. Production of dissociated sensory neuron cultures and considerations for their use in studying neuronal function and plasticity. *Nature protocols* **2**, 152–60 (2007).
260. Wang, T. *et al.* Neurturin overexpression in skin enhances expression of TRPM8 in cutaneous sensory neurons and leads to behavioral sensitivity to cool and menthol. *The Journal of neuroscience* **33**, 2060–70 (2013).
261. Wang, T. *et al.* Phenotypic switching of nonpeptidergic cutaneous sensory neurons following peripheral nerve injury. *PloS one* **6**, e28908 (2011).
262. Kang, R. *et al.* The receptor for advanced glycation end products (RAGE) sustains autophagy and limits apoptosis, promoting pancreatic tumor cell survival. *Cell death and differentiation* **17**, 666–76 (2010).
263. Ceyhan, G. O. *et al.* Pancreatic neuropathy results in “neural remodeling” and altered pancreatic innervation in chronic pancreatitis and pancreatic cancer. *The American journal of gastroenterology* **104**, 2555–65 (2009).
264. Koide, N. *et al.* Establishment of perineural invasion models and analysis of gene expression revealed an invariant chain (CD74) as a possible molecule involved in perineural invasion in pancreatic cancer. *Clinical cancer research* **12**, 2419–26 (2006).
265. Cain, D. M. *et al.* Functional interactions between tumor and peripheral nerve: changes in excitability and morphology of primary afferent fibers in a murine model of cancer pain. *The Journal of neuroscience* **21**, 9367–76 (2001).
266. Herner, A. *et al.* Glutamate increases pancreatic cancer cell invasion and migration via AMPA receptor activation and Kras-MAPK signaling. *International journal of cancer*. **129**, 2349–59 (2011).
267. Jancso, N., Jancso-Gabor, A. & Szolcsanyi, J. Directe evidence for neurogenic inflammation and its prevention by denervation and pretreatment with capsaicin. *British journal of pharmacology and chemotherapy* **31**, 138–151 (1967).
268. Jancso, G., Kiraly, E. & Jancso-Gabor, A. Pharmacologically induced selective degeneration of chemosensitive primary sensory neurones. *Nature* **270**, 741–743 (1977).